CHALMERS
UNIVERSITY OF TECHNOLOGY

Compressed Stabilised Earth Blocks in Nepal

A study of the rehabilitation of buildings in rural villages after the Gorkha Earthquake

Master's Thesis in the Master's Programme Structural Engineering and Building Technology

HERMAN MELLEGÅRD
AXEL STEINERT

Department of Civil and Environmental Engineering
Division of Structural Engineering
Steel and Timber Structures
CHALMERS UNIVERSITY OF TECHNOLOGY
Gothenburg, Sweden 2016
Master's Thesis BOMX02-16-139

MASTER'S THESIS BOMX02-16-139

Compressed Stabilised Earth Blocks in Nepal

Master's Thesis in the Master's Programme Structural Engineering and Building Technology

HERMAN MELLEGÅRD
AXEL STEINERT

Department of Civil and Environmental Engineering
Division of Structural Engineering
Steel and Timber Structures
CHALMERS UNIVERSITY OF TECHNOLOGY
Göteborg, Sweden 2016

Compressed Stabilised Earth Blocks in Nepal
A study of the rehabilitation of rural villages in Nepal after the Gorkha earthquake

Master's Thesis in the Master's Programme Structural Engineering and Building Technology

HERMAN MELLEGÅRD

AXEL STEINERT

Examensarbete BOMX02-16-139/ Institutionen för bygg- och miljöteknik,
Chalmers tekniska högskola 2016

Department of Civil and Environmental Engineering
Division of Structural Engineering
Steel and Timber Structures
Chalmers University of Technology
SE-412 96 Göteborg
Sweden
Telephone: + 46 (0)31-772 1000

Cover:
Construction of the first CSEB building in Majhi Gaun, Nepal.
Department of Civil and Environmental Engineering.
Göteborg, Sweden, 2016

Compressed Stabilised Earth Blocks in Nepal
A study of the rehabilitation of rural villages in Nepal after the Gorkha earthquake

Master's thesis in the Master's Programme Structural Engineering and Building Technology

HERMAN MELLEGÅRD
AXEL STEINERT
Department of Civil and Environmental Engineering
Division of Structural Engineering
Steel and Timber Structures
Chalmers University of Technology

ABSTRACT

In the spring of 2015 Nepal was hit by the Gorkha Earthquake. Remote and poor villages suffered severe consequences. The non-profit organization *Build up Nepal* is working with the rehabilitation of these villages after the Gorkha Earthquake. They teach villagers how to build earthquake resistant houses with local materials and local labour. *Build up Nepal* has taught villagers to build earthquake resistant with Compressed Stabilised Earth Blocks (CSEB) and steel reinforcement. CSEB is made from soil, cement and water and then compressed to a block. The blocks are cured to gain strength. CSEB has a large potential for remote villages in Nepal since it only requires simple machines and most material can be found nearby almost any construction site. *The Nepali Building Code* (NBC) does not cover design of CSEB buildings and there is also little knowledge of the actual properties of CSEB and the behaviour of CSEB buildings in Nepal.

The aim of this study was to make a structural analysis of a CSEB building and thereby investigate the actual material properties of CSEB and the structural behaviour of a CSEB building in Nepal. Through in field testing, this study focused on finding values for parameters used in design calculations today, that is: Young's modulus, the density, the compressive and tensile strength and the first natural period of a CSEB building. This study also aimed to find a good numerical model of a CSEB building. The dynamic response of a CSEB building, when excited with an impulse, was tested in field. This test was used to verify the numerical model and to calibrate the mass and stiffness distribution of the model. Suggestions of design improvements for the CSEB buildings build by *Build up Nepal* were made based on the findings of a literature study of earthquake design of masonry and CSEB structures. Also three questions regarding deviations in design raised as a result of observations during the construction of a CSEB building were treated.

This study showed that the values for the density of CSEB could be lower than given in literature. Young's Modulus, the tensile and compressive strength are often times higher than given in literature. These parameters are highly dependent on the machine being used in the production of CSEB, also the cement proportions and the amount of coarse particles in the soil have an impact on these parameters. The first natural period of the first CSEB building built by *Build up Nepal* was much lower than estimated by the empirical formulas for "other structures" in *NBC 105:1994*.

Key words: compressed stabilised earth blocks, CSEB, design improvements, dynamic response, dynamic testing, earthquake engineering, field studies, finite element method, Gorkha Earthquake, Kathmandu, Majhi Gaun, masonry, modal analysis, Nepal, numerical modelling, rehabilitation process.

Contents

Preface

First of all we would like to express our gratitude for writing this Master Thesis together with *Build up Nepal,* it has been both extremely fun and rewarding. *Build up Nepal* has been a great organization to work with providing an open and effective work environment. The collaboration has been a clear success for both sides. Therefore a long term agreement between *Engineers without Borders* at Chalmers and *Build up Nepal* has been established as a result of our collaboration. More students will now get the opportunity to go to Nepal and to work in another dimension of reality where their technical knowledge is desperately needed.

Working with a, for us, completely new building material has not been easy all the time but we have learnt a great deal. We learnt almost as much from things we did not manage to do or had to change, as from the things we did and that ultimately ended up in this report. It is a sometimes frustrating but a great way of learning to find out what pieces of information that are missing for you to succeed. This Master Thesis has been a perfect ending of our time at Chalmers University of Technology. It has given us the opportunity to use almost all our acquired knowledge as structural engineers; we have not only studied the construction of a whole building but also the making of the material used in that building and the testing needed for development of design provisions. This Master Thesis has also truly inspired us to work as structural engineers in the future, we have seen the need for the profession and the great things a structural engineer can accomplish also at a completely different place in the world.

We would also like to take the opportunity to direct a special thanks to our supervisors: Reza Haghani and Thomas Abrahamsson that have been very understanding with this slightly different way of writing a Master Thesis. We would also like to thank Åke Solfelt and Mikael Mangold that also have helped us a great deal especially in the preparations for our field trip.

It has been very valuable to have our opponents, Mathilda Larsson and Henrik Mayor, as a sounding board in the writing and development of this Master Thesis. Thank you Mathilda and Henrik.

Last but not least, a big thanks to all employees of *Build up Nepal*, to Björn Söderberg, Kulendra Neupane, Sonal Gupta, Sontos and Madhu for their warm welcome to Nepal and their organization.

1 Introduction

In the spring of 2015 Nepal was hit by an earthquake, over 500000 houses were totally destroyed. Remote and poor villages suffered severe consequences (Söderberg, 2015). This study was written in the wake of this crisis. This first chapter covers the background, the purpose, the aim, the methodology and finally the limitations of this study.

1.1 Background

The non-profit organization *Build up Nepal* is working with the rehabilitation of villages. *Build up Nepal* teaches villagers how to build earthquake resistant houses with local materials and local labour. In Majhi Gaun, a small village outside Kathmandu *Build up Nepal* has taught villagers how to build with Compressed Stabilized Earth Blocks (CSEB) and steel reinforcement. CSEB is a masonry construction material. The blocks are made from soil, cement and water and then compressed to a block. The blocks are finally cured to gain strength. CSEB has a large potential for remote villages in Nepal since it only requires simple machines and most material can be found nearby almost any construction site. The reception of the CSEB has been extremely positive among the people of Majhi Gaun. The community has a strong belief in the technology and is eager to build up their village with CSEB. A technology and design well anchored in the community has proven to be of great importance in rehabilitation work for long term success (Sandersson & Burnell, 2013). *Build up Nepal* will provide Majhi Gaun with the machines to produce CSEB, design of buildings and additional training courses in how to build with the blocks. Furthermore *Build up Nepal* will also supervise important phases of the construction. The aim is however that the villagers, who are neither engineers nor masons, eventually shall be able to build the CSEB houses all by themselves. The Master Thesis was written during the construction of the first CSEB building in Majhi Gaun.

The Nepali Building Code (NBC) does not cover design of CSEB buildings why today usually guidelines from *Indian Standard 1905:1987* combined with *IITK-GSDMA* and *Auroville Earth Institute* often are used. There is also little knowledge of the actual properties of CSEB and the behaviour of CSEB buildings in Nepal. Furthermore, the material properties of CSEB are also variating widely with production method and composition, especially compression ratio, curing and amount of stabilization have large impact on the final behaviour of the block (Maïni, Production and Use of Compressed Stabalised Earth Blocks, 2010).

1.2 Purpose

The extensive work of rehabilitation that the people of Nepal now are facing will take years. In the wake of this national crisis Nepal also has to manage a technical change. In order to build up a sustainable society with building structures that can withstand earthquakes of the future, new methods and techniques have to be used. Nepal needs all the help they can get in managing this change. The purpose of this study was to help to improve the quality and the performance of CSEB buildings built by people with a non-engineering background.

1.3 Aim of the Study

The aim of this study was to make a structural analysis of a CSEB building in Majhi Gaun and thereby investigate the actual material properties of CSEB and the structural behaviour of a CSEB building in Nepal. The study focused on finding values for Young's modulus, the density, the compressive and tensile strength and the first natural period for CSEB and a CSEB building in Nepal. These parameters are used in design calculations of CSEB in Nepal. This study also aimed to find a good numerical model of a CSEB building and to come up with suggestions of design improvements for the CSEB building in Majhi Gaun. An additional aim of this study was to treat three questions raised during the construction of the first CSEB building in Majhi Gaun (these are further described in Chapter 2):

Q1. Could failures in production result in a CSEB with too poor quality?
Q2. Does a bent rebar in one of the corners make the building unsafe?
Q3. Does a poorly anchored rebar next to one of the openings make the building unsafe?

1.4 Methodology

Existing theory of earthquakes, earthquake effect on structures and earthquake design of masonry and CSEB structures were covered in a literature review. Existing knowledge of some relevant material properties of CSEB, is also covered here. The next part of the study covered needed theory for dynamic analysis of structures. This part covered analysis methods, modelling approaches and justified simplifications.

The material properties of various types of CSEB were measured in field. The blocks used in Majhi Gaun were tested to find the actual material properties of the CSEB used in the CSEB building in Majhi Gaun. With reference to the observations made in field (see Chapter 2 Section 2.1) also variations of CSEB were tested in order to increase the knowledge of the influence of different composition of soil, proportions of cement and production method. The compressive and tensile strength of CSEB were tested and calculated by a method and a machine from *Auroville Earth Institute*. Values for Young's modulus were calculated with an equation which was proposed in *Advances in Composite Materials-Analysis of Natural and Man-made Materials* (Panzera, Christoforo, Cota, Borges, & Bowen, 2011). The ultrasonic pulse velocity was tested with a Pundit Lab Ultrasonic Instrument and two standard 54 kHz transducers (a more detailed description of this testing methodology can be found in Chapter 10). The density of the CSEB was also measured.

The dynamic behaviour of the CSEB building in Majhi Gaun was tested and measured using accelerometers and a data acquisition device of model: Data Translation DT9837A (a more detailed description of this testing methodology can be found in Chapter 11 Section 11.1). From the acceleration time-history a calculation and an estimation of some natural frequency modes were made.

3D solids were used to model the CSEB building in Majhi Gaun in Abaqus/CAE 6.13-3. The result of the testing of the material properties of the CSEB used in Majhi Gaun was used as input material properties. The natural frequencies of the model were calculated by a modal analysis. The aim was to find a model with the same dynamic behaviour as tested in field. The natural frequency modes found in field were compared with the natural frequency modes of the model. The model was calibrated to find a mass and stiffness distribution that corresponded

well to reality. This was done by varying the input values for Young's Modulus and the density in the ranges found in the testing of the blocks. Also the values found in literature were used as input values.

Q1 was treated based on the result of the material property testing of CSEB. In *Q1* "*too poor quality"* was defined as values of E, σ_t and σ_c lower than given in literature since these values are used in design calculations today. *Q2* and *Q3* were answered by calculating the earthquake design load on the CSEB building in Majhi Gaun and the resistances of the segments of interest. The earthquake design load was calculated according to the *Nepali Building Code 105:1994*. An amplification of this load was made with reference to *IITK GSDMA Guidelines for Structural Use of Masonry*.

1.5 Limitations

The structural analysis was in this study limited to the elastic behaviour of the CSEB building. Cracking patterns, stiffness redistribution and failure modes were not analysed. The reinforcement was assumed to have little influence on the dynamic behaviour in the uncracked state why it was neglected in the modal analysis. No durability aspects were taken into account.

The amount of time and equipment available for in field testing of both the material properties of CSEB and the dynamic behaviour of the CSEB building in Majhi Gaun was limited. Even if tests failed slightly or did not give as clear result as desired there was no time for retakes. Therefore all tests are limited to the equipment at hand and conditions at the time of the testing.

The answers to the questions raised during the construction of the CSEB building in Majhi Gaun are adapted to the time frame of the project. The answers are only based on the investigations of this study and in order to answer some of the questions more thoroughly also other aspects should be investigated.

2 In-Field Observations

This chapter covers some observations made in field at construction sites in Nepal. These observations have functioned as additional background to this study and also raised some important questions. It was relevant to take part in the construction process of a CSEB building to better understand the construction environment in Nepal and what affects the material properties of CSEB and the performance of a CSEB building.

During any construction unforeseen problems arise, these are then often solved by an experienced and skilled site engineer. Majhi Gaun and many other rural villages of Nepal do not always have that option. Today many aid organisations who previously ran education projects or orphanages now need to build up their facilities. The demand for skilled engineers is larger than the supply. During the construction of the first CSEB building in Majhi Gaun examples of solutions lacking engineering understanding were found. When mistakes during construction lead to deviations from the original design *Build up Nepal* has limited knowledge of the structural impact.

2.1 Production of CSEB in Majhi Gaun

There are many crucial steps in the production of a CSEB. They all influence the material properties of the final result. Due to various reasons during the production process there is a potential deviation in expected performance and actual performance.

2.1.1 Measuring

The equipment available for measuring the different compounds have a large margin of error. The cement is bought in 50 kg bags. The same type of bag is then, for convenience, used to measure the volume of the soil (see Figure 1). The amount of soil that is put in the bag is not weighted and there is no way of controlling the density or the moisture content in it. It is likely that the amount might differ from bag to bag.

Figure 1. Bags used for measuring compounds in Majhi Gaun.

2.1.2 Composition

The methods to determine the soil type also have a large margin of error. The composition of fractions in the soil are determined by a sedimentation test and ocular inspection. This test is usually performed in an irregular plastic bottle (see Figure 2).

Figure 2. Plastic bottle used for sedimentation test.

2.1.3 Mixing

The mixing of the different contents usually takes place on a thin steel sheet placed on the ground and the mixing of soil and cement is done by hand while water is added to the mix. It is likely that the content is not 100 % evenly distributed over the mix. It is also likely that some of it could get spilled outside the steel sheet and thereby get lost. One mixing process in Majhi Gaun is shown in Figure 3.

Figure 3. Mixing cement and soil in Majhi Gaun

2.1.4 Curing

The curing process is an important part of the production of CSEB. Different weather conditions make this process difficult to plan. It is plausible that the timing sometimes might fail since monitoring systems do not exist. The construction work is for many villagers a new and only one part of their work day. It should be balanced with all other tasks they must attend to, agriculture, cooking etc. It is therefore likely that the watering may be forgotten altogether when other tasks are in need of a lot of attention. The curing of CSEB is shown in Figure 4.

Figure 4. Curing of CSEB in Majhi Gaun.

These observations regarding the production of CSEB raised the question:
Q1. Could failures in production result in a CSEB with too poor quality?

2.2 Bending of Rebars

The vertical rebars should be placed when building the foundation. They have to be casted in the foundation in order to get proper anchorage. The positions of the rebars are decisive for the rest of the construction since the blocks are placed in the spacing of the vertical rebars. This is especially important when using hollow interlocking blocks. Many villagers lack experience in measuring technique and cannot foresee the total consequence of a small mismeasurement. In the foundation, often made by irregular stone blocks, it is also difficult to find suitable reference points. If the vertical rebars are misplaced the planned number of whole and half blocks will not fit in the spacing between them. To tear up the whole foundation is a costly and time consuming process why other solutions might appear. One observed solution was how the rebars were simply bent into the correct position when misplaced (see Figure 5).

Figure 5. Bent rebars in Majhi Gaun

The observation of bending of rebars raised the question:
Q2. Does a bent rebar in one of the corners make the building unsafe?

2.3 Forgotten or Misplaced Rebars

Rebars are sometimes entirely misplaced, forgotten during the casting of the foundation or needed to be replaced due to some redesign of the building after the foundation had been casted. There was an observed example of a solution to this where rebars were placed in drilled holes in the already cured plinth beam (see Figure 6). This will result in a shorter anchorage length than prescribed.

Figure 6. Drilling holes for anchorage of rebars.

Observations of forgotten rebars raised the question:
Q3. Does a poorly anchored rebar next to one of the openings make the building unsafe?

3 Earthquakes

Earthquakes are dynamic vibrating movements of the earth. They usually do not last longer than one minute but larger earthquakes often have numerous aftershocks.

3.1 Seism Types

There are two main types of earthquakes: tectonic and volcanic. Different natural phenomena create different types of earthquakes or seisms. Human activity could also create vibrations in the ground but for a limited region and duration. The most severe and most frequently occurring types stem from movement in the tectonic plates. 200 million years ago the earth was a single land area. Over time the land has separated and created different tectonic plates. Tectonic plates could be described as slices of the earth crust floating around on the more viscous magma. The tectonic plates are still moving and many plates and many continents are composed of several different plates. The plates are by their movements (towards, alongside and from each other) building up a huge amount of energy that gets stored in the earth's crust. The plasticity of the crust limits the amount of energy that can be stored, when this limit is reached it fails elastically and creates a tectonic earthquake. The volcanic earthquakes are usually less severe than the tectonic. When the magma under the earth crust is pushing up it sometimes break it and creates an earthquake. Also the opposite, when the magma is caving, can cause an earthquake. Finally, also volcanic eruptions and explosions can make the earth quake (Shrestha, Manual for EQ Safe Building Construction, 2012).

3.2 Seismic Waves

The focus of the earthquake is called hypocentre. The epicentre lies on the surface straight above the hypocentre. At the hypocentre, spherical pulses are induced that propagate as concentric waves in all directions. An earthquake can induce four different types of waves and each type is dependent on the medium that the wave is travelling in. The different types of waves have different types of actions and periods. All waves are reversible and ultimately the ground vibrates in all directions during an earthquake. Records of the occurrence of different wave types and their reflections are used to determine the depth and the hypocentre of an earthquake. Figure 7 gives an overview of some features of an earthquakes and one pattern of wave propagations (Shrestha, 2012).

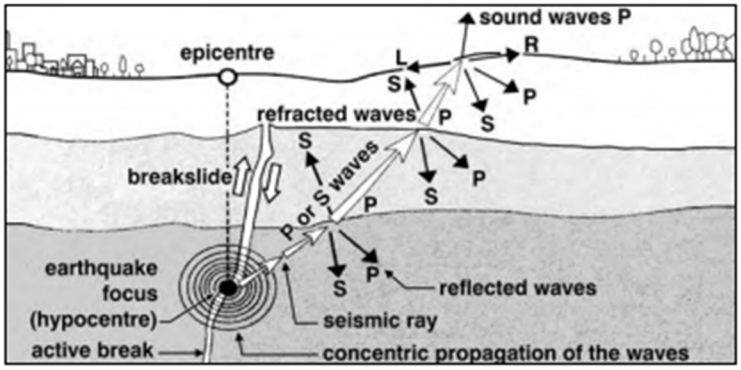

Figure 7. Schematic view of an earthquake (Shrestha, Manual for EQ Safe Building Construction, 2012).

3.2.1 Wave types

The P-wave also called the primary wave is the first that propagates deep down in the crust of the earth. Its action is longitudinal and creates compression and dilation in the ground (see Figure 8 a). The velocity of a P-wave is 5-8 km/s. The S-wave has a shear and transversal action on the ground creating an oscillating movement on the ground. The oscillation is vertically perpendicular to its progression (see Figure 8 b). The velocity of the S-waves is slower than the P-wave, around 3-5 km/s. Love waves also called L-waves, are similar to the S-waves but creates an oscillation horizontally perpendicular to the wave progression (see Figure 8 c). Rayleigh waves, also called R-waves, create vibrations through an elliptical movement counter clockwise to the wave propagation direction (see Figure 8 d) (Shrestha, 2012).

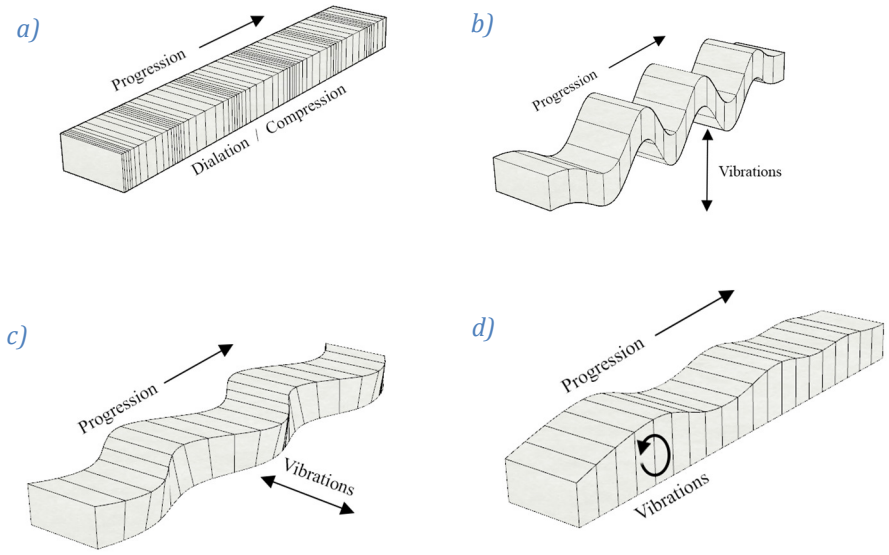

Figure 8. Four different wave types of an earthquake. a) P-wave b) S-wave c) L-wave d) R-wave.

3.3 Measurement of Earthquakes

In the measurement of an earthquake there are two major measuring scales and systems: the Richter and the Mercalli Scale.

3.3.1 The Richter Scale and the Moment Magnitude Scale

The Richter scale measures the magnitude of an earthquake, it measures the amount of energy that an earthquake releases. The original Richter scale that was developed in 1935 by Charles F. Richter has today been modified to cover more types of earthquakes. The scale is logarithmic in shaking amplitude, for every increase in magnitude by one unit the increase in amplitude is tenfold and the increase in terms of energy is about 32 times. The highest measured value is 8.9 on the Richter Scale (Spence, Sipkin, & Choy, 1989). The Gorkha earthquake the 25 April 2015 measured 7.8 on the Richter scale (Seneca, 2015). An indication of the severity and the occurrence frequency of earthquakes is given by Table 1.

Table 1. Number of earthquakes and their typical effect of them (The University of Liverpool, 1999).

Richter Scale	Number of earthquakes (per year)	Typical effect of this magnitude
< 3.4	800000	Detected only by seismometers.
3.5-4.2	30000	Just about noticeable indoors.
4.3-4.8	4800	Most people notice them, windows rattle
4.9-5.4	1400	Everyone notices them, dishes may break, open doors swing.
5.5-6.1	500	Slight damage to buildings, plaster cracks, bricks fall.
6.2-6.9	100	Much damage to buildings: chimneys fall, houses move on their foundations.
7.0-7.3	15	Serious damage: bridges twist, walls fracture, buildings may collapse.
7.4-7.9	4	Great damage: most buildings collapse.
>8.0	One every 5 to 10 years	Total damage: surface waves seen, objects thrown in the air.

Seismographs at surface level around the whole world record the oscillations of the ground and with this data the magnitude can be calculated. Different magnitude scales have been developed, one for body waves and one for the Rayleigh surface waves. Geographic variations exist in order to get the result to comply with the original Richter Scale developed for California (Spence, Sipkin, & Choy, 1989).

The two Richter Magnitude Scales are not equivalent for all earthquakes. Larger earthquakes send out more energy on long-period frequencies which may result in underestimations of the true size of the earthquake. The Moment Magnitude Scale has been developed to better estimate the size of larger earthquakes. Instead of ground motions it is based on the mechanical work in the fault. This scale is adapted to the Richter scale for medium sized earthquakes to give the same magnitudes. However damages to structures are usually caused by shorter period vibrations why separate scales for energy released and physical effects could be of interest (Spence, Sipkin, & Choy, 1989).

3.3.2 The Modified Mercalli Intensity Scale

The Modified Mercalli Intensity Scale evaluates the effects of an earthquake. The scale has no mathematical base but is a ranking of the observed effects at the site (U. S. Geological Survey, 1989). A short version of the 10 steps of ranking is given in Table 2.

Table 2. Ranking and description of damage according to the Modified Mercalli Intensity Scale (U. S. Geological Survey, 1989).

Intensity	Shaking	Description/Damage
I	Not felt	Not felt except by a very few under especially favourable conditions.
II	Weak	Felt by a few persons at rest, especially on upper floors of buildings.
III	Weak	Felt quite noticeably by persons indoors, especially on upper floors of buildings. Many people do not recognize it as an earthquake. Parked cars may rock slightly. Vibrations similar to the passing of a truck.
IV	Light	Felt by many indoors, only by few outdoors during the day. At night, some awakened. Dishes, windows, doors disturbed; walls make cracking sound. Vibration like a heavy truck striking a building. Parked cars rock noticeably.
V	Moderate	Felt by nearly everyone; many awakened. Some dishes and windows brake. Unstable objects overturned. Pendulum clocks may stop.
VI	Strong	Felt by all, many frightened. Some heavy furniture moved; a few instances of fallen plaster. Damage slight.
VII	Very Strong	Damage negligible in buildings of good design and construction; slight to moderate in well-built ordinary structures; considerable damage in poorly built structures; some chimneys broken.
VIII	Severe	Damage considerable in specially designed structures; considerable damage in ordinary substantial buildings with partial collapse. Great damage in poorly built structures. Fall of chimneys, factory stacks, columns, monuments, walls. Heavy furniture overturned.
IX	Violent	Considerable damage in specially designed structures; well-designed frame structures thrown out of plumb. Great damage in substantial buildings, with partial collapse. Buildings shifted off foundations.
X	Extreme	Some well-built wooden structures destroyed; most masonry and frame structures destroyed with foundations. Rails bent.

3.4 Seismic Zones

90 % of the world's earthquakes occur in an area in the Pacific Ocean called "the Ring of Fire" also known as the Circum-Pacific belt. The Alpide belt, which stretches through the Himalayas and Nepal, has 5-6 % of the earthquakes of the world (U.S Geological Survey, 2016). Figure 9 shows the Circum-Pacific belt and the Alpide belt on a map.

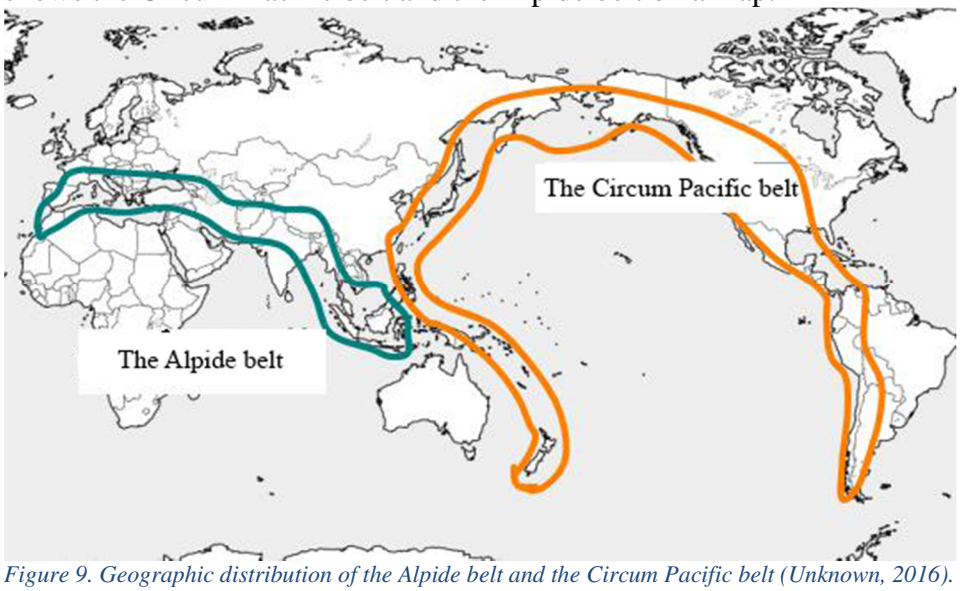

Figure 9. Geographic distribution of the Alpide belt and the Circum Pacific belt (Unknown, 2016).

3.5 Seismic Predictions in Nepal

The Himalayas and Nepal are located at the boundary of the Eurasian and the Indo-Australian plates. Here the Indo-Australian plate moves under the Eurasian plate which induces stresses in the crust. Over the years this fault has ruptured many times and it is likely to continue to. This is how far science goes. It is possible to predict that an earthquake is likely to occur in a specific area but the exact magnitude and the time of the event is impossible to foresee. There are expectations of another "great Himalayan earthquake". Past large earthquakes in the region have induced uneven stresses that needs to be evened out. The earthquake of 25 April did not deform the fault all way through why there is a risk for another large earthquake sometime in the future (Varshney, 2015).

3.6 The Gorkha Earthquake

The Gorkha Earthquake of 25 April 2015 reached a magnitude 7.8 on the Richter scale and on the Modified Mercalli Intensity Scale it reached up to the IX which means violent shaking. The epicentre was 75 km west-northwest of Kathmandu. The major aftershock the 12th of May reached a magnitude of 7.3 on the Richter scale, this time the epicentre was placed 83 km east of Kathmandu. A large part of this Himalayan fault was previously locked but during the quake it unzipped. In Kathmandu high rise buildings and towers were damaged the most. The portion of high frequency waves were limited, instead the long period waves were oscillating and amplified by the soft soil of the Kathmandu basin. The ground in Kathmandu was therefore vibrating with a period of around five seconds generating a frequency equal to the natural frequency of the first mode for many taller buildings. In the mountainous area the major cause of collapse was the large and numerous landslides induced by the earthquake (Seneca, 2015).

4 Compressed Stabilised Earth Blocks (CSEB)

Constructing masonry using earth or soil is one of the oldest building techniques in the world. Masonry has historically during long time been the dominant building material. Building with masonry is simple and straightforward which is one of the reasons for its substantial role as a building material historically. The availability of materials, tools and field of application differs between cultures and results in a multitude of various appearances. It can be used to build both structural and non-structural walls (Lourenço, Rots, & Blaauwendraad, 1995). The Compressed Stabilized Earth Block is a technique for making blocks out of soil. CSEB is different to ordinary kiln fired bricks in its production process, no kiln is needed instead it is compacted. Taking soil, cement and water and then pressing it all together in a machine gives a block with similar behaviour and properties as that of concrete or ordinary kiln fired bricks (Riza, Rahman, & Zaidi, 2010). A CSEB machine is shown in Figure 10.

Figure 10. CSEB machine used in Majhi Gaun.

CSEB has many advantages, the most important properties can be summarised as its structural strength, environmentally friendliness, durability, architectural beauty, low maintenance and comparably low cost (Lourenço, Rots, & Blaauwendraad, 1995). In Nepal CSEB has gained a lot of attention after the Gorkha Earthquake since it allows people to rebuild strong houses to a large extent using local soil. In Nepal it has many advantages compared to ordinary kiln fired bricks: higher strength, less emissions and lower cost (Nankhwa, 2015).

4.1 General Properties of CSEB

Masonry in general is a heterogeneous and anisotropic composite construction material. Blocks or bricks, also referred to as units, are held together by intermediate layers of mortar. Both the units and the mortar can have several compositions and shapes which influence the properties of the masonry. The production of CSEB relies on compressing a mixture of soil, cement and water and then letting it hydrate to gain strength. The mortar is a mix of either lime or cement, water and sand in different proportions. For both the CSEB units and the mortar the compressive strength of the materials is greater than the tensile strength. In addition, the joints between the materials are weak when subjected to tensile forces. This joint is also fragile when subjected to shear stresses. The units and mortar are tied together with friction and chemical bonding where friction is dominant in resisting shear and the chemical bonding the tensile stresses (Bernier, Glascoe, & Mosalam, 2009).

4.2 Some Variations of CSEB

The blocks come in a lot of different sizes and shapes. Depending on the type of structure different types of blocks are used. There are often hollow sections in the blocks in order to decrease the weight and to enable the placement of reinforcement. The wall can then either be fully grouted, where all the hollow sections are grouted or partially grouted where grout is placed only where rebars are present. The most common way to introduce reinforcement into a CSEB wall is to embed it in grout, a form of concrete with high slump, in these hollow sections of the CSEB. The function of the grout is to keep the rebars in place and also to create bonding strength between the rebars and the masonry. The grout increases the cross sectional area which enhances the overall strength. The grout must have a high slump in order to reach all voids (Anderson & Brzev, 2009) (Bakeer, 2009)**.** The way the blocks connect to each other can also differ. One way is the typical masonry approach where a layer of mortar is used to secure interaction of the blocks at their interfaces. Another way, where no mortar is used, is a self-interlocking approach where the blocks are designed with profiles that interlock with each other (see Figure 11) (Maïni, Earthquake Resistant Buildings With Hollow Interlocking Blocks, 2005).

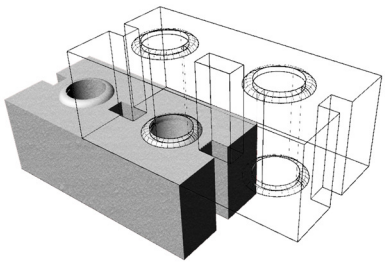

Figure 11. Visualisation of the interlocking of two hollow interlocking CSEB.

4.3 Composition of CSEB

The composition of the soil used is very important when producing CSEB. A soil with a high content of sand is wanted in order to get a high compressive strength and reduced shrinkage (Riza, Rahman, & Zaidi, 2010). A high amount of silt and clay fractions will simplify the production of the blocks but contribute less to the strength. According to the *Auroville Earth Institute* the optimal composition is given by Table 3 using the definition of fractions given in Table 4. Not all soils in Nepal are suitable for CSEB production why sometimes sand has to be added to reach the required sand content (Maïni, Earthquake Resistant Buildings With Hollow Interlocking Blocks, 2005).

Table 3. The optimal soil composition of CSEB (Maïni, Earthquake Resistant Buildings With Hollow Interlocking Blocks, 2005)

Gravel	Sand	Silt	Clay
15 %	50 %	15 %	20 %

Table 4. Definition of fractions of soil (Maïni, Earthquake Resistant Buildings With Hollow Interlocking Blocks, 2005).

Pebbles	Gravel	Sand	Silt	Clay
200 to 20 mm	20 to 2 mm	2 to 0.06 mm	0.06 to 0002 mm	<0.002 mm

4.3.1 Stabilisation of CSEB with Cement

The silt and the clay binds the soil together and stabilizes it. When the soil gets damp this effect is reduced why also cement has to be added. A minimum of 5 % is needed and the economic upper limit is around 9-10 % (Maïni, Earthquake Resistant Buildings With Hollow Interlocking Blocks, 2005). To reach maximum strength it is necessary to keep the blocks moisty during the first three to four weeks. Also, if the clay particles dry they shrink and cracks start to propagate. Therefore, watering of the blocks should be done at least one time per day depending on the weather and also shading of the blocks should be provided (Maïni, Production and Use of Compressed Stabalised Earth Blocks, 2010).

4.4 CSEB Data

The properties of CSEB will vary with soil composition and production method why the values in Table 5 only give ranges. It is based on these values that design calculations of CSEB are made in Nepal today.

Table 5. Material properties of CSEB (Maïni, Earthquake Resistant Buildings With Hollow Interlocking Blocks, 2005) (Shrestha, Standard Norms and Specification for CSEB Block, 2012).

Data on CSEB	
Apparent bulk density, ρ	1700-2200 kg/m^3
Young's Modulus, E	700-1000 MPa
Poisson's ratio, μ	0.15-0.5
Compressive strength, σ_c	3-6 MPa
Tensile strength, τ	0.5-2 MPa
Bending strength, σ_b	0.5-2 MPa
Shear strength, S	0.4-0.6 MPa
Water absorption	5-20 %
Damping coefficient, ξ	5-30 %
Coefficient of thermal expansion, α	0.010-0.015
Swell after saturation	0.5-2 mm/m
Shrinkage (due to natural air drying)	0.2-2 mm/m
Permeability	1.10-5 mm/s

4.5 Durability of CSEB

Studies have shown that the block will remain stabilised under fairly wet conditions also for long exposure times. Problems could arise first if the block reaches saturation level for a long time. CSEB could have a somewhat reduced strength in wet conditions (Riza, Rahman, & Zaidi, 2010). Humus in the soil should be removed since it can cause problems with stabilisation. The amount of unstabilised material in the block has a considerable impact on the durability of the block. Freeze and thaw has shown to cause no damage to CSEB (Maïni, Earthquake Resistant Buildings With Hollow Interlocking Blocks, 2005).

4.6 Sustainability of CSEB

The main sustainability advantage of CSEB compared to most material is that it often is a super local material. To many construction sites no transport is needed. The production process can be labour intensive which has less negative environmental impact compared to electricity or internal combustible engine driven productions. Compared to other brick materials it has both a lower energy consumption and pollution emission which can be seen Table 6.

Table 6. Energy Consumption and Pollution emissions of some brick materials (Maïni, Earthquake Resistant Buildings With Hollow Interlocking Blocks, 2005).

	Energy Consumption [MJ/m^2]	CO_2-emission [kg/m^2]
CSEB	110	16
Kiln Fired Bricks	539	39
Country Fired Bricks	1657	126
Plain Concrete Blocks	235	26

4.7 Quality of CSEB

A good block should have a uniform and regular shape, all angles should be straight. The blocks should not have any cracks or chips. All lumps and pebble sized fractions should be removed before compaction and the block should not contain any salts since it can damage the mortar surrounding the blocks in a wall (Maïni, Earthquake Resistant Buildings With Hollow Interlocking Blocks, 2005).

4.8 Reinforcement of CSEB

Reinforcement will add to the non-linear behaviour of a CSEB structure, in the uncracked state the contribution of the reinforcement is negligible (Anderson & Brzev, 2009). However, using horizontal reinforcement increases the ultimate shear resistance greatly. It also strengthens the out of plane behaviour and when connected to vertical rebars the wall elements become stiffer. Vertical reinforcement also helps the wall to resist tensile stresses perpendicular to the horizontal bed-joint. The reinforcement gives the structure a wanted box behaviour and in addition results in a more ductile behaviour which is generally sought in seismic design (this is further described in Chapter 6 Section 6.3) (Bakeer, 2009).

4.8.1 Reinforcement Bondage

The bondage between the rebars and the confining material is a keystone in the overall performance of a reinforced CSEB structure. The anchorage as well as the quality of the splicing of rebars depend on a good bondage. This field of research lacks a good assessment method for the bondage strength. The problem lies in the attempt to create a test that correlates well to reality since the conditions differ a lot from structure to structure (Park & Sungnam, 2012). In partially grouted CSEB the rebars are often directly confined by grout which is subsequently confined by units or blocks. This results in two possible main failure mechanisms. The first possible failure is slippage at the interface between rebar and grout and the second slippage at the interface between the grout and the surrounding blocks (Anderson & Brzev, 2009) (Bakeer, 2009).

5 Earthquake Effect on Structures

The vibrations of an earthquake do not kill people themselves. People are killed when structures collapse. The real cause of death could therefore be derived to poorly designed structures in combination with earthquakes (Maïni, Earthquake Resistant Buildings With Hollow Interlocking Blocks, 2005).

The forces induced by the earthquake will act on and displace the base of the structure. This creates a relative displacement to the top and will therefore create inertia forces in the structure. In this way the vibrations of the ground will be transferred up in the structure. The motions of the ground are cyclic and the dynamics of the structure have to be taken into account (Paultre, 2011).

5.1 Dynamic Response of a Structure

In contrast to a static problem there is not one single solution to a dynamic problem. To solve a structural dynamic problem it is necessary to calculate the displacement of the structure over time which in turn gives the dynamic response, also called displacement time history. The main difference of a static and a dynamic problem is not the time but the inertia forces, forces that counteract the applied dynamic loading. Dynamic problems can be treated as static only if the inertia forces are negligible compared to the applied loading. From the displacement time history it is possible to calculate the maximum dynamic response, the maximum values of forces, reaction and stresses needed for design purposes (Paultre, 2011).

5.2 Earthquake Loading

An earthquake is an arbitrary dynamic loading, it is as opposed to a periodic loading not cyclic and give cause to a large variation of acceleration over time. The earthquake load is applied at the base of a structure which induces a time variation of the inertia forces over the height of the structure (Paultre, 2011). Figure 12 shows a schematic representation of an earthquake load on a single degree of freedom system.

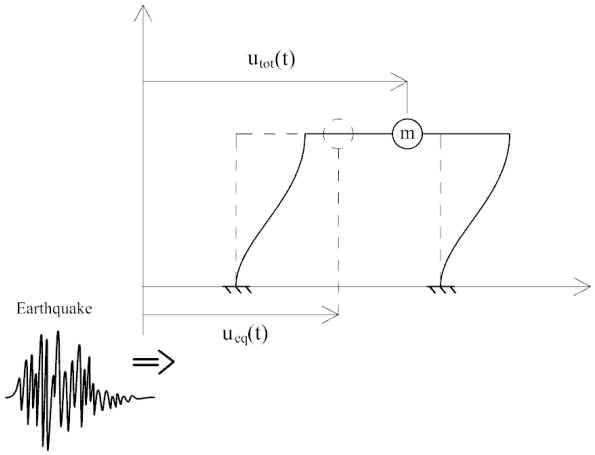

Figure 12. Schematic representation of an earthquake load on a single degree of freedom system.

5.3 Dynamic Motions of Structures

For the simplest of system, a single degree of freedom, the equation of dynamic equilibrium can be written as an differential equation of the time varying parameters displacement(u), velocity($\dot{u}$), acceleration($\ddot{u}$) and force(p) combined with the constants mass(m), damping(c) and stiffness(k):

$$m\ddot{u}(t) + c\dot{u}(t) + ku(t) = p(t)$$

If $p(t) = 0$ and the initial conditions are non-zero the solution of this equation is called the free response. The equation above could then also be written as:

$$\ddot{u}(t) + 2\zeta\omega\dot{u}(t) + \omega^2 u(t) = 0$$

where the damping ratio $\xi = \frac{c}{c_{cr}} = \frac{c}{2m\omega}$ and the angular frequency of motion is defined as:

$$\omega^2 = \frac{k}{m}$$

This frequency is also called the natural angular frequency and corresponds to the natural period as:

$$T = \frac{2\pi}{\omega}$$

If $\xi = 0$ the system is undamped and the solution will be:

$$u(t) = Acos(\omega t) + Bsin(\omega t)$$

In other words the system will continue to oscillate forever. In real life there are no undamped systems. Energy losses in the system will damp the motion. Depending on the amount of damping in the system the motion will be different. $\xi < 1$ is called subcritical damping and gives an oscillatory motion. $\xi = 1$ is called critical damping and $\xi > 1$ is called over critical damping and they both give non-oscillatory motions. Most structures have a damping ratio of between 0-0.2 giving an oscillatory motion. To determine the damping ratio is, in real life, difficult since it is not easily derived solely from the system's mechanical properties. Energy losses in structures are due to radiation, friction and fluid's resistance to motion which have complex energy dissipation mechanisms. The damping behaviour is for the sake of simplicity therefore simplified to a viscous damping in simple models. The damped angular frequency is defined as $\omega_d = \omega\sqrt{1-\xi^2}$ and for damping ratios between 0-0.2 the ratio $\frac{\omega_d}{\omega}$ is almost constant and equal to 1 why the damped angular frequency can be taken equal to the natural angular frequency (Paultre, 2011).

The behaviour of more complex structures cannot be reduced to a single degree of freedom system with one deformation mode. More nodes are needed to represent the deformation and behaviour of the structure adequately. A modal analysis is required where different modes describe the shapes which the structure naturally displace into. The displacement modes could be both longitudinal, rotational and translational. The response of such a system will be a combination of all modes oscillating at their natural frequency. When a mode is excited by a dynamic force of its natural frequency a resonance response is built up. The dynamic amplification at this frequency goes towards infinity but in real life this resonance will cause

plastic deformation in the structure, which changes the natural frequency, why the extreme values are never reached. Earthquake excitations are of multi-frequency why this full amplification also rarely gets time to build up. The earthquake response of a structure will instead be the combined effect of the energy at different frequencies and the natural frequencies of the different modes of the structure (Goswami, Mehta, Murty, & Vijayanarayanan, 2012).

5.4 Inelastic and Elastic Response

Any structure has a limit in elastic displacement. When this is exceeded the structure deform inelastically. The inelastic response of the structure is thought to soften the structure and thereby increase the period and the displacement but at the same time yielding materials in the structure are dissipating energy which increases the damping of the structure and decreases the displacement (Bakeer, 2009).

5.5 Damages on Masonry Structures during Earthquakes

When a building has suffered total collapse it is difficult to tell what failure mechanism that led to the collapse. But when inspecting structures that have withstood an earthquake many typical damages can be seen (Maïni, Earthquake Resistant Buildings With Hollow Interlocking Blocks, 2005). In this section some common damages are treated.

5.5.1 Damages to Walls

The ground motion during an earthquake can make a wall segment fail in various ways, both in-plane and out of plane failures exist. Cracks in walls of different size, direction and length can cause a total collapse of a wall or a partition of a wall. (Anderson & Brzev, 2009)

5.5.2 In-Plane Failure of a Wall

A reinforced masonry wall will be subjected to axial and shear forces but also bending moments simultaneously. The performance of a shear wall is influenced by the degree of the axial stresses, the dimensions of the wall, the material properties, the amount and distribution of vertical and horizontal reinforcement. The failures of a masonry wall are often located in between openings of a facade, such as doors and windows, where the shear resistance is reduced. These areas are called piers and spandrels (see Figure 13) (Anderson & Brzev, 2009).

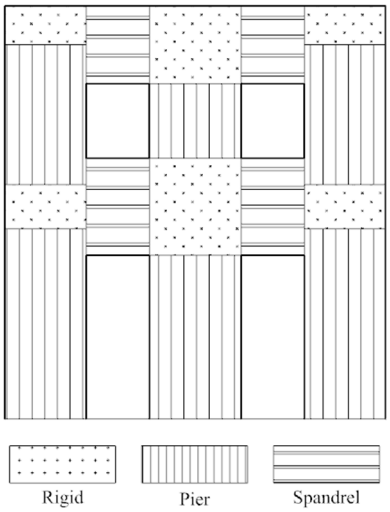

Figure 13. Visualization of division of rigids, piers and spandrels of a wall section.

Typically a masonry brick wall has three failure modes in the in-plane direction. Two of them are due to the shear stresses and the third is due to the overturning moment combined with axial stresses (see Figure 14). The first and the second failure modes are common in masonry buildings subjected to horizontal loads and can often be observed in areas where earthquakes have struck. A cause of failure with regard to the third mode is when the anchorage length or the splicing is insufficient when subjected to tension. This will lead to degradation of the strength of the wall and can eventually lead to failure if the stresses are large enough (Tomaževič, 2009).

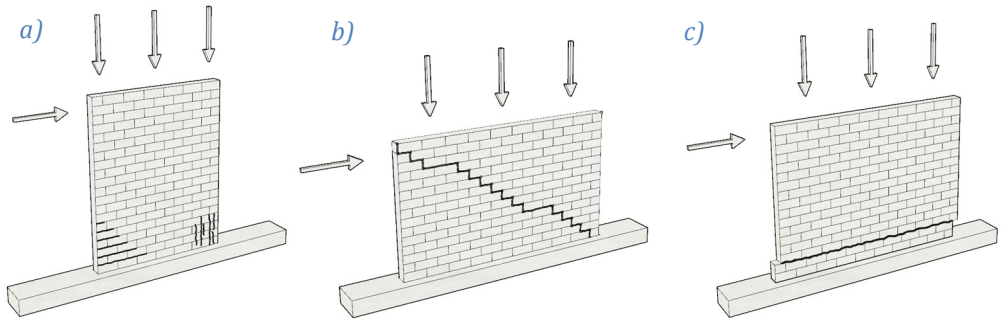

Figure 14. a) The stresses from the acting moment together with the axial stresses can cause both crushing of the masonry and tensile cracking. More common when height/length ratio is high. b) Diagonal shear failure in tension leading to cracks either within the units or along the joints. More common when height/length ratio is low. c) Horizontal cracks due to sliding along the horizontal joints between units or a unit and a bed joint. Common when there is a low compressive stress and the mortar is weak. Usually it occurs close to the bed joint (Tomaževič, 2009).

5.5.3 Out of Plane Failure of a Wall

Horizontal loads acting in the perpendicular direction of a wall are causing out of plane action. Out of plane failures are more likely to happen in multi-storey buildings since the accelerations are larger. The ground motions of an earthquake can cause an overturning moment called toppling which is usually prevented with good connections to a diaphragm. The wall can bend in both a vertical way where the floors/roof provide support but also in a horizontal way where cross walls or pilasters provide support (see Figure 15). A sufficient amount of reinforcement, vertical and horizontal, is needed to withstand the expected bending moments (Anderson & Brzev, 2009).

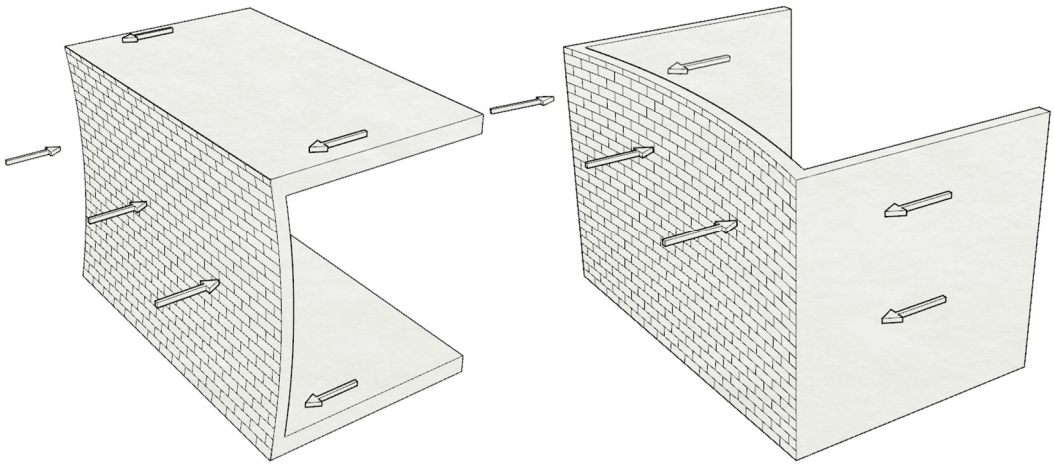

Figure 15. The two types of out of plane failure modes of a wall.

5.5.4 Damages to Roof and Floors

A poorly constructed roof can lead to damages such as dislocation of roof members (trusses, purlins or other beams) that can, if dislocated enough or if the connections are weak, lead to collapse of the roof. If not connected properly, smaller elements of the roof such as railings, cornices, chimneys or roof tiles can fall off the roof and in that way be a danger to people on the ground. Floorings in multi-storey buildings that are not properly connected to the walls can easily collapse when shifted away from its supports.

5.5.5 Damages to the Foundation

The ground motions of an earthquake can cause movement of the soil around the foundation that can lead to sinking, tilting, or cracking of the foundation. The damages to the foundation will, in turn, affect the rest of the structure by inducing stresses (Shrestha, 2012).

5.5.6 Pounding

Pounding is a well-recognized phenomena in seismic design. When two buildings are located close to each other with different dynamic characteristics they oscillate differently and hammer onto each other which causes structural damages. This problem is avoided by introducing a sufficiently large separation gap between two buildings (Sharma, 2008).

6 Design for Earthquake Resistance with CSEB

The design for earthquake resistance includes some basic building techniques that have proven to work well. CSEB structures are relatively heavy constructions and will therefore generate large inertia forces when subjected to seismic action. These structures are prone to cracking because of their many joints between CSEB units and mortar but also due to the brittle property of the material. In order to keep the structure safe a thoughtful design that utilizes the different materials of the structure in the right way is necessary (Murty).

6.1 Symmetry

During an earthquake the movements of the mass of a structure cause inertia forces. Therefore the centre of mass and the centre of rigidity should coincide. This is achieved by a symmetric building in both plane and elevation. In a plan view the outer walls should be as symmetric as possible and if it has the shape of a rectangle the proportion of short and long side should not exceed 1:3. If the building has an elongated shape it should be divided into smaller boxes with rigid inner walls or buttresses that can provide resistance in the vulnerable direction. The in plan symmetry also regards the orientation of shear walls to avoid a rigidity centre that is shifted to far away from the centre of mass (see Figure 16). Elevation symmetry refers primarily to openings such as doors and windows that should be placed as symmetric as possible but it also concerns the structure of the roof. In buildings with several floorplans a constant thickness of the exterior wall is recommended. Floors should act as one rigid unit to enable the distribution of loads to the load resisting members of the structure (Åstrand, 1994) (Maïni, Earthquake Resistant Buildings With Hollow Interlocking Blocks, 2005).

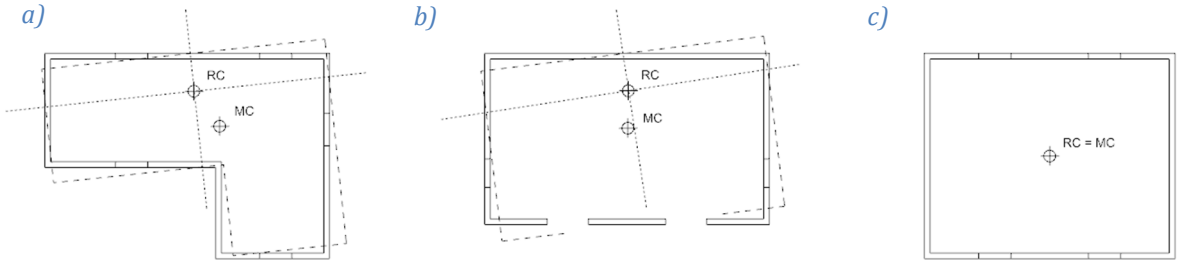

Figure 16. Illustration of torsional effects due to different positions of the centre of mass and the centre of rigidity. a) The shape of the building creates a shifted position of the two centres. b) Here the shape of the building is proper, however the openings of the building is focused to one side which causes weaker shear walls in this area. The result is a rigidity centre that gets shifted to the opposite side whilst the centre of mass remains rather close to the geometrical centre. c) A symmetric shaped building with symmetrically placed openings lead to a coincided centre of rotation and mass which is desirable.

6.2 Ductility

The structure should have a design for ductility. The ductility of a structure is a measurement of the capacity of the structure to displace inelastically. The ductility ratio describes the amount of damage the structure can take without collapsing and is defined as:

$$\mu_{\Delta} = \frac{\Delta_u}{\Delta_y}$$

Where Δ_u is the nonlinear displacement and Δ_y is the displacement at yielding. When a force exceeds the elastic region a nonlinear deformation starts. Creating ductility in the design means that the structure should sustain large deformations without a brittle collapse (Bakeer, 2009).

6.3 Box Behaviour

Depending on the direction of an earthquake some structural elements are be weakened while other elements remain stronger. A good performance structure should be able to, in the greatest extent possible, take advantage of the strong elements. Good horizontal connectors between the different structural elements enable utilization of all elements and make them work together. This design approach is called box behaviour and helps the structure to act as one big rigid unit. An example of this can be seen in Figure 17 where wall segments A1 and A2 are acting in their strong direction. Wall segments B1 and B2 are acting in their weak direction and need support from wall A1 and A2. If the earthquake would act in a perpendicular direction the relation would be the opposite. This transfer of loads requires sufficiently rigid connections at the corners. Therefore, many building codes such as the Indian Standard 4326:1993 prescribes minimum distances for openings to corners and other junctions, this is to ensure the rigidness of these connections (Murty).

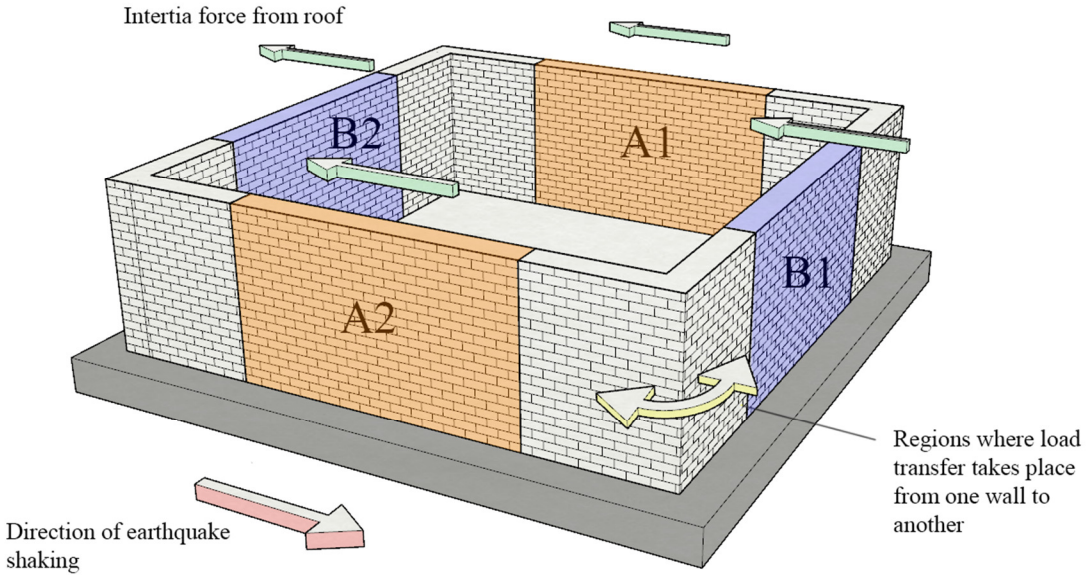

Figure 17. Example of force transfer from weak walls to strong walls in a CSEB building.

6.3.1 Shear Walls

Shear walls play a big part in resisting horizontal forces. They can be of different lengths and material. To enhance the box behaviour of a structure, shear walls should be present in all exterior walls and placed as symmetric as possible. If necessary, inner walls can also be constructed as shear walls which should also be designed symmetrically. The strength of the shear wall is along its length, i.e. in-plane, and has considerably less strength in the normal plane of the wall. From the connections to horizontal elements, loads are transferred to the shear walls that will result in uplift forces and shear forces that the wall has to resist. Obviously, if the stresses are too high, the wall fails (Anderson & Brzev, 2009).

6.3.2 Tie Beams

A good way to ensure the box behaviour is via steel reinforcement embedded in concrete. Both vertical and horizontal rebars will help achieving the wanted behaviour. In CSEB structures it could be difficult to place horizontal reinforcement. A good solution is to make tie bands where horizontal rebars are placed in either hollowed out CSEB units or in casted concrete beams (Maïni, Earthquake Resistant Buildings With Hollow Interlocking Blocks, 2005). It is advisable to place tie bands at several levels. There are usually four types of tie bands in a one floor masonry building: plinth beam, sill beam, lintel beam and top beam. In Figure 18 the construction of a tie beam at sill level is shown. The plinth beam is casted directly on the foundation. The sill beam is located right under the windows and is interrupted when doors are present. The lintel beam is casted right above doors and windows and is probably the most important beam of the four. It acts as a support for walls loaded in their weak direction and strengthens the stability by reducing the unsupported height of the wall. At the top of the wall the top beam is found. Also, when a building has a pitched roof an inclined gable beam should be used (Murty, Why are Horizontal Bands necessary in Masonry Buildings?). The bands reduce the length of cracks by restricting them to be in between the tie beams (LIU & Wang, 2000).

Figure 18. The construction of a tie beam at sill level in Majhi Gaun.

6.3.3 Diaphragms

A diaphragm is a horizontal structural member which design purpose is to transmit lateral loads to vertical load resisting elements e.g shear walls or frames. Typical diaphragms are floors and roof structures that contribute to the box behaviour by tying structural members together to make the structure act as one entity during an earthquake. It is very important for diaphragms to remain in an elastic state to fulfil their purpose of transferring the loads to other elements that may yield (RangaRajan, 2016).

Diaphragms are distinguished as rigid or flexible. There are different ways of dividing them into these two categories. Eurocode 8 provides one definition where the maximum horizontal displacement of the diaphragm cannot exceed more than 10 % of a corresponding absolute rigid

body's displacement to be considered rigid. A rigid diaphragm is assumed to distribute the lateral loads to resisting elements in direct proportion to their stiffness which will lead to equal displacement of the vertical elements. A typical rigid diaphragm is the reinforced concrete slab. As opposed to rigid diaphragms a flexural diaphragm is limited in distributing torsional and rotational forces and can in a less extent distribute the lateral loads in proportion to the stiffness of the vertical elements. Simple roof structures and timber floorings are examples of flexural diaphragms (RangaRajan, 2016).

6.4 Roof Structure

The symmetry rule applies also for the roof structure. The preferred shape is the four pitched roof that possesses double symmetry: in both plan and elevation. A desired feature when designing a roof structure is to make it act as one rigid diaphragm in order to distribute lateral loads to the stiff vertical elements of the structure. In order for this transition of loads to work the connections between roof and wall elements need to be rigid (Åstrand, 1994). A lightweight roof construction will decrease the seismic weight and therefore also reduce the inertia forces (Reid, u.d.). Concerning the roof cladding it is preferable to use larger elements like sheeting of metal or plastic instead of using smaller elements like tiles that more easily can fall down when not properly anchored to the roof structure (Åstrand, 1994).

6.5 Other Design Aspects of CSEB in Nepal

In addition to a few already covered topics such as symmetry and structural layout the *Auroville Earth Institute* and the Ministry of Education in Nepal have composed some guidelines that are based on the Indian Standard 1905:1987 for other aspects that are important when designing CSEB buildings with regard to earthquakes.

6.5.1 Max Heights/Wall Thicknesses

The thickness of walls should not be less than 200 mm and the height is limited to 3 m for each storey of the building (Shrestha, 2012).

6.5.2 Openings

According to *Auroville Earth Institute* the total amount of openings in a structural wall for a one storey CSEB building should not exceed 50 % of the total length of the wall. This ratio decreases with the number of floors in a building. As was discussed in Chapter 6 Section 6.3. they also recommend a distance from an opening to an adjacent corner not shorter than 25 % of the height of the opening (Maïni, Earthquake Resistant Buildings With Hollow Interlocking Blocks, 2005).

6.5.3 Buttresses

For a wall to be able to resist the bending moments induced by the ground motions the measurement of the wall has to be of reasonable length. A good way could be to divide the wall into shorter segments by using either cross walls or buttresses. A rule of thumb that is suggested by *Auroville Earth Institute* is that a wall segment longer than eight meters should be supported in at least one of these two ways (Maïni, Earthquake Resistant Buildings With Hollow Interlocking Blocks, 2005).

6.5.4 Foundation

It is advisable to use the same type of foundation throughout the whole building. Mixing foundation types can easily lead to settlements. Isolated foundations e.g. footing foundations for each column should therefore be avoided and instead trench foundations are advisable to use (Maïni, Earthquake Resistant Buildings With Hollow Interlocking Blocks, 2005).

A reinforced concrete strip footing is the most effective solution but masonry footings are much more common in Nepal. A depth of 750 to 900 mm below ground level is necessary for the footing to get under the weathering zone. In special cases when surrounded by unstable soil the depth needs to be even larger. Moreover, the width of the footings have to be wide enough to sustain the pressure from the superstructure. In one storey buildings 750 mm is set as a recommendation and this measurement increases with the number of floors (Shrestha, 2012).

7 Dynamic Analysis of Structures

A dynamic analysis of a structure could be divided into three basic steps. First an analytical model has to be set up. Based on the structural drawings, the parameters that affect the dynamic behaviour should be found. Thereby the simplifications that could be made are decided. In this step the damping characteristics, the mass distribution, the stiffness and the boundary conditions should be defined (Paultre, 2011).

In the next step a mathematical model should be created. In the finite element method differential equations derived from the laws of physics are used. The number of dynamic degrees of freedom needed to represent the behaviour of the structure should also be determined in this step. For a static structural system the number of degrees of freedom is the number of separate displacement coordinates needed to describe the displaced or deformed shape of the structure. To represent the effects of the inertia forces of a dynamic problem *dynamic degrees of freedom* are to be used. The effect of local variations of deformation on the nodal displacement that control the inertia forces are the reason to why fewer degrees of freedom are usually needed for a dynamic model than for a static. Concentrating the masses at a given number of nodes gives a discrete system. This could simplify the model since then the response is only defined at these point. The number of masses needed are as many as needed to represent the behaviour of the structure adequately. Creating a system of concentrated masses will simplify the calculations but the approach requires extensive experience when the structures are complex. To verify and calibrate a created model a dynamic test can be used in order to confirm calculated natural frequencies and damping values. Finally, as a last step, the time history response should be calculated from the differential equations and the finite element model (Paultre, 2011).

7.1 Modal Analysis

By using the global mass and stiffness matrices of a structure it is possible to solve the equation of motion as an eigenvalue problem to find the natural frequencies of the different vibration modes (Ewins, 1984). The equation of motion of a MDOF undamped system can be written as:

$$M\ddot{u} + Ku = 0$$

Knowing that the motion of a discrete system can be harmonic the displacement vector can be written as:

$$u(t) = \phi\cos(\omega t - \Theta)$$

where ϕ represents the possible deformed shapes that are constant in time and Θ the phase angle. The acceleration can then be written as:

$$\ddot{u}(t) = -\omega^2 u(t)$$

since the equation must be valid for all t which means all values of the cosine term the equation can be rewritten as

$$K\phi = \omega^2 M\phi$$

which is a generalized eigenvalue problem and can be written as a standard eigenvalue problem ($Ax = \lambda x$):

$$M^{-1}K\phi = \omega^2\phi$$

or

$$[K - \omega^2 M]\phi = [K - \lambda M]\phi = 0$$

All solutions with a non-zero motion can be found by what is called the *Characteristic Equation* of the system:

$$\det(K - \omega^2 M) = \det(K - \lambda M) = 0$$

Expanding the determinant for an n-degree of freedom system will form a polynomial equation of n degrees with n solutions to λ. The roots of these solutions gives the natural angular frequencies of the system $\lambda_n = \omega_n^2$ and are all giving a certain mode shape (Paultre, 2011).

7.2 Methods for Seismic Analysis

In this part the most widely used seismic design methods are introduced and described.

7.2.1 Equivalent Static Method

As mentioned in Chapter 5 the ground motions of an earthquake are cyclic. The dynamics should therefore be taken into account. However, for a fairly regular, simple and low-rise structure it is, according to most codes, sufficient to represent the dynamic load by an equivalent static horizontal load. The first mode is in this method assumed to dominate the dynamic response and the response is assumed to be linear. The equivalent static load is proportional to the mass of the structure (Koboevic, 2015). Site considerations, type of load-bearing system and type of building are usually also taken into account. The analysis should be performed in the two main directions of the building. The exact prescribed methodology of the method varies from code to code but the main principle is to express the base displacements of the structure during an earthquake as one base shear force. It is in many codes possible to account for accidental torsion. Accidental torsion is not to be confused with the torsion from geometrical asymmetry. Accidental torsion can arise for various reasons: uneven distribution, presence of non-structural members in the building, uneven live-load distribution etc. (Council Building Seismic Safety, 2016).

The *Equivalent Static Method* is sometimes also referred to as the *Lateral Force Method* and in *NBC 105:1994* it is called the *Seismic Coefficient Method*.

7.2.2 Modal Response Spectrum Method

The *Modal Response Spectrum Method* is a linear statistical analysis method. In contrast to the *Equivalent Static Method* it calculates the contribution of each natural mode of the structure. This method gives a better representation of the dynamic behaviour of the structure and could also be used on more complex structures. In the calculation of seismic action this method relates the response spectra of the ground motions at a certain location to the response spectra of different types of structures. This method take into account that the response of a structure is a

function of both frequency content of the ground motion and the dynamics of the structure itself. Based on time-histories of different earthquakes a smoothened response curve is developed describing the maximum acceleration and velocity of displacement for time periods of a SDOF system. For a MDOF system there are different mathematical methods of calculating the combined peak response of all modes, the most commonly used are: the *Absolute Sum Method*, the *Square Root of Sum of Squares Method* and the *Complete Quadratic Combination Method* (Jangid, 2013).

There are methods to extend the *Modal Response Spectrum Method* to, in a simplified way, represent the nonlinear response as well. These methods requires a nonlinear load-deformation relation (Villaverde, 1988).

7.2.3 Time-History Response Method

The inelastic response of the structure is of great importance for the seismic resistance of a structure. This nonlinear response is only possible to analyse through integration of the equation of motion at each time step (Villaverde, 1988). The *Time-History Response Method* requires the full accelerograms of a design earthquake. By step-by-step integration the *Time-History Response Method* can express the internal forces of a structure as a function of time for a specific ground motion. This method is more time consuming and costly than the *Modal Response Spectrum Method* (Music, 2016). However, there are numerical ways of performing the calculations more efficiently such as the *Central Difference Method*, the *Newmark Method* and the *Wilson-θ Method* (Paultre, 2011).

7.3 Digital Signal Processing of Dynamic Testing

In dynamic testing a critical step is digital signal processing. In order to get any valuable information from the accelerogram of a dynamic modal testing the raw data should be processed. Some standard methods of processing data are given in this section.

7.3.1 Fast Fourier Transform

A *Fourier Series* is an expansion of a periodic function expressing it in terms of sines and cosines. By taking advantage of the mutual orthogonality of a sine and a cosine function it is possible to express any periodic function as an infinite number of sine and cosine functions. It is then also possible to solve any operation for each term individually (Weisstein, 2016). The *Discrete Fourier Transform* is an extension of the *Fourier Series* valid for any periodic function which is defined only at *N* discrete points at t_k and $k = 1, N$. Any such function could then be represented by a finite series. The *Discrete Fourier Transform* will thereby reveal any periodicity of an input signal and could be used to transfer an input signal in the time domain to the frequency domain (Ewins, 1984). In the *book Modal Testing: Theory and Practice* (Ewins, 1984) the *Discrete Fourier Transform* is written as:

$$x(t_k)\ (=\ x_k) = \sum_{n=0}^{N-1} X_n e^{2\pi i n k/N}$$

where:

$$X_n = \frac{1}{N}\sum_{k=1}^{N} x_k e^{-2\pi i n k/N}$$

n = 1, N

Finally the *Fast Fourier Transform* is a computationally efficient algorithm to estimate the *Discrete Fourier Transform* (Mathworks, 2016).

7.3.2 Averaging

It is advisable to perform an averaging process of a number of individual time records. By using an average from a number of tests will increase the reliability of the result. The response that is measured in each time-history will be clarified whereas the response that fluctuate each time will be averaged out (Ewins, 1984).

7.3.3 Anti-Aliassing

This phenomena has to do with the relation between frequency and the sampling rate. For instance, if the frequency is high and the sampling rate is relatively low the real frequency can be misinterpreted as a lower one because the samples of the real curve accidently generates an imaginary frequency see Figure 19. To avoid this occurrence filters can be used to exclude the undesirable frequencies. The influence of aliassing is strongest near the *Nyquist frequency*. The *Nyquist frequency* is half of the sampling rate and is also known as the folding frequency. The highest digital signal that can be reproduced is according to the *Nyquist Theorem* half of the sampling rate (Ewins, 1984).

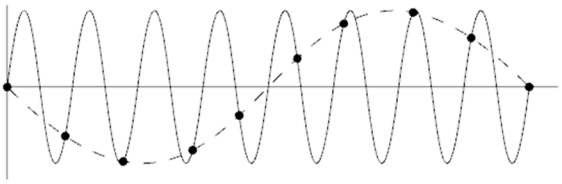

Figure 19. Illustration of misinterpretation of signal due to sampling rate.

7.3.4 Leakage and Windowing

When using only a finite length of a time-history with the assumption of periodicity a leakage problem could arise. If the signal is not perfectly periodic in the time window used some of the energy leaks into other frequencies when using the *Discrete Fourier Transform*. A simple case of this problem is described in Figure 20. A solution to this could be to adjust the time window prior to using the *Discrete Fourier Transform*. For a transient impact load, where the most important information is in the beginning of the time-history, it could be useful to use an exponential window see Figure 21 (Ewins, 1984).

a)

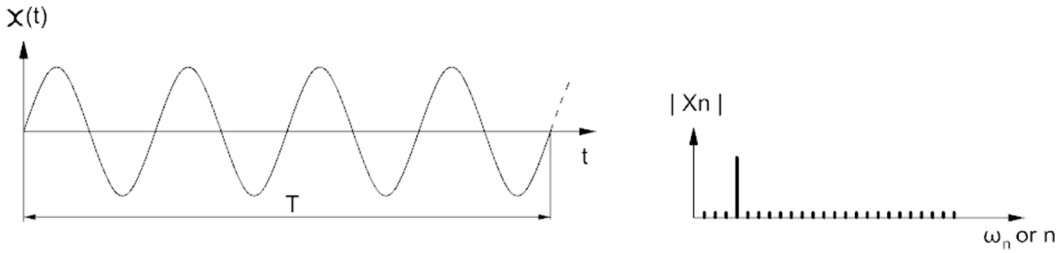

b)

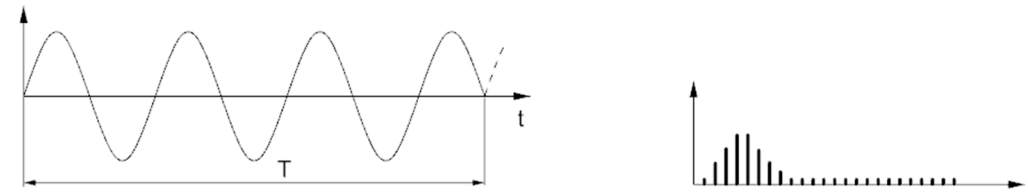

Figure 20. Illustration of Leakage problems and effects of Leakage. a) A perfectly periodic function b) A non-periodic function.

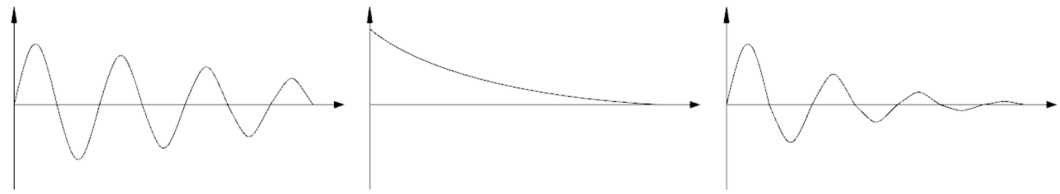

Figure 21. Illustration of the effects of an exponential window on a transient load.

8 Modelling of Masonry and CSEB

Numerical modelling of masonry is complex, it is difficult to compile a generic model that has sufficient experimental data to be justified. Experimental data is needed for numerous parameters affecting the cracking pattern and the stiffness redistribution. The interaction of concrete, CSEB and mortar is also difficult to properly represent since it will vary with both the specific material compositions and the craftsmanship of the mason. There are no well-established ways of determining the support conditions of the masonry joints why this is another uncertainty (Lourenço, Rots, & Blaauwendraad, 1995). Numerical modelling of masonry, and thereby CSEB, can be divided into two main categories: macro and micro modelling. The difference between the two approaches is the precision and the interpretation of the uniformity of the masonry, whether to consider it homogeneous or heterogeneous. In lack of enough detailed knowledge the homogenous approach is advisable (Bolhassani, Hamid, Lau, & Moon, 2014).

8.1 Macro Modelling

In a homogenous approach the mortar joints and units are smeared together into one simplified uniform material using the average properties of the initial materials. The behaviour of the homogenous material can either be isotropic or anisotropic. This method is practical to use when analysing the overall behaviour of a masonry structure but is not sufficient to determine what will happen on a more detailed local level (Bolhassani, Hamid, Lau, & Moon, 2014).

8.2 Micro Modelling

The micro modelling approach is considered to be very difficult since there are an immense number of parameters to take into account when considering the material to be heterogeneous. Micro modelling is usually divided into simplified and detailed. The detailed modelling takes all the characteristics of masonry into consideration and should predict the real behaviour. This is very time consuming on larger structures since the number of elements and nodes increase intensively. In order to, in some extent, simplify this one way is to model the mortar as an interaction condition and to formulate a cracking condition at the interface that takes the mortar properties into account (Bolhassani, Hamid, Lau, & Moon, 2014).

9 Description of the CSEB Building in Majhi Gaun

The building is located on a slope of a hill side in the village Majhi Gaun, 30 kilometres northeast of Kathmandu in the Sindhupalchok province (see Figure 22). This building was designed as a three room building but with the possibility to build a fourth room which would offer prospects for the future to the family living in the house.

Figure 22. CSEB building in Majhi Gaun before and after painting.

The construction site was excavated in order to get a flat surface to build on and an adequately stable soil. The building was built on a foundation of stone block-cement-mortar with a reinforced concrete strip for anchorage of the vertical rebars (see Figure 23). On top of the plinth beam the first layer of the CSEB were placed. In the building in Majhi Gaun a hollow interlocking block with the dimensions 300x150x115 mm^3 was used (see Figure 25 a). All hollow sections of the CSEB were grouted with concrete and all corners also have vertical steel reinforcement all the way to the top (HYSD with yield stress of 415 MPa and permissible stress of 230 MPa). Steel reinforcement was also placed on each side of every opening and in the span of the long wall sections as described in the reinforcement drawing (see Appendix A.2). The building has additional reinforced concrete tie-beams at sill, lintel and top level. The configuration for the sill level is given in Appendix A.2. The tie-beams are connected with vertical reinforcement at crucial points such as corners and next to doors and windows. Finally steel profiles are casted in the concrete beams at the top of the building. These profiles support the corrugated steel used as roof cladding. The plan drawing is shown in Figure 24 and the section drawings of the building are given in Appendix A.1.

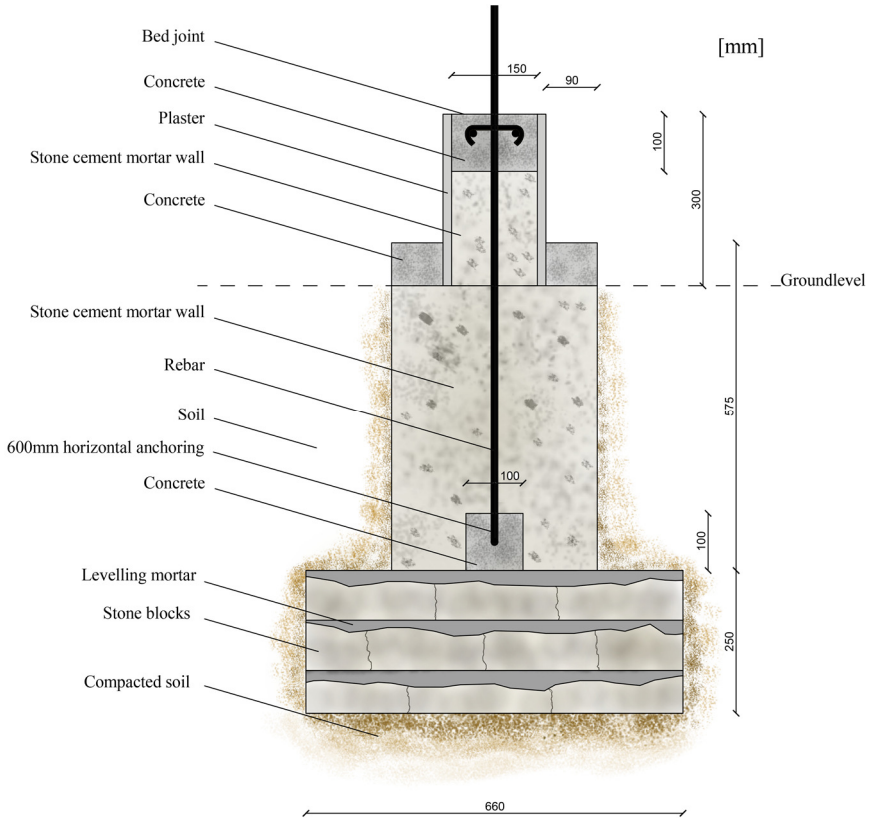

Figure 23. Detailed drawing of the foundation.

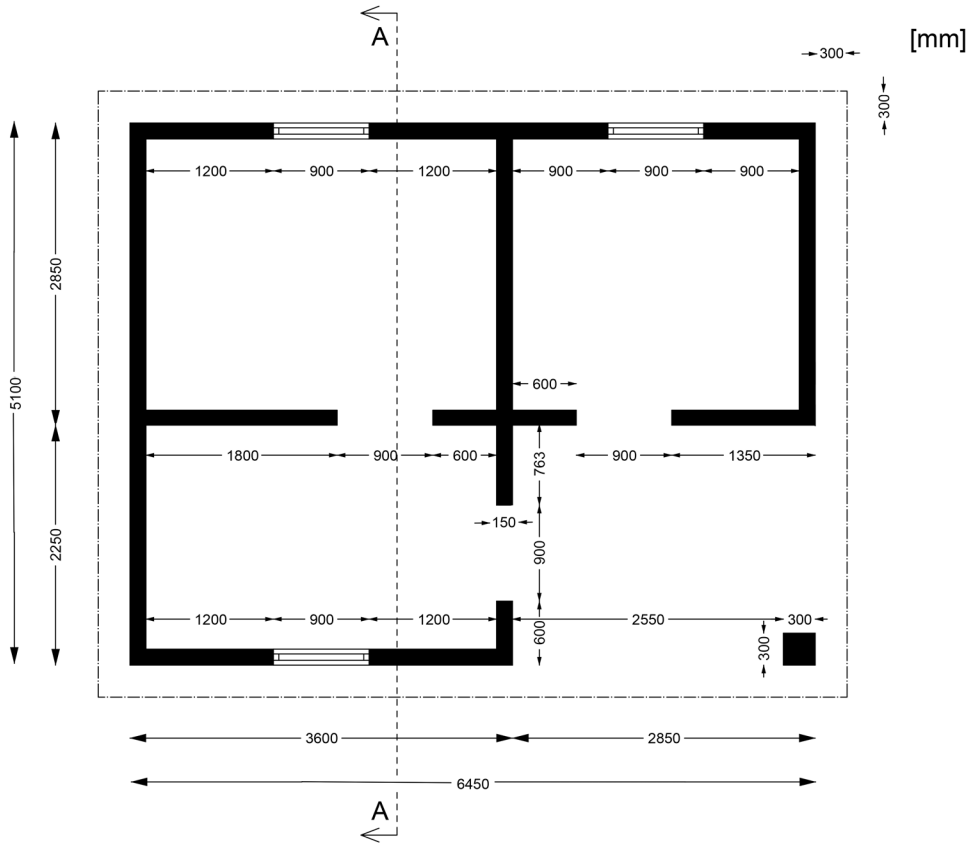

Figure 24. Plan drawing of building in Majhi Gaun.

10 Testing of CSEB Material Properties

Build up Nepal has focused on two types of blocks that are used in their buildings. In the building in Majhi Gaun a hollow interlocking block with the dimensions 300x150x115 mm^3 was used (see Figure 25 a). For larger buildings such as school projects a larger block with the dimensions 240x240x90 mm^3 is used (see Figure 25 b). The larger block has cut outs at the edges in order to make room for steel reinforcement. These blocks are also produced with a machine providing a higher degree of compaction. *Build up Nepal* tries to produce blocks with the ideal soil composition described in Chapter 4 Section 4.3 and a cement content of 10 % is used.

a) *b)*

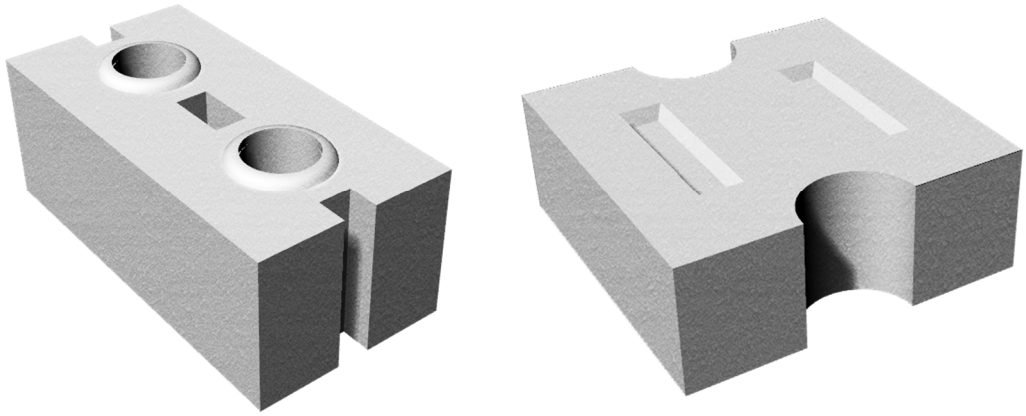

Figure 25. a) The Hollow Interlocking block used by Build up Nepal. b) The 240x240x90 mm^3 block.

10.1 Testing Methodology

In Chapter 4 Section 4.4 literature values of the material properties of CSEB were given and as described in Chapter 1 section 1.1 the material properties of CSEB differs a lot dependent on the composition, proportions and production method. In order to find the actual ranges of the density, Young's Modulus, the compressive and the tensile strength for the CSEB produced by *Build up Nepal* and the CSEB used in the building in Majhi Gaun these properties were tested in field. 20 hollow interlocking blocks used in Majhi Gaun and 12 other blocks with the dimensions 240x240x90 mm^3 were tested. The 12 blocks with the dimensions 240x240x90 mm^3 had varying composition, proportions and production methods, the purpose of this was to investigate the influence of these aspects on the CSEB. The testing methodologies of these tests and the results are given in this chapter.

10.1.1 Ultrasonic Wave Testing of Young's-modulus

An ultrasonic pulse velocity test is a non-destructive test that can be performed in field measuring the velocity of a P-wave in the material. Since the velocity of a P-wave in a solid material depends on the elastic properties and the density of the material it is possible to calculate Young's-modulus. The following formula describes the relationship between Young's-modulus, the density, the Poisson's ratio and the velocity of the P-wave (Panzera, Christoforo, Cota, Borges, & Bowen, 2011):

$$E = \frac{(1+\nu)(1-2\nu)}{(1-\nu)}\rho V_p^2$$

10.1.2 Compressive and Tensile Strength Testing

A destructive strength test was performed on both the hollow interlocking blocks used in Majhi Gaun and on the blocks with the dimensions 240x240x90 mm^{3}. A field block tester from *Auroville Earth Institute* was used, a drawing of the block tester is shown in Figure 26. As can be seen in Figure 26 a lever arm is used to decrease the required load to break the block. It is also important that the field tester has a proper counter-weight. From the results of a three point bending test the compressive and tensile strength were calculated by formulas derived by *Auroville Earth Institute* (Maïni, Production and Use of Compressed Stabalised Earth Blocks, 2010). The force applied on the block is given by:

$$F = (load\ on\ plate + load\ of\ plate) * L_e \qquad [\text{kg}]$$

The compression strength conversion formula is given by:

$$\sigma_c = \frac{F * L}{1.56 * W * H} * \sqrt{1 + \frac{L^2}{4 * H^2}} \qquad [\text{kg/cm}^2]$$

The tensile strength conversion formula is given by:

$$\sigma_t = \frac{3 * F * L}{2 * W * H^2} \qquad [\text{kg/cm}^2]$$

Where L is the distance between supports, L_e is the length of the lever arm, W is the width of the block and H is the height of the block.

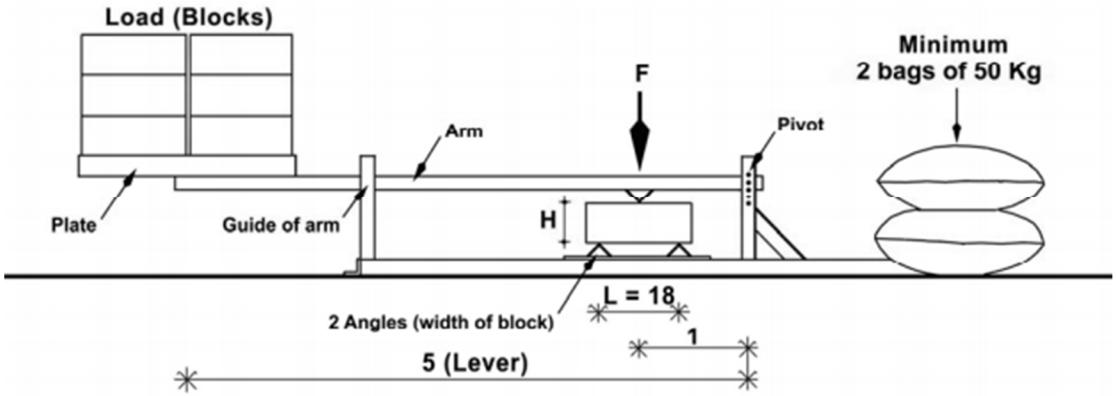

Figure 26. Drawing of field block tester used in the destructive strength tests (Maïni, Production and Use of Compressed Stabalised Earth Blocks, 2010).

10.2 Testing of Young's Modulus and Density of CSEB used in Majhi Gaun

Two standard 54 kHz transducers and a Pundit Lab were used to measure the velocity of a P-wave in 20 different blocks in Majhi Gaun (see Figure 27)**.** The blocks were taken from two different production occasions including various different batches of each occasion. The blocks were to be used in the final parts of the first CSEB building. The blocks were weighted in order to calculate their density. The value for Poisson's ratio was assumed to be 0.25 with reference to Table 5. The cement content was supposedly around 10% in the Majhi Gaun CSEB why the Poisson's ratio was assumed to be in the upper range of the values given in Chapter 4 Section 4.4.

Figure 27. Ultrasonic Pulse velocity test with a Pundit lab and two 54 kHz transducers in Majhi Gaun.

10.2.1 Results of Test

Table 7 shows the calculated values of Young's-modulus for the 20 blocks. The table shows that Young's-modulus of the CSEB in Majhi Gaun ranged from 1.63-4.91 GPa, with an average value of 2.74 GPa. The density ranged from 1470.6-1719.5 kg/m^3 with an average of 1548 kg/m^3.

Table 7. Results for the 20 tested blocks.

Block	Density	P-Velocity	Poisson's ratio	Young's Modulus
	[kg/m^3]	**[m/s]**	**-**	**GPa**
1	1583.7	1654.7	0.25	3.61
2	1538.5	1419.8	0.25	2.58
3	1470.6	1228.7	0.25	1.85
4	1583.7	1597.2	0.25	3.37
5	1538.5	1432.1	0.25	2.63
6	1470.6	1273.6	0.25	1.99
7	1470.6	1466.8	0.25	2.64
8	1583.7	1666.7	0.25	3.67
9	1629.0	1608.4	0.25	3.51
10	1696.8	1782.9	0.25	4.50
11	1719.5	1851.9	0.25	4.91
12	1538.5	1312.8	0.25	2.21
13	1583.7	1315.8	0.25	2.28
14	1538.5	1127.5	0.25	1.63
15	1515.8	1321.8	0.25	2.21
16	1493.2	1382.2	0.25	2.38
17	1493.2	1357.7	0.25	2.29
18	1538.5	1280.6	0.25	2.10
19	1493.2	1360.9	0.25	2.30
20	1493.2	1283.5	0.25	2.05

10.3 Test of Young's Modulus and the Density of Various CSEB

In this test the larger blocks with the dimensions 240x240x90 mm^3 were used. In order to find the influence of the soil composition, the proportions of cement and the production method of CSEB tests of various types of CSEB were performed. In order to test the influence of the composition on the performance of the CSEB three different mixes were prepared. The blocks in Test 1 had a mixture which was intended to represent the ideal composition presented in Chapter 4 Section 4.3. In Test 2 a mixture with the same soil composition as in Test 1 was used but the proportion of cement was less. In Test 3 the soil composition had an increased amount of sand and gravel. In addition to the three tests of different mixes a fourth test was performed to investigate the influence of the curing process. In Test 4 the blocks were not watered sufficiently and thereby not cured properly. This test was performed on the same type of mixture as in Test 1 Table 8 gives the composition of each test.

Table 8. Proportions of water, cement and soil and composition of the soil used in the four tests.

	Proportions:	Composition of Soil:
Test 1 (Ideal)	1 water : 1 cement : 8 soil	35 % silt and clay 65 % gravel and sand
Test 2 (less cement)	1 water : 0.5 cement : 8.5 soil	35 % silt and clay 65 % gravel and sand
Test 3 (more coarse)	1 water : 1 cement : 8 soil	25 % silt and clay 75 % gravel and sand
Test 4 (poorly cured)	1 water : 1 cement : 8 soil	35 % silt and clay 65 % gravel and sand

In total 12 blocks were produced: three for each test. All blocks were, after compression, placed on a metallic sheet with minimum exposure to sunlight and covered with a plastic sheet. They were all watered sufficiently except the blocks of the fourth test. They were weighed and an ultrasonic pulse velocity test was performed after three weeks of curing. Two standard 54 kHz transducers and a Pundit Lab were used to measure the velocity of a P-wave in the 12 blocks.

10.3.1 Results of Test

Table 9 shows the density and the calculated values of Young's-modulus of the 12 blocks. The test showed that Young's-modulus ranged from 8.04-8.92 GPa with an average of 8.51 GPa for the blocks in Test 1. For the blocks in Test 2 with the lowest cement content the values were the lowest with a range of 3.77-4.26 GPa and an average of 4.02 GPa. Test 3 showed the highest values with a range of 10.85-12.47 GPa and an average of 11.49 GPa. The poorly cured blocks of Test 4 showed a slightly lower range of Young's modulus than that of Test 1, Young's modulus ranged from 7.03-8.25 GPa with an average of 7.77 GPa.

Table 9. Result for the 12 tested blocks.

Block	Density	Velocity	Poisson's	Young's-modulus
	[kg/m^3]	**[m/s]**	**-**	**[GPa]**
Test 1				
1	1932.9	2353	0.25	8.92
2	1894.3	2330	0.25	8.57
3	1888.5	2260	0.25	8.04
Test 2				
1	1894.3	1643	0.25	4.26
2	1848.0	1565	0.25	3.77
3	-	-	-	-
Test 3				
1	1992.7	2592	0.25	11.16
2	2008.1	2730	0.25	12.47
3	1981.1	2564	0.25	10.85
Test 4				
1	1915.5	2241	0.25	8.02
2	1884.7	2116	0.25	7.03
3	1905.9	2279	0.25	8.25

10.4 Test of Tensile and Compressive Strength of Interlocking Blocks

For various reasons only two hollow interlocking blocks, the type of blocks used in Majhi Gaun, could be tested.

10.4.1 Result of Tensile and Compressive Test

The mean values for the tensile and compressive strength of the two interlocking blocks were $\sigma_t = 1.78\ MPa$ and σ_c =11.1 MPa. The result for each block is given in Table 10.

Table 10. Result for the two tested blocks.

Block	Applied load [kg]	$\sigma_t[MPa]$	$\sigma_c[MPa]$
1	250	1.74	10.9
2	260	1.81	11.3

10.5 Test of Tensile and Compressive Strength of Various CSEB

In order to find the influence of the soil composition, the proportions of cement and the production method of CSEB also on the tensile and the compressive strength the same 12 blocks as described in Section 10.3 were tested.

10.5.1 Result of Tensile and Compressive Test

The test showed that the field tester could not provide enough force to break the blocks. Therefore the test was aborted before all blocks were tested. At a load of 300 kg none of the five tested blocks broke. Above 300 kg the test was considered not safe to continue. The pile of blocks on the plate risked to fall uncontrollably see Figure 28. Using the formulas given in Section 10.1.2 this would result in a minimum value of $\sigma_c = 9.7$ MPa and $\sigma_t = 1.7\ MPa$.

Figure 28. Test of CSEB with 250 kg on the loading plate.

11 Dynamic Testing of Building in Majhi Gaun

As described in Chapter 7 the dynamic response of a structure could be used to calibrate a numerical model. The first natural frequency should also be used in force calculations using the NBC 105:1994. Therefore the dynamic response of the building in Majhi Gaun was tested. From the measured response the first natural frequency and some consecutive natural vibration modes of the building were estimated. The free vibration response was tested for a transient impact load.

11.1 Testing Methodology

The response was tested at three different locations and in each test a force was excited three times. The response was measured by three accelerometers mounted at different parts of the structure. The accelerometers were directed to collect data in the direction of the applied force. A big log (approximately 20 kg) was used to create an impulse load on the building. A Data Translation DT9837AT data acquisition unit together with three PCB Piezotronics accelerometers model 333B32 with frequency ranges of 0.5-3k Hz were used. For all tests the response of the accelerometers were measured before the impact and as long as any oscillation could be detected. The sampling rate was 600 Hz. The force was always excited directly onto the top beam in all three tests.

11.1.1 Dynamic Test 1

In this test the force was applied as shown in Figure 29. The accelerometers were placed at the farther wall close to the top beam as shown in Figure 29.

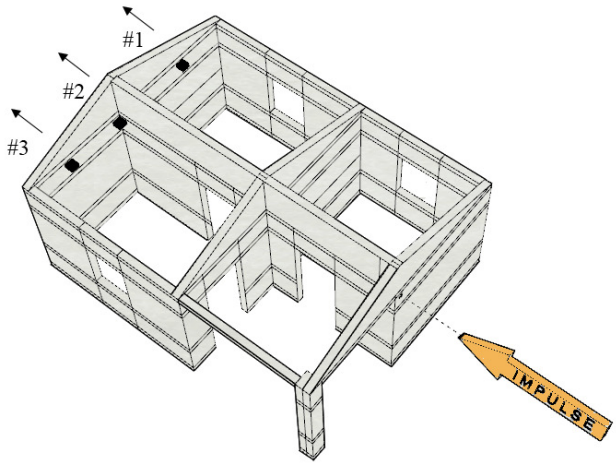

Figure 29. Visualization of position of applied impact and position of accelerometers during Dynamic Test 1.

11.1.2 Dynamic Test 2

In this test the force was applied as shown in Figure 30. The accelerometers were placed at the wall as shown in Figure 30.

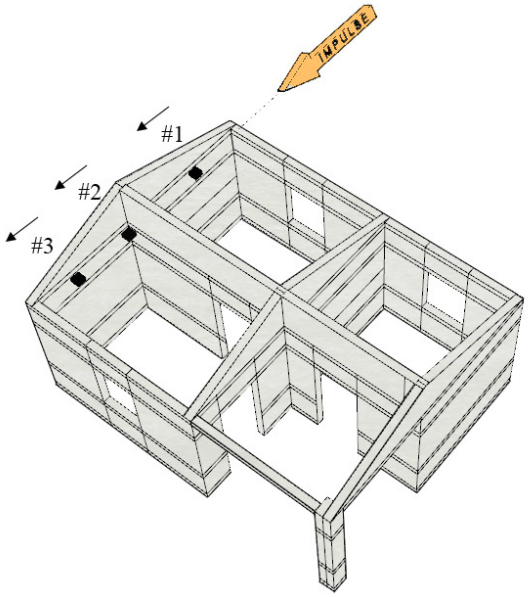

Figure 30. Visualization of position of applied impact and position of accelerometers during Dynamic Test 2.

11.1.3 Dynamic Test 3

In this test the force was applied as shown in Figure 31. The accelerometers were placed at the wall as shown in Figure 31.

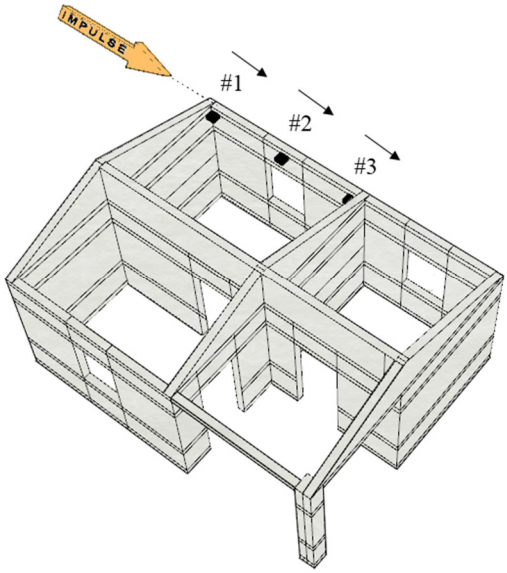

Figure 31. Visualization of position of applied impact and position of accelerometers during Dynamic Test 3.

11.2 Processing and Results of Dynamic Testing

First the parts of the accelerograms with a significant response to the impact loads were found. Then the accelerograms of all excitations of each test were used to create an average of the response for each test. In Dynamic Test 1 the sampling rate at the first excitation was mistakenly 195 Hz why this accelerogram was excluded. The averaged data was then normalized in order to account for varying amplitude of the impulse load. A band pass filter filtering out frequencies above 80 % of the *Nyquist frequency* was then created. A *Fast Fourier Transform* was finally performed on the averaged and filtered data in order to find the frequency spectra of the three tests. The plotted raw data of each test and excitation as well as all processing steps are given in a *Matlab*-file in Appendix B. In Appendix B the averaging process and the similarity in the response of each excitation is shown. The processing of the response signals was made after the creation of the Fe-model described in Chapter 12. This model offered a better understanding of the natural vibration modes of the building. From the modal analysis of the Fe-model it was clear that the accelerometers at the midpoint of a wall would have a better observability (a larger displacement). Therefore only the response signal of accelerometer #1 was chosen for Dynamic Test 1 and 2 and accelerometer #2 for Dynamic 3.

11.2.1 Result of Dynamic Test 1

In Figure 32 the processed data and the averaged data of the two excitations are shown. The processed data represents only the response of the lower frequency modes of the building.

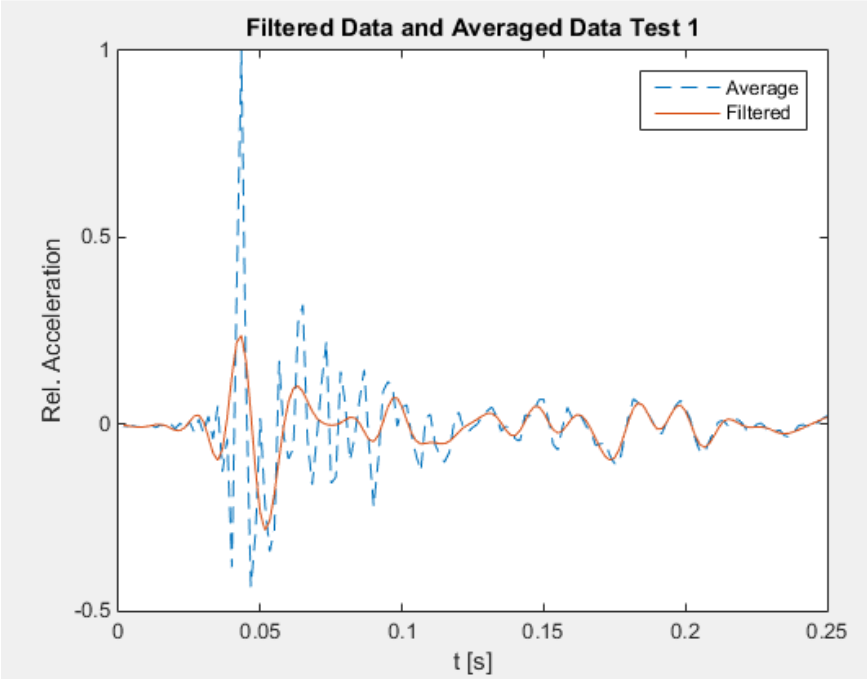

Figure 32. Processed signal plotted against the unfiltered signal of Dynamic Test 1.

Figure 33 shows the frequency spectra of the processed data of Dynamic Test 1. Clear peaks can be seen around frequencies of 18 Hz and 33 Hz. Also frequencies around 51 Hz and 59 Hz have noticeable peaks.

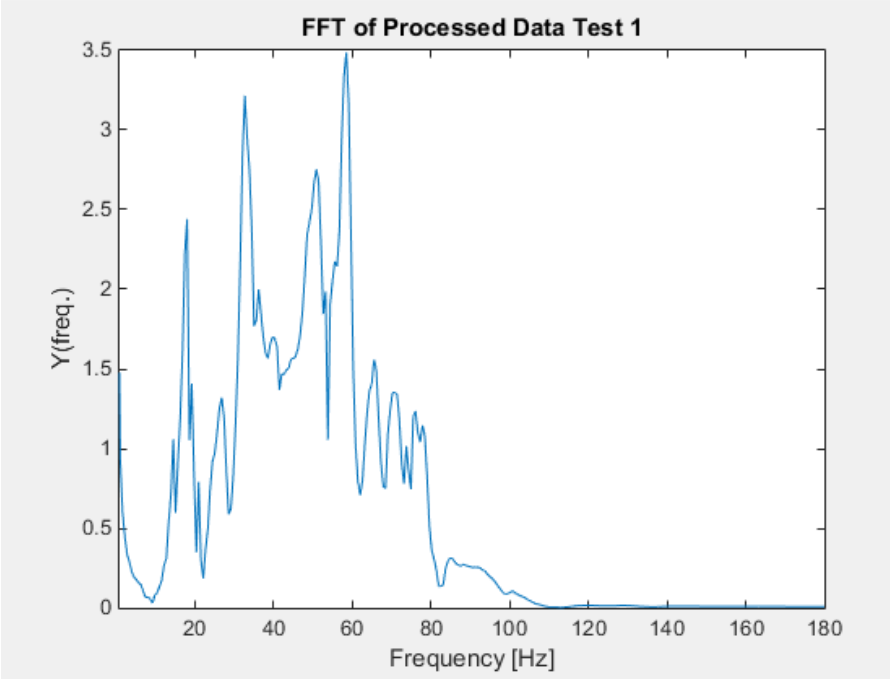

Figure 33. Resulting frequency spectra of the filtered signal of Dynamic Test 1.

11.2.2 Result of Dynamic Test 2

In Figure 34 the processed data and the averaged data of the three excitations are shown. The processed data represents only the response of the lower frequency modes.

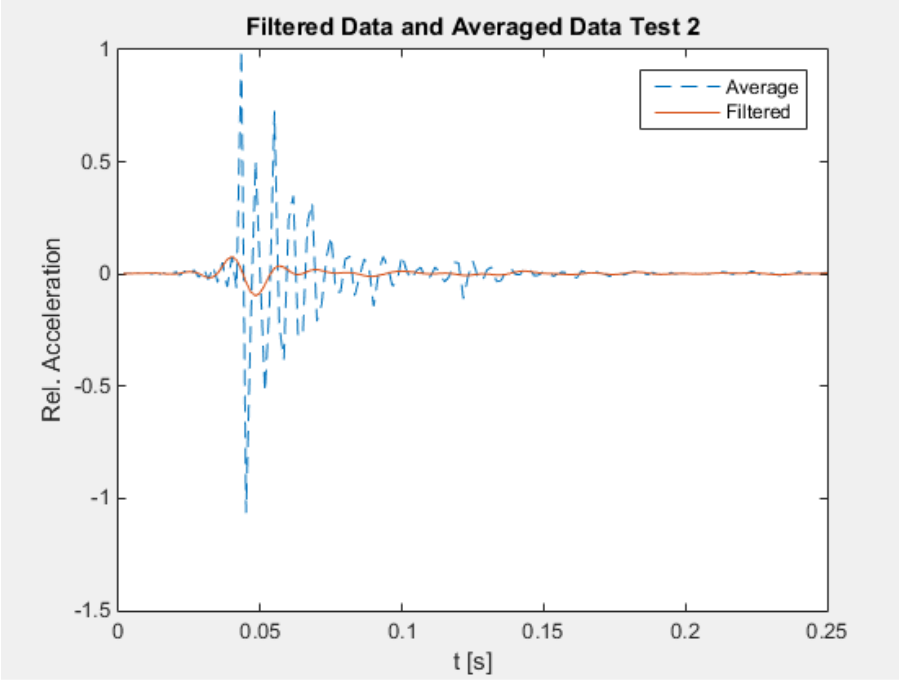

Figure 34. Processed signal plotted against the unfiltered signal of Dynamic Test 2.

Figure 35 shows the frequency spectra of the averaged and filtered data of Dynamic Test 2. A peak can be observed at 18 Hz. There is also a cluster of peaks in the range of 28 Hz up to 39 Hz and again in the range 48-70 Hz.

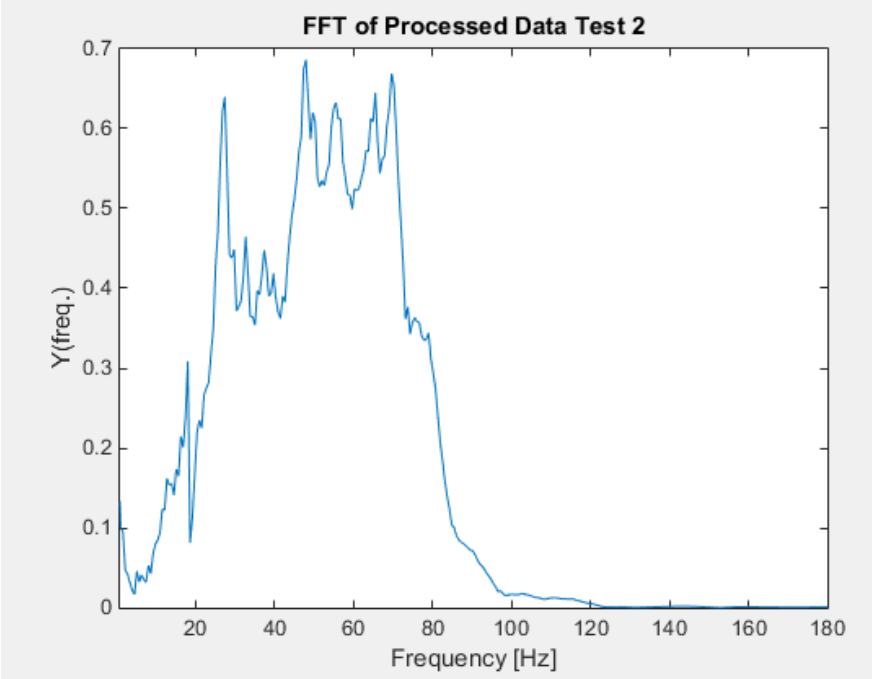

Figure 35. Resulting frequency spectra of the filtered signal of Dynamic Test 2.

11.2.3 Result of Dynamic Test 3

In Figure 36 the processed data and the averaged data of the three excitations are shown. The processed data represents only the response of the lower frequency modes.

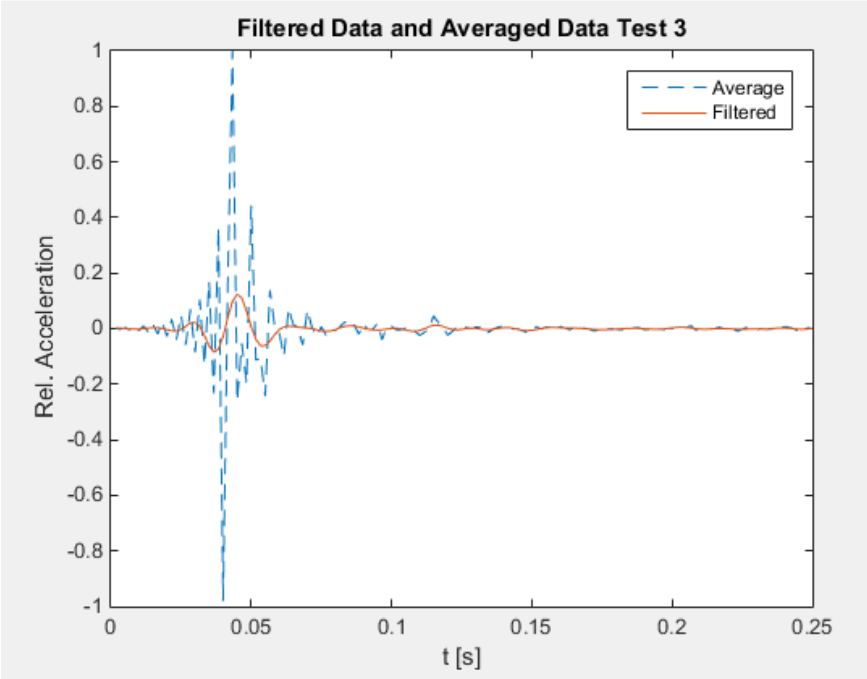

Figure 36. Processed signal plotted against the unfiltered signal of Dynamic Test 3.

Figure 37 shows the frequency spectra of the averaged and filtered data of Dynamic Test 3. A minor peak can be seen just short of 20 Hz. Also a cluster of peaks are visible around 50 Hz.

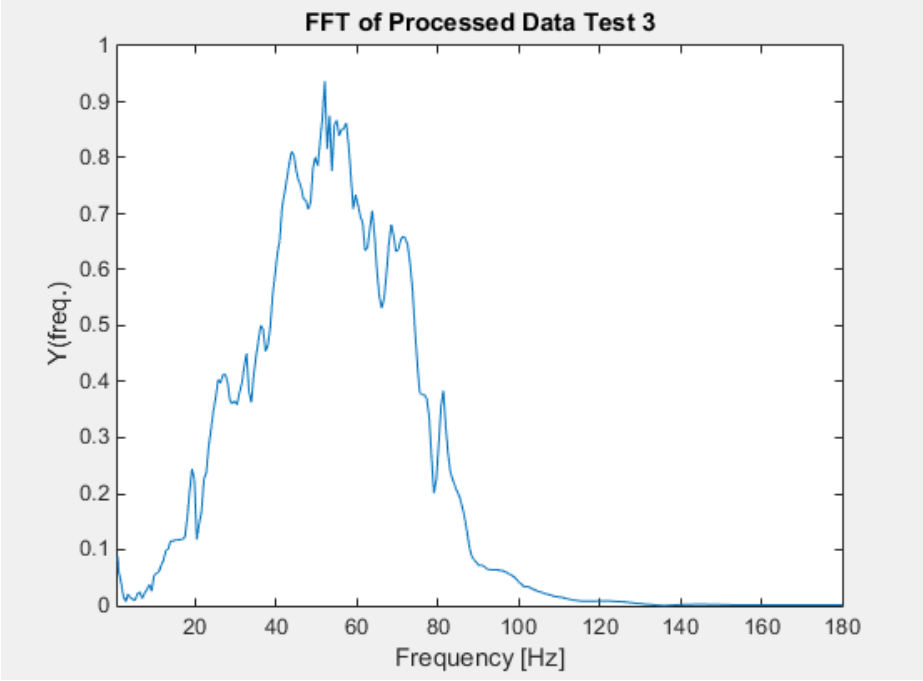

Figure 37. Resulting frequency spectra of the filtered signal of Dynamic Test 3.

11.3 Analysis of Dynamic Test Result

In this section the processed test results of the dynamic testing are analysed. The purpose of the analysis was to find a useful result to use as a verification parameter for a finite element model.

11.3.1 Discussion of Dynamic Test 1, 2 and 3

In Dynamic Test 1 the processed data showed a good representation of the overall trend of the average raw data. Excluding higher frequency modes the processed data still showed a good representation of the response. In the frequency spectra there were clear peaks at around 18 Hz, 33 Hz and a cluster of peaks around 50 Hz.

In Dynamic Test 2 the filtered data did not follow the response of the averaged raw data as clearly as in Dynamic Test 1. The frequency spectra also showed less clear peaks in the lower regions. However it is visible that the building again exhibit contribution from a mode at 18 Hz. There are also many potential modes in the range 28-39 Hz.

Dynamic Test 3 shows a doubtful relation between the filtered and the averaged raw data. The frequency spectra of test 3 only shows a clear peak up around 55 Hz.

A possible explanation to why Dynamic Test 1 represents the lower frequencies better could be the excitation points of the applied impact loads during the tests. In Dynamic Test 1 the force was applied at the midpoint of the building triggering lower frequency sway modes. In Dynamic Test 2 and 3 on the other hand the loads were applied at corners which may have triggered higher frequency torsional modes to a larger extent. Another reason to why Dynamic Test 2 and 3 showed less significant result for the lower frequencies could be that the excitation took place relatively close to the accelerometers which may have caused a lot of high frequency local vibrations.

11.3.2 Conclusion of Dynamic Testing

Dynamic Test 1 represented the response of the lower frequency modes of the building best therefore the result of Dynamic Test 1 will be used in the verification of the finite element model. It is considered to have the best accuracy for the earlier and globally dominant modes. The first natural frequency of the building is estimated to f_1=18 Hz in both direction with reference to Dynamic Test 1 and Dynamic Test 2. This is equivalent to a first natural period of T_1=0.06s.

12 Modal Analysis of Building in Majhi Gaun

The building in Majhi Gaun was modelled in the finite element software Abaqus/CAE 6.13-3. The purpose of the model was to calibrate and verify the mass and stiffness distribution of the model. To do so, a modal analysis was performed and the resulting modes were compared with the founding from the dynamic testing from Chapter 11 Section 11.3.2. All modes in the range of 0- 45 Hz were included.

12.1 Calibration Methodology

In the first iteration the average values found in the testing of Chapter 10 Section 10.2.1: $E = 2.74\ GPa$ and $\rho = 1548$ kg/m^3. The Young's-modulus and the density were then iteratively altered in the ranges given in the same section $E = 1.63 - 4.91\ GPa$ and $\rho = 1470.6 - 1719.5$ kg/m^3. The aim was to find the configuration that gave a model with the most similar natural frequencies to those found in the dynamic testing of Chapter 11 Section 11.3.2. Finally also the literature value of Young's-modulus and density given in Chapter 4 Section 4.4 were modelled.

12.2 Description of Abaqus Model

All elements were modelled as homogenous 3D solids with isotropic elastic materials and the material properties given in Section 12.2.1. The interfaces between CSEB units were neglected and instead the macro approach mentioned in Chapter 8 Section 8.1 was chosen. The CSEB was modelled as infill segments between each tie beam. These infill segments had circular openings every 150 mm, corresponding to the openings of the hollow interlocking blocks used by *Build up Nepal*. In these openings circular concrete columns were modelled. All reinforcement were neglected since the analysis was linear elastic.

12.2.1 Material Properties

The concrete was modelled with a Young's modulus of 20 GPa which was fairly low but a reasonable assumptions with reference to production methods available. The Poisson's ratio of the concrete was set to 0.2 and the density to 2400 kg/m^3. Steel profiles were modelled with a Young's modulus of 210 GPa and a Poisson's ratio equal to 0.3 with a density of 7800 kg/m^3. The CSEB had a Poisson's ratio equal to 0.25. The density and Young's Modulus were altered as described in Section 12.1.

12.2.2 Boundary Conditions

The plinth beam was at all nodes of the lower surface fully constrained to the ground which was the only boundary condition present in the model (see Figure 38).

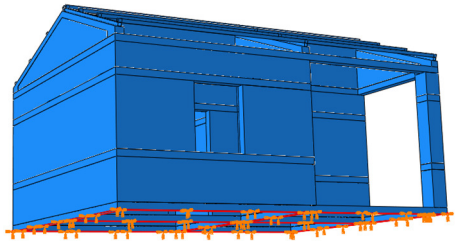

Figure 38 Visualization of applied boundary conditions in Abaqus/CAE-model.

12.2.3 Constraints

All interfaces between tie beams, infill and the cylindrical shaped concrete were modelled as tied together. This type of constraint is justified since the deformations during the dynamic test were very small and elastic. It was assumed that all cross-sections remained planar and that a compatibility condition saying that the strain on each side of an interaction surface was fulfilled. Therefore full interaction between CSEB and concrete was chosen for the modal analysis. Also the hollow steel profiles on the roof were tied to the inclined concrete beams. Some constrained interaction surfaces can be seen in Figure 39.

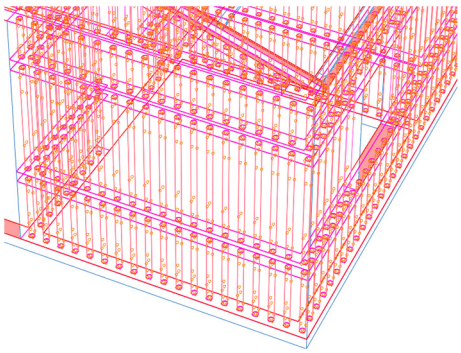

Figure 39.Visualizations of some constrained interaction surfaces in Abaqus/CAE-model

12.2.4 Meshing

Each part of the model was meshed separately with 3D hexahedrons. The fineness of the meshing varies from part to part. The meshing is shown in Figure 40.

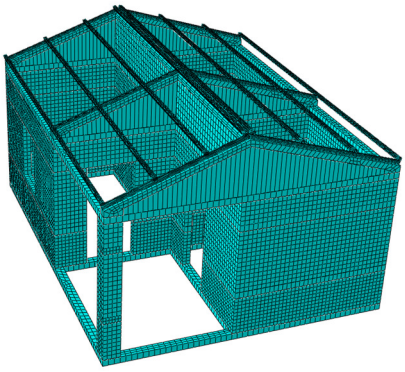

Figure 40 Visualization of meshing in Abaqus/CAE-model

12.2.5 Modal Analysis of Abaqus/CAE Model

A modal analysis of all natural frequency modes between 0 and 45 Hz was run.

12.2.6 Result of Modal Analysis

The modal analysis resulted in a number of natural modes. The local modes where the roof steel bars buckled in different directions were neglected. The modes that were either not observable at the position of the accelerometer in Dynamic test 1 or not controllable at the position of the impact were also, for all iterations, neglected but placed in Appendix C.

The two first global modes that were both observable and controllable for the initial input values are shown in Figure 41**.** The natural frequencies of these two modes are 24.6 Hz and 35.5 Hz which are both higher than the first and the second frequencies calculated from the Dynamic test 1 of Chapter 11 Section 11.2.1.

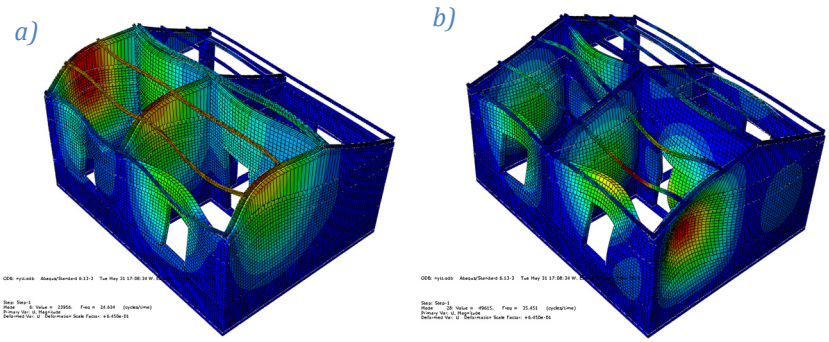

Figure 41. a) First observable and controllable mode at 24.6 Hz b) Second observable and controllable mode at 35.5 Hz

In the next iteration the lower bound values of the ranges given by the test of Chapter 10 Section 10.2.1 were used as input values: Young's Modulus = 1.63 GPa and the density = 1470 kg/m^3. The three first global modes that would have been both observable and controllable in dynamic test 1 are shown in Figure 42**.** The natural frequencies of the modes are 21.7 Hz, 24.4 Hz and 34.9 Hz. There was a first mode which was still slightly higher than the one calculated from the dynamic test. The third mode was somewhat higher than the second frequency calculated from the dynamic test. A second mode at 24.4 Hz was placed in between these two.

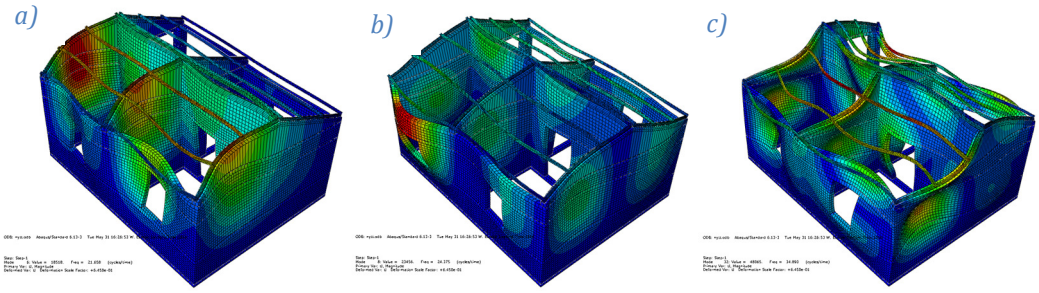

Figure 42. a) First observable and controllable mode at 21.7 Hz b) Second observable and controllable mode at 24.4 Hz c) Third observable and controllable mode at 34.9 Hz.

Finally values for Young's Modulus and the density given in Chapter 4 Section 4.4 were tested. This time only one mode was found that would have been both observable and controllable in dynamic test 1. This mode is shown in Figure 43**.** The natural frequency of that mode was 18 Hz which is almost the exact value of the first frequency calculated from dynamic test 1.

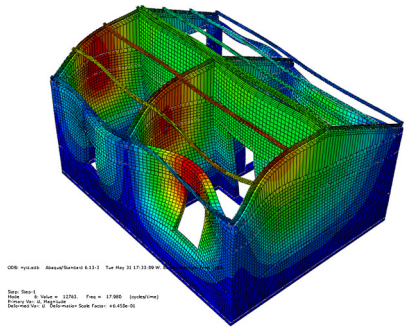

Figure 43. First observable and controllable mode at 18 Hz.

12.2.7 Calibration of Material Properties

The values of Young's-modulus and the density given in literature gave one frequency mode that was almost totally consistent with one of the frequencies calculated from the Dynamic test 1. However, this material configuration gave a less accurate result for the next and higher natural frequencies. There was no mode to be found that fitted with the second mode calculated from the Dynamic test 1. The lower bound configuration with a Young's modulus 1.63 GPa and a density of 1548 kg/m^3 gave modes with slightly too high natural frequencies but with an acceptable deviation for both the first and the second mode. Given that this material configuration of Young's modulus and density actually also was measured at site gave it extra credibility this configuration was considered the best.

13 Suggested Design Improvements of the CSEB Building

The design of this building was based on structural safety but also on an architectural vision of a family home. Oftentimes the architectural vision do not coincide with the structurally optimal design. A conflict of what is most important then takes place. The building in Majhi Gaun was designed as a three room building but with the possibility to build a fourth room. This offers prospects for the future to the family living in the house but also results in an asymmetrical building. The following chapter will address the improvements of the design of the building only with regard to structural safety.

13.1 Symmetry

The importance of symmetry, which is mentioned in Chapter 6 Section 6.1, is of great importance when designing an earthquake resistant building. As can be seen in Figure 44 and mentioned in the section above the plan symmetry is not ideal (in neither x- or y-direction) when only three rooms are built. Also, the three existing rooms are of different sizes since the two orthogonal inner walls are not centred. This in turn results in openings, for both windows and doors, that are not symmetric around the centre-point of the building.

13.2 Isolated Column

Another consequence of the three room design is the isolated column. It is separated from the other vertical resisting members of the structure and placed in one of the corners. This column will experience high stresses during seismic action which are likely to initiate an early failure.

13.3 Roof Structure

As mentioned in Chapter 6 Section 6.4 it is desirable to make the roof as rigid as possible, to make it act like one entity and in this way enable the redistribution of lateral forces. The rigidness of the parallel steel girders that are supposed to act as support for the roof cladding could therefore be improved. The corrugated steel panels does, to some extent, increase the rigidness but it is not enough.

13.4 Suggested Design Improvements

With reference to Section 13.1-13.3 some improvements in the layout of walls and openings were made. The actual layout and the improved layout are given in Figure 44. In the improved layout a fourth room is drawn. The isolated column is in this design removed. It is possible to reduce the size of the other rooms if the same total floor area is wanted as for the three room design. All openings but one are in this design symmetrical. One of the inner doors does not have a counterpart on the other side of the symmetry line. In the improved design it is placed further to the centre in both x- and y-direction (in x-direction as a result of the symmetric layout of the walls). Also a suggestion of an improved roof structure with diagonal bracing members were made. The actual roof structure and the improved roof structure are given in Figure 45. This improved design is more likely to resemble a rigid diaphragm in two directions.

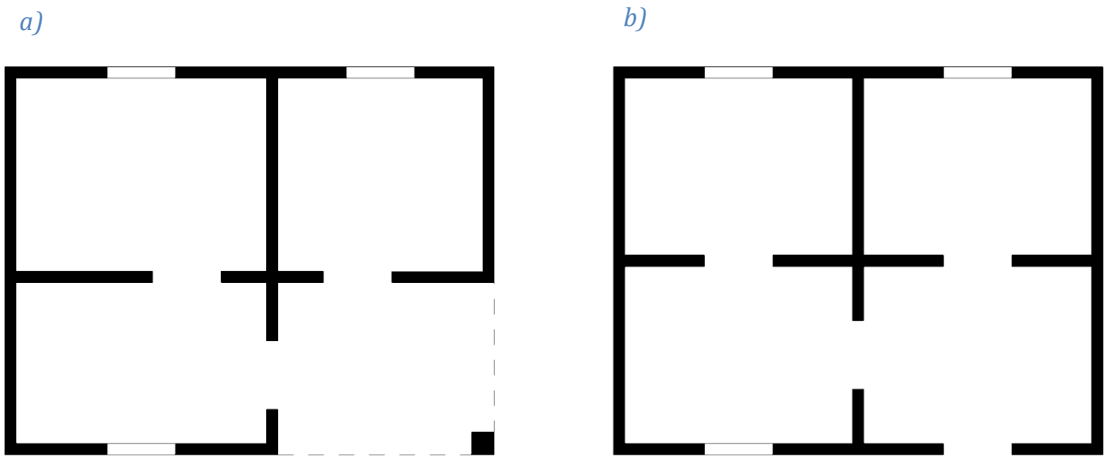

Figure 44. a) The actual layout of openings and walls b) The improved layout of openings and walls.

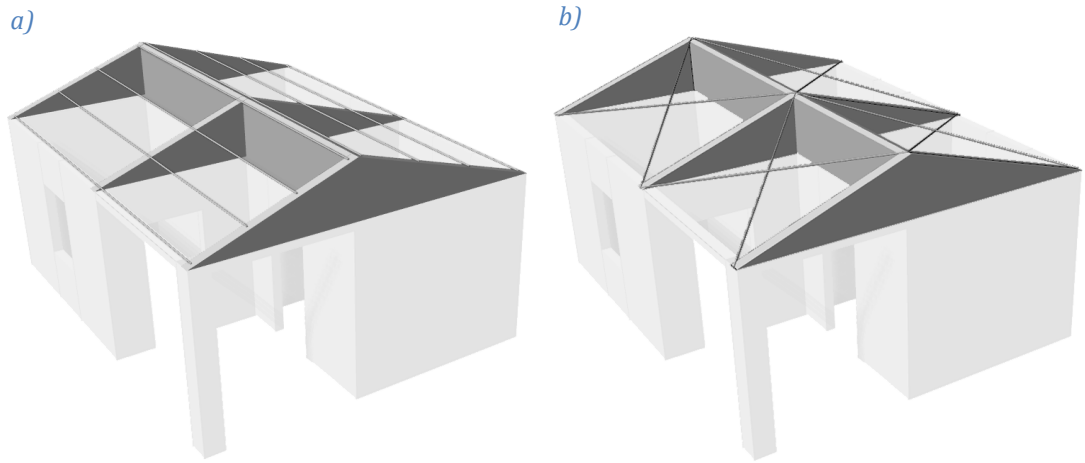

Figure 45. a) The actual roof structure b) The improved roof structure.

14 Analysis of Q1, Q2 and Q3

In this chapter the questions raised by observations in field were treated. In order to analysis Q2 and Q3 the earthquake design load first had to be calculated.

The earthquake design load was calculated according to the *Nepali Building Code 105:1994*. All calculations are given in Appendix D. An amplification of the load was made with reference to *IITK GSDMA Guidelines for Structural Use of Masonry*. In the load calculation the value of the density was conservatively chosen to the upper value tested in Majhi Gaun, $\rho = 1719.5\ kg/m^3$ since this resulted in the largest load:

$$V_b = C_d * W_{seismic} \quad \text{(NBC 105:1994)}$$

The value for the first natural period of the CSEB building was taken as measured in the Dynamic Testing in both directions. The formula proposed by the NBC would have resulted in the same value of C (for detailed calculations see Appendix D).

$$T_{1measured} = 0.06\ s \qquad => C = 0.08$$

$$T_{1NBC} = \frac{0.09H}{\sqrt{D}} = 0.12\ s \qquad => C = 0.08$$

Finally the load was considered to be distributed on the vertical reinforced sections with regard to tributary wall area. In the x-direction eccentricity had to be taken into account.

Q1. Could failures in production result in a CSEB with too poor quality?
As stated in Chapter 1 Section 1.4 "*too poor quality"* was defined as values of E, σ_t and σ_c lower than given in literature. By this definition none of the material property tests of this study showed a result that would indicate a risk of CSEB with too poor quality for the CSEB produced by *Build up Nepal*. However, the quality of the test performed in this study should be taken into account and are discussed in Chapter 15.

Q2. Does a bent rebar in one of the corners make the building unsafe?
As can be seen in Appendix A.2 there are three vertical rebars in each corner of the building. These rebars were confined in a concrete cylinder which in turn was confined by the hollow interlocking CSEB. The concrete cylinder around the block was considered too slender to be considered a column. The interaction between the concrete and the CSEB was as mentioned in Chapter 12 assumed to be full in the elastic state. In the elastic state the corner was therefore considered as a symmetric L-shaped column with three reinforcement bars (see Figure 46). The L-shaped columns were considered to not be free in lateral bending why they were treated as symmetrical T-section columns in the design calculations. The boundary conditions of the columns were conservatively chosen as fixed at the bottom and free at the top. In the resistance calculation the values of E, σ_t and σ_c were conservatively chosen as the lowest values measured in Majhi Gaun: $E = 1470.6\frac{\text{kg}}{\text{m}^3}, \sigma_t = 1.74\ GPa$ and $\sigma_c = 10.9\ GPa$.

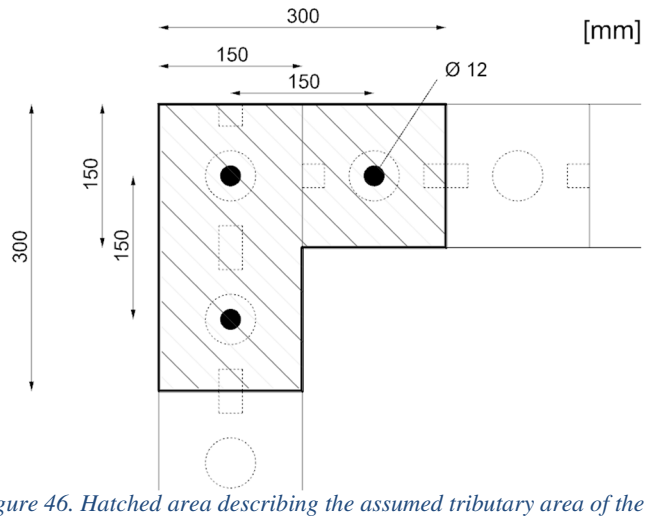

Figure 46. Hatched area describing the assumed tributary area of the L-shaped column.

The corner with the maximal force was conservatively chosen $Q_{y3} = 0.522 \frac{kN}{m*rebar}$ (see Appendix D). The design calculations in Appendix F.1 showed that the L-shaped columns in the corners remained in state 1, the uncracked state, when subjected to the earthquake design load. The minimum reinforcement requirement was checked. According to *IITK-GSDMA* the minimum reinforcement in a corner should be 100 mm^2 (Indian Institute of Technology Kanpur, 2005). This is equivalent to three rebars with a diameter of $\emptyset\, 6.51\, mm$ or two rebars of $\emptyset\, 7.98\, mm$. The actual rebars in the corners were of $\emptyset\, 12\, mm$ as can be seen in Appendix A.2. The answer to the question above was therefore that a bent rebar in one of the corners would not make the building unsafe. Even in the worst case, where one rebar was totally put out of order the corner column remained uncracked and the minimum reinforcement requirement was fulfilled.

Q3. Does a poorly anchored rebar next to one of the openings make the building unsafe?
As given in Appendix A.2 there is one rebar on each side of each opening in the building. These rebars were in the same way as described earlier in this section confined in a concrete cylinder which in turn was confined by the hollow interlocking CSEB. Therefore the section around these rebars were again considered as columns. The thickness of the column was considered the same as the thickness of the block and the length as the length of one block. The position of the reinforcement in the column was considered differently depending on the direction of the force (see Figure 47). The boundary conditions of the columns were conservatively chosen as fixed at the bottom and free at the top. In the resistance calculation the values of ρ, σ_t and σ_c were again conservatively chosen as the lowest values measured in Majhi Gaun: $\rho = 1470.6 \frac{\mathrm{kg}}{\mathrm{m}^3}$, $\sigma_t = 1.74\, GPa$ and $\sigma_c = 10.9\, GPa$.

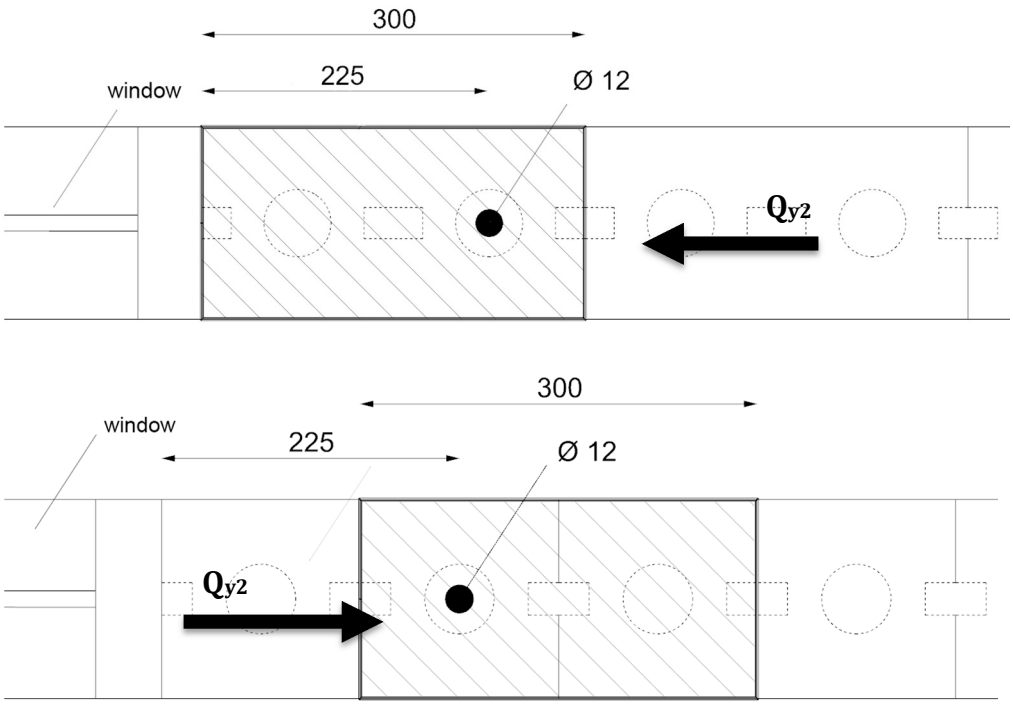

Figure 47. Hatched area describing the assumed tributary area of the column depending on force direction.

The maximum force next to an opening was as described in Appendix D, $Q_{y2} = 0.419 \frac{kN}{m*rebar}$. In this wall the check was then performed for the tallest column next to an opening, $h_c = 3.1\ m$. The design calculations in Appendix F.2 showed that the columns next to an opening remained in state 1, the uncracked state, when subjected to the earthquake design load. The minimum reinforcement requirement was checked. According to *IITK-GSDMA* the minimum reinforcement next to an opening should be 100 mm^2 and should be placed within a distance of 400 mm from the opening (Indian Institute of Technology Kanpur, 2005). This is equivalent to a rebar of a diameter of $\emptyset\ 11.3\ mm$. The actual rebars next to openings were of $\emptyset\ 12\ mm$ as can be seen in Appendix A.

The answer to the question is not as straightforward as for Q2. On the one hand the section did not crack when subjected to the earthquake design load. On the other hand if the poorly anchored rebar was considered to be totally out of order the minimum reinforcement requirement would not be fulfilled. However, the cracking of the section should be considered the most important aspect with regard to safety. Other global aspects such as the box behaviour of the structure should also be taken into account. The vertical rebars are supposed to create ties between the horizontal bands and preferably also to the foundation in the inelastic state. As a result of a poorly anchored rebar the tie to the foundation would be put out of order but the column itself would probably eventually create anchorage to the rebar. This would result in proper action of the rebar further up in the structure. This means that also a poorly anchored rebar would create proper ties between at least some of the horizontal bands.

In summary a poorly anchored rebar next to an opening is unwanted and will change the behaviour of the structure. At a local level it should not be considered unsafe but the effects on a global level cannot be determined. More knowledge of the exact behaviour of a poorly anchored rebar and the properties of the stiffness redistribution of structure in the inelastic state are needed in order to answer this question more accurately.

15 Discussion

In this chapter some uncertainties of the study will be discussed together with alternative approaches that could have improved the results.

In the testing of Young's Modulus only the P-wave was measured with the ultrasonic pulse velocity instrument. Therefore Poisson's ratio had to be estimated. The Poisson's ratio was assumed to be the same for all blocks which has to be considered as a simplification. Also the accuracy of the value (Poisson's ratio of 0.25) should be regarded as an uncertainty. If S-wave transducers also had been available and the velocity of the S-wave had been measured too this estimation would not have been necessary and Young's modulus could have been calculated only using tested data.

It would also have been valuable to be able to make laboratory tests of the compressive and tensile strength since the field testing in many ways lacked in quality. The field tester used could not provide enough pressure in order to break the 240x240x90 mm^3 blocks. Therefore the conclusions from those tests were limited. In a laboratory the full working curve could have been obtained and thereby also an indication of the nonlinear behaviour of the blocks could have been acquired. Regarding the interlocking blocks in Majhi Gaun the attempts were unfortunately only two. The field tester could not be brought to Majhi Gaun and the testing had to be performed at the office in Kathmandu. More attempts were needed here.

Despite the uncertainties due to the testing conditions in Nepal all blocks tested showed values of Young's Modulus, density, compressive and tensile strength that in most cases deviated from the quite wide ranges given in literature. The machine being used showed to have a clear influence on the material properties but also the amount of cement. It is also likely that the same machine could give variating properties depending on the amount of mixture that is compressed. Therefore if an organization, a machine or a village could get a quality assurance of their CSEB the values used in design could be altered and the structures could thereby be optimized with regard to material use and funds, savings of funds have an unlimited importance in villages with barely none.

The dynamic testing showed a relatively consistent result. Taking the testing environment and the equipment available into account it is considered successful. However, with better equipment at hand and the chance to create a numerical model before performing the testing the result would most likely have been both clearer and more reliable. If potential natural vibration modes could have been analysed on beforehand the location of both the accelerometers and the location of the force application could have been adjusted. In some cases the accelerometers were placed at nodes with limited oscillation thereby not yielding any valuable information. It should also be mentioned that the length of the cables did limit the possible locations of the accelerometers. In hindsight the building should probably not have been excited at the corners at all since this presumably triggered high frequency torsional modes which then were governing the response. Instead more attempts should have been made at the midpoints to increase the amount of data here and thereby lowering the uncertainty of the result. The method of exciting the building with a timber log straight on the top beam could also have been improved. If a rubber protection would have been placed at the top beam it would have created a smoother impulse and reduced the local high frequency vibrations that created noise in the response. Another alternate approach could have been to use a basketball tied to a rope as a sledge hammer. Creating a periodicity in the application of the impulse itself could also have simplified the processing of the data.

From the result of the modal analysis of the CSEB building in Majhi Gaun it could be argued that the *Equivalent Static Method* should not be used. The torsional modes have a clear impact and it is doubtful if it can be concluded that the first natural mode is governing the dynamic behaviour. A *Modal Response Spectrum analysis* could potentially give a better design.

The numerical Abaqus/CAE model includes simplifications. As mentioned in Chapter 12 a macro approach with the assumption of full interaction between the blocks at the interfaces was used. As a consequence this model cannot show relative displacement between blocks. If the interface would be the weak link of the masonry this model could not show this behaviour. However in the elastic state it is assumed to represent the behaviour well. The model was considered to show a good representation of the elastic dynamic response. Furthermore, also in the elastic state, there are non-investigated aspects that could have influence. Therefore it is necessary to be careful in order to not arrive at false conclusions. The model showed that Young's Modulus of the CSEB masonry was lower than tested for the 20 blocks. This could be correct, but also non-investigated aspects could have influenced. For instance, the fact that the blocks used in the beginning of the construction process were not included in the testing of the material properties was not considered. Potentially these blocks were of lower quality since the workers had less experienced in the beginning of the construction process. The actual average value of the CSEB in the building could then also be lower and equal to the CSEB masonry.

The suggested design improvements of Chapter 13 only consider structural aspects. As mentioned in the background in Chapter 1 it is also important that the architectural vision has good anchorage in the community. Therefore the suggested design improvements should only work as a leading line for the architect in the design of new CSEB buildings.

16 Conclusions

In addition to the suggested design improvements of Chapter 13 and the analysis of the question Q1-3 in Chapter 14 this study also arrived at some other conclusions.

Based on the investigations of this study it can be concluded that Young's modulus is very dependent on the machine being used in production of the block (that is the degree of compaction of the mixture). It was also shown that the proportion of cement used in the mix has considerable influence. The use of an increased amount of coarse particles in the soil composition increases the value of Young's modulus whereas the curing does not seem to have a considerable influence.

Regarding the tensile and compressive strength ($\sigma_{t,}\, \sigma_c$) these properties are also dependent on the machine being used however the exact variation from one machine to another could not be decided nor the variation for other variations of CSEB.

This study also showed that the density of CSEB could be lower than the values given in literature. This would in turn result in a smaller seismic load than used in design calculations today (as seen in Chapter 14):

$$V_b = C_d * W_{seismic} \quad \text{(NBC 105:1994)}$$

The first natural frequency of a CSEB building could be higher than calculated using the empirical formulas given in the *NBC 105:1994*. This did not have an impact on the calculations in Chapter 14 since both the calculated and the measured values were at the plateau of the graph in Table 8.1 from *NBC 105:1994* (given in Appendix D). However, for all other cases, where both values are not at the plateau, there is a risk that the empirical formulas underestimates the factor C and thereby the equivalent earthquake load.

Finally, the calibrated numerical model of Chapter 12 Section 12.2.7 was considered to, in the elastic state, give a good representation of the CSEB building in Majhi Gaun.

17 References

Anderson, D., & Brzev, S. (2009). *Seismic design guide for masonry buildings.* Toronto: Canadian Concrete Masonry Producers Aassociation.

Bakeer, T. (2009). *Collapse analysis of masonry structures under earthquake actions. Vol. 8.* Dresden: Technische Universität, Dresden.

Bernier, J., Glascoe, L., & Mosalam, K. (2009). *Mechanical Properties of Unreinforced Brick Masonry, Section 1.* Livermore: US Departement of Energy by Lawrence Livingmore National Labaratory.

Bolhassani, M., Hamid, A., Lau, A., & Moon, F. (2014). Simplified micro modeling of partially grouted masonry assemblages. *Elsevier*.

Council Building Seismic Safety. (2016, May). *Evaluation of the Accidental Torsion Requirement in ASCE 7 by the FEMA P695 Methodology.* Retrieved from Civil, Environmental and Architectural Engineering-University of Colorado: http://civil.colorado.edu/~balajir/CVEN6833/projects/jared.pdf

Ewins, J. E. (1984). *Modal Testing: Theory and Practice.* Letchworth: Research Studies Press LTD.

Geological Survey of Canada. (n.d.). *Earthquake Glossary*. Retrieved from U.S Geological Survey: http://earthquake.usgs.gov/learn/glossary/?term=locked%20fault

Goswami, R., Mehta, V. V., Murty, C., & Vijayanarayanan, A. R. (2012). *Some Concepts in Earthquake Behaviour of Buildings.* Gujarat: Gujarat State Disaster Management Authority-Government of Gujarat.

Indian Institute of Technology Kanpur. (2005). *IITK-GSDMA Guidlines for Structural Use of Reinforced Masonry.* Kanpur: Indian Institute of Technology Kanpur and Gujarat State Disaster Mitigation Authority.

Jangid, D. S. (2013, April 5). *Introduction to Earthquake Engineering.* Retrieved from Nptel: http://www.nptel.ac.in/courses/105101004/downloads/04%20Chapter.pdf

Koboevic, S. (2015, February). *CIV6510 Conception Parasismique des Structures.* (S. Koboevic, Performer) École Polytechnique de Montréal, Montréal, Quebec, Canada.

LIU, D.-h., & Wang, M.-z. (2000). Masonry Structures Confined with Concrete Beams and Columns. *Paper. No. 2720.* Auckland: 12 World Conference on Earthquake Engineering.

Lourenço, P. B., Rots, J. G., & Blaauwendraad, J. (1995). *Two approaches for the analysis of masonry structures: micro and macro-modelling.* Delft, Netherlands: HERON.

Maïni, S. (2005). *Earthquake Resistant Buildings With Hollow Interlocking Blocks.* Auroville: Auroville Earth Institute.

Maïni, S. (2010). *Production and Use of Compressed Stabalised Earth Blocks.* Auroville: Auroville Earth Institute.

Mathworks. (2016, May). *Fast Fourier Transform (FFT)*. Retrieved from Mathworks: http://se.mathworks.com/help/matlab/math/fast-fourier-transform-fft.html?requestedDomain=se.mathworks.com

Mosalam, K., Glascoe, L., & Bernier, J. (2009). *Mechanical Properties of Unreinforced Brick masonry, Section 1.* US Department of Energy by Lawrence Livermore National Laboratory.

Murty, C. (n.d.). *Why are Horizontal Bands necessary in Masonry Buildings?* New Dehli: IIT Kanpur and BMTPC.

Murty, C. (n.d.). *Why should Masonry Buildings have simple Structural Configuration?* New Dehli: IIT Kanpur and BMTPC.

Music, R. (2016). *Construction of Design Response Spectrum-The Chilean Way.* Retrieved from Berkeley Seismological Labaratory-Earth and Planetary Science: https://seismo.berkeley.edu/eqw_presentations/RodrigoMusic_DesignResponse.pdf

Nankhwa, S. (2015, May 26). The Building Blocks of Reconstruction. *Nepali Times*.

Panzera, T. H., Christoforo, A. L., Cota, F. P., Borges, P. H., & Bowen, C. R. (2011). *Advances in Composite Materials - Analysis of Natural and Man-Made Materials.* Rijeka: Intech.

Park, S.-K., & Sungnam, H. (2012). Uniaxial bond stress-slip relationship of reinforcing bars in concrete. *Advances in Materials Science and Engineering* .

Paultre, P. (2011). *Dynamic of Structures.* Croyden: ISTE.

RangaRajan, T. (2016, May 20). Retrieved from Structural Engineering Forum of India: http://www.sefindia.org/forum/files/floor_diaphragms_353.pdf

Reid, R. (n.d.). *Earthquake Resistant Buildings*. Retrieved from Reidsteel: http://www.reidsteel.com/information/earthquake_resistant_building.htm

Riza, F. V., Rahman, I. A., & Zaidi, A. M. (2010). A Brief Review of Compressed Stabilized Earth Brick (CSEB). Kuala Lumpur: International Conference on Science and Social Research.

Sandersson, D., & Burnell, J. (2013). *Beyond Shelter After Disaster: Practice, Process and Possibilities.* New York: Routledge.

Seneca. (2015, August 9). *Scientists shed a new light on the Gorkha 2015 earthquake: the methods used in predicting the shaking and resulting damage could be used for earthquakes elsewhere*. Retrieved from The Watchers: http://thewatchers.adorraeli.com/2015/08/09/scientists-shed-a-new-light-on-the-gorkha-2015-earthquake-the-methods-used-in-predicting-the-shaking-and-resulting-damage-could-be-used-for-earthquakes-elsewhere/

Sharma, I. J. (2008). *Seismic pounding effects in buildings.* Rourkela: National Institute of Technology, Rourkela.

Shrestha, H. D. (2012). *Manual for EQ Safe Building Construction.* Kathmandu: Government of Nepal, Ministry of Education, Department of Education.

Shrestha, H. D. (2012). *Standard Norms and Specification for CSEB Block.* Kathmandu: Government of Nepal Ministry of education Departement of Education.

Spence, W., Sipkin, S. A., & Choy, G. L. (1989). *Measuring the Size of an Earthquake*. Retrieved from U.S Geological Survey: http://earthquake.usgs.gov/learn/topics/measure.php

Söderberg, B. (Director). (2015). *Build up Nepal - Rebuilding and fighting poverty* [Motion Picture].

The University of Liverpool. (1999). *Richter Scale*. Retrieved from Matter: http://www.matter.org.uk/schools/content/seismology/richterscale.html

Tomaževič, M. (2009). Shear resistance of masonry walls and Eurocode 6: shear versus tensile strength of masonry. *Materials and Structures*.

U. S. Geological Survey. (1989). *The Severity of an Earthquake.* Retrieved from U. S. Geological Survey: http://pubs.usgs.gov/gip/earthq4/severitygip.html

U.S Geological Survey. (2016). *Earthquake Glossary*. Retrieved from U.S Geological Survey: http://earthquake.usgs.gov/learn/glossary/?term=Ring%20of%20Fire

Unknown. (2016). *Ring of Fire*. Retrieved from Japaneseclass: http://japaneseclass.jp/trends/about/%E7%92%B0%E5%A4%AA%E5%B9%B3%E6%B4%8B%E7%81%AB%E5%B1%B1%E5%B8%AF

Varshney, V. (2015, April 26). *'The great Himalayan earthquake', yet to arrive* . Retrieved from Down to Earth: http://www.downtoearth.org.in/news/-the-great-himalayan-earthquake-yet-to-arrive-49559

Weisstein, E. (2016, May). *Fourier Series*. Retrieved from Mathworld-A Wolfram Web Resource: http://mathworld.wolfram.com/FourierSeries.html

Villaverde, R. (1988). Modal Superposition Method for Seismic Design of Non-Linear Structures. *Earthquake Engineering & Structural Dynamics* .

Åstrand, J. (1994). *Att bygga i u-land : vägledning vid planering och genomförande av byggprojekt.* Stockholm: Svenska missionsrådet (SMR).

Appendices

Appendix A

Drawings

In this appendix drawings and reinforcement drawings of the building in Majhi Gaun are given.

A.1 Drawings of house in Majhi Gaun

A.1.1 Plan and section

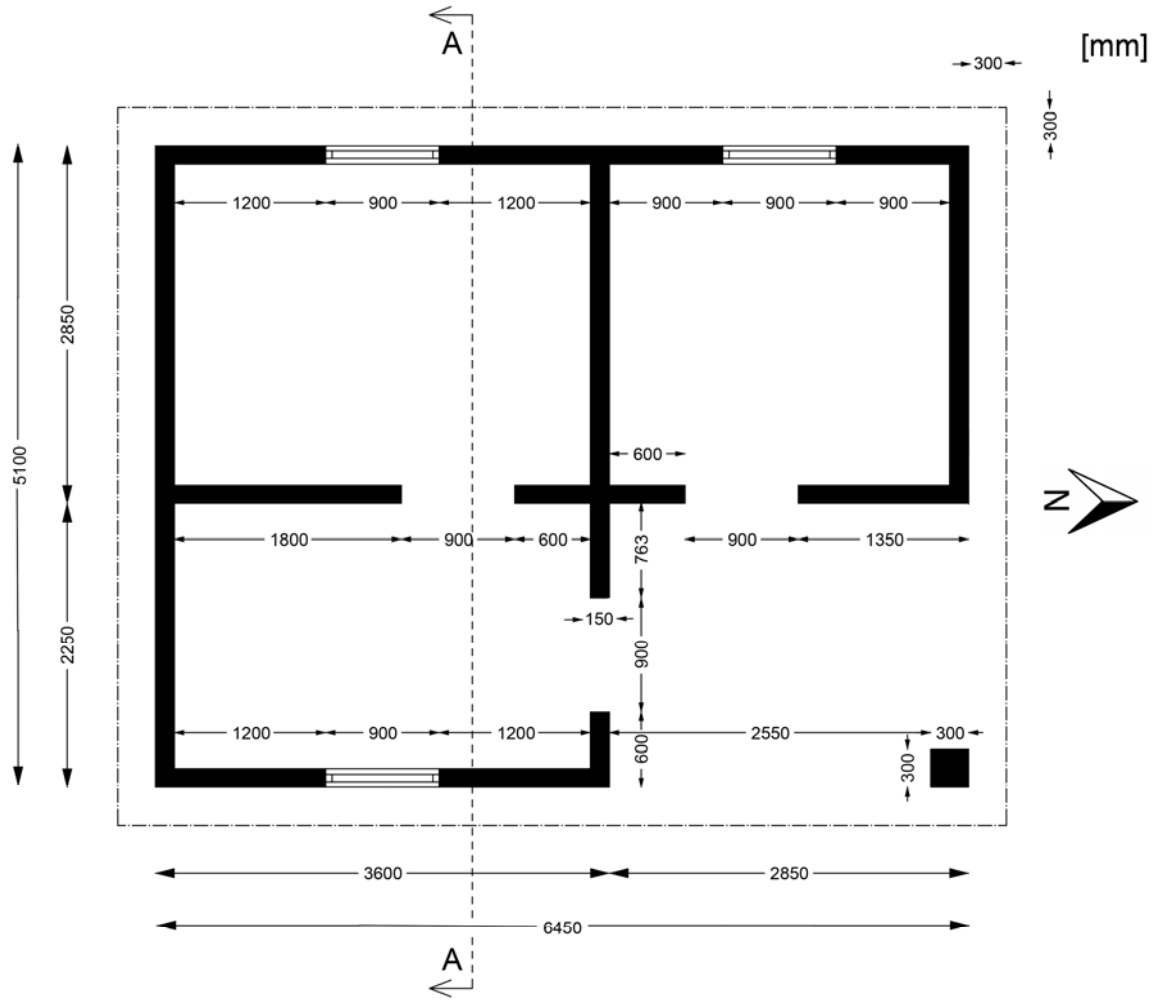

Figure 1 Plan drawing

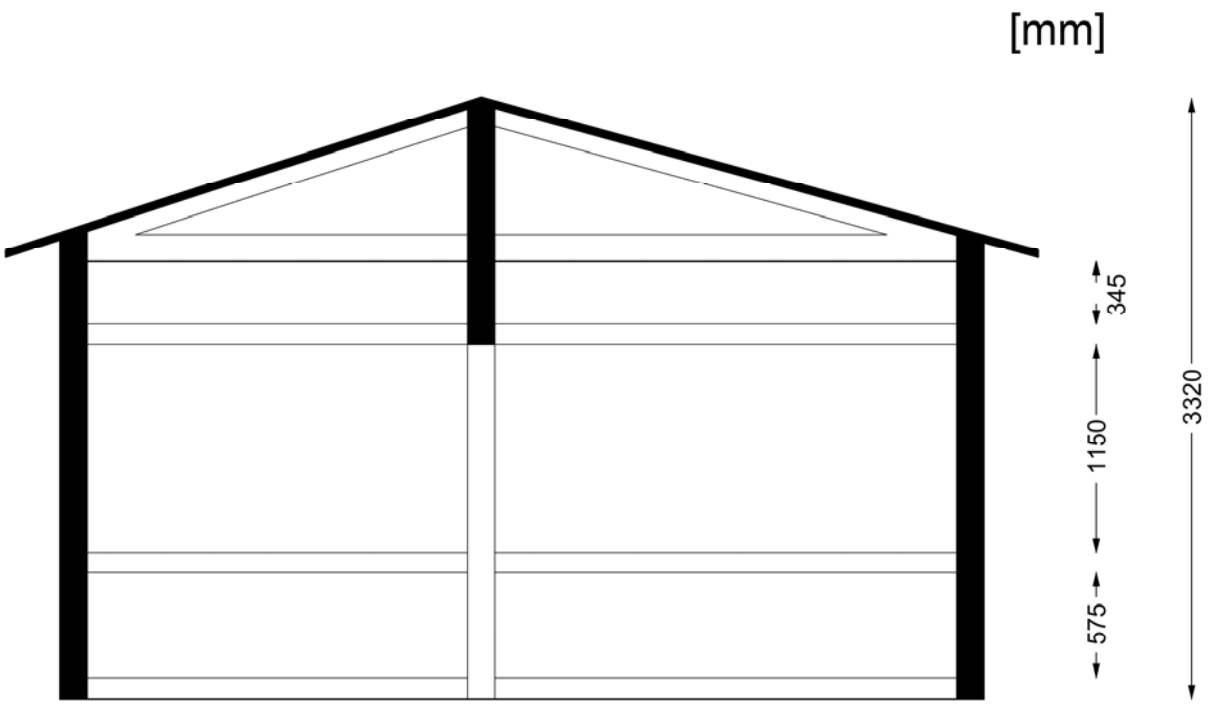

Figure 2 Section drawing

A.1.2 Facades

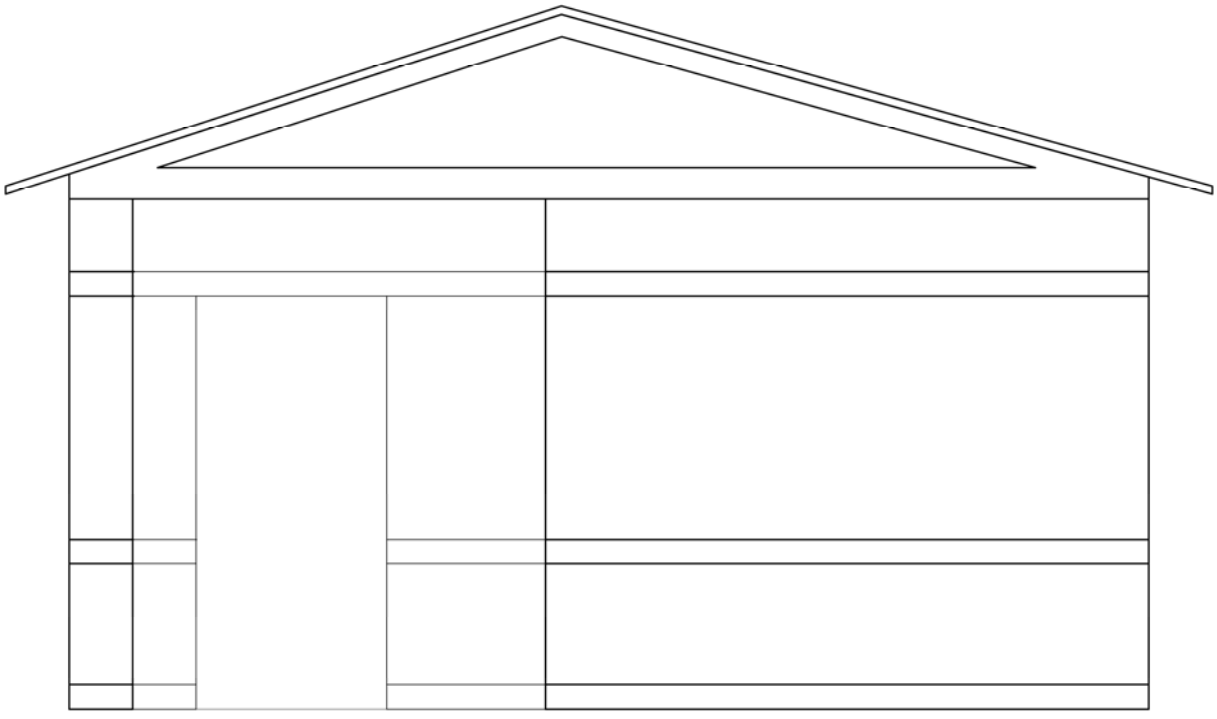

Figure 3 North facade

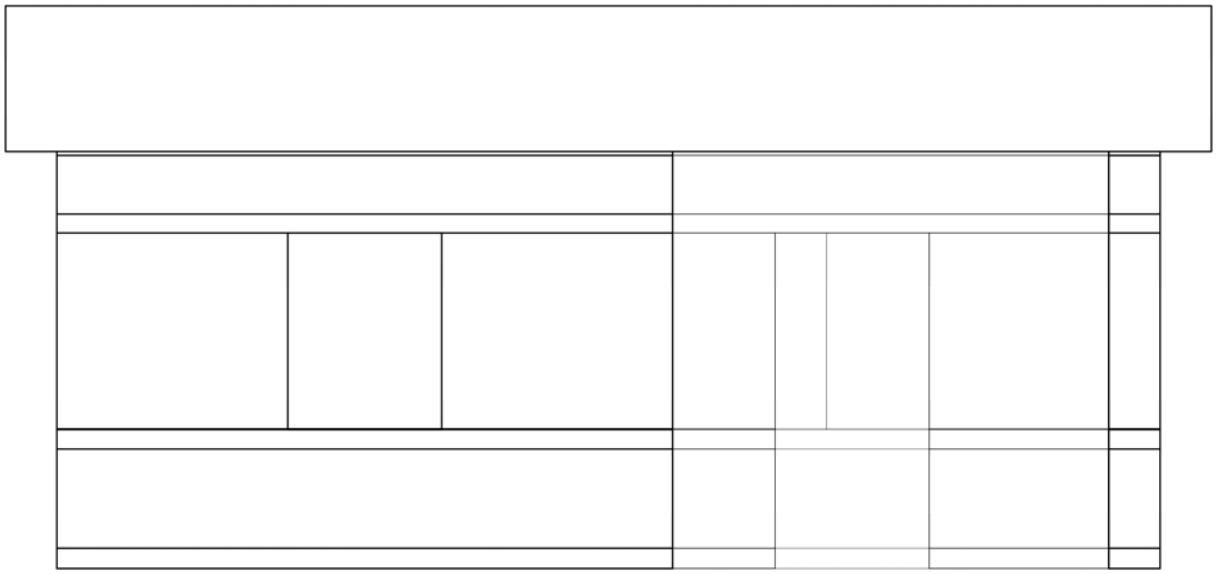

Figure 4 East facade

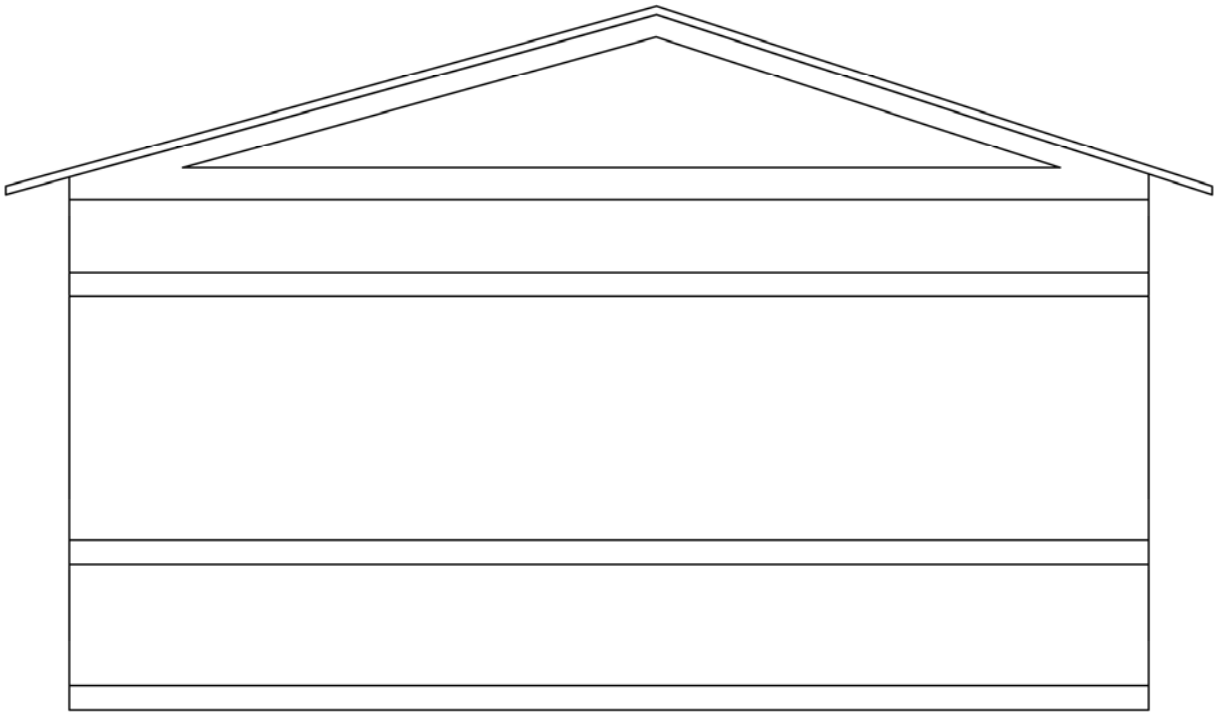

Figure 5 South facade

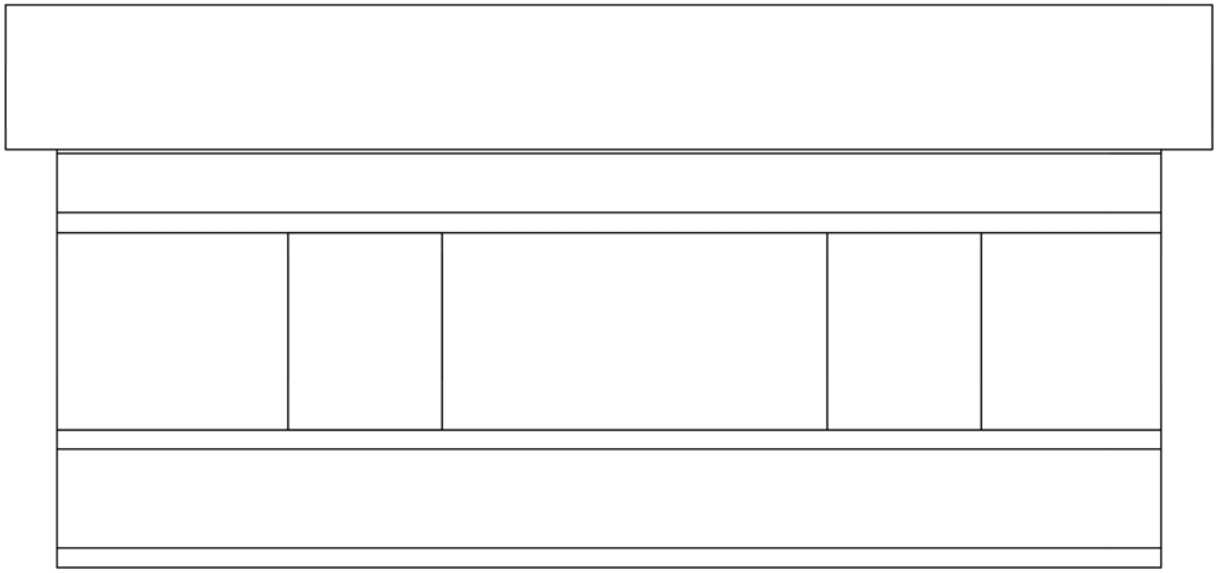

Figure 6 West facade

A.2 Reinforcement drawings

A.2.1 Sill Beam Reinforcement

In Figure 7 the layout of reinforcement at sill beam level of the house in Majhi Gaun is presented. The two parallel horizontal bars going along the walls have a diameter of 10 mm. The stirrups that hold these two together have a diameter of 8 mm. Also the hooks present in all the corners and intersections have a diameter of 8 mm. All the vertical reinforcement that is anchored in the foundation has a diameter of 12 mm. These vertical bars are spliced between sill and lintel level and are anchored at the top of the building, either in the top beam or the inclined roof beams. The appearance of the reinforcement at the other beam levels have identical detailing in the junctions. The only difference is where the openings are placed.

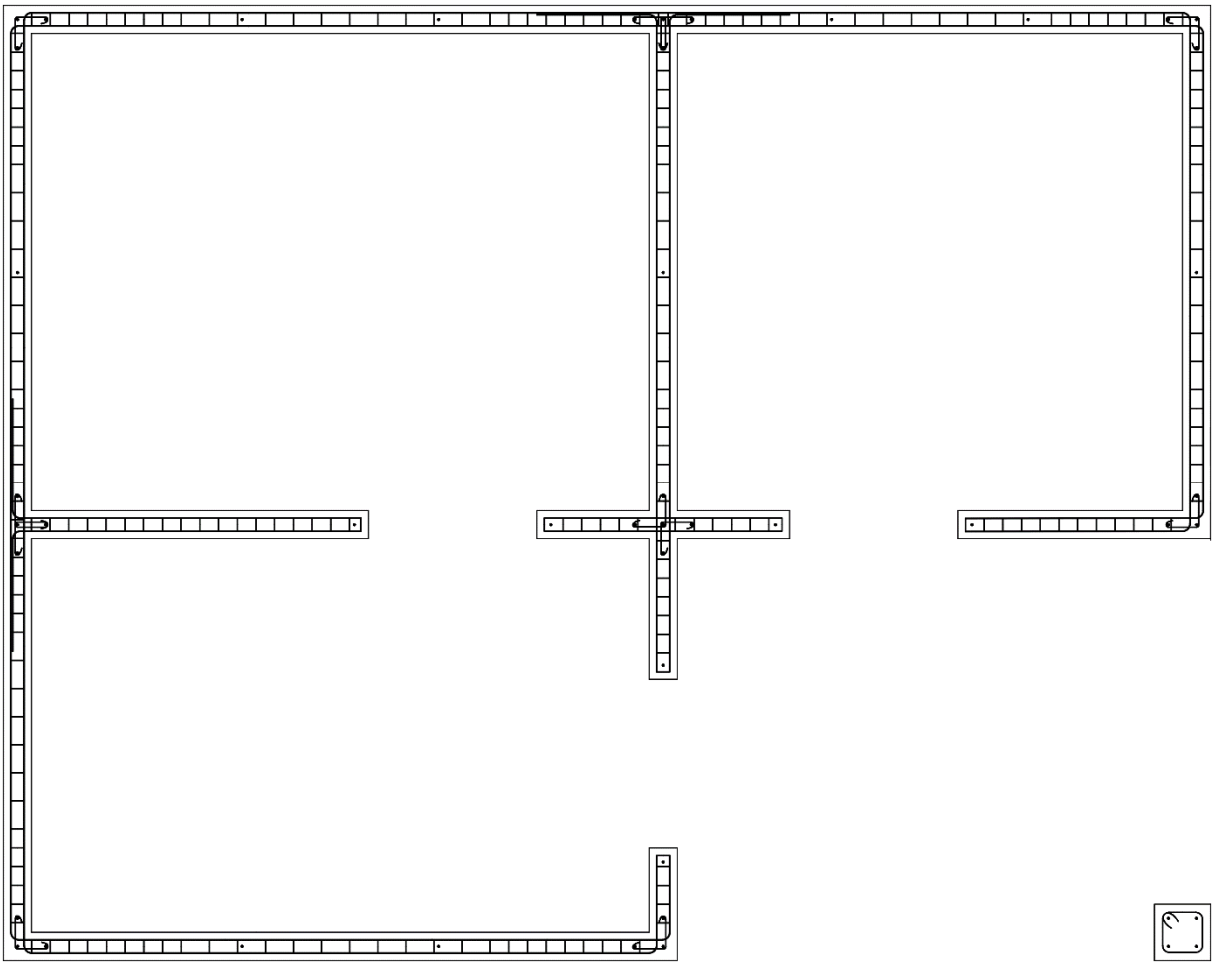

Figure 7 Reinforcement drawing of the sill beam

A.2.2 Details of Reinforcement

A detailed reinforcement drawing of corners can be seen in Figure 8. The outer bar swops position with the inner bar when passing the corner. Stirrups are holding the two parallel bars

together with a spacing of 100-150 mm. On every beam level there is a hook present to hold the three vertical bars together.

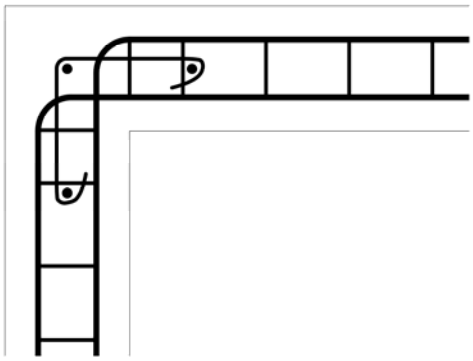

Figure 8 Detail of reinforcement in a corner (Sill beam)

In Figure 9 a detail of a 4-way crossing can be seen. All bars are passing the crossing continuously in both directions. Two hooks are used to connect the five vertical rebars on every beam level.

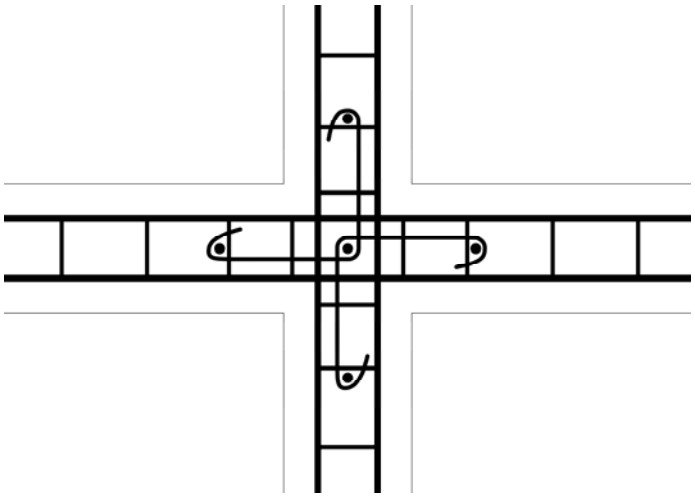

Figure 9 Detail of reinforcement in a 4 way crossing of walls (Sill beam)

Figure 10 shows the detailed reinforcement of a T-crossing. The bars coming from the inner wall go to the outer bars of the outer wall and are anchored with a length of 600 mm. Also here two hooks connect the four vertical bars.

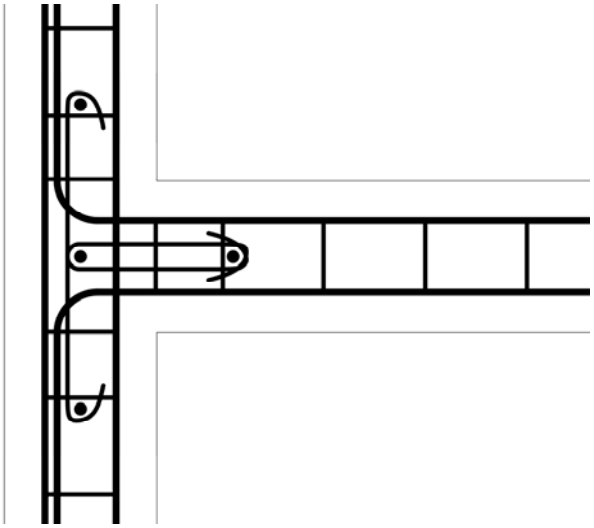

Figure 10 Detail of reinforcement in a T-crossing (Sill beam)

Appendix B

Digital Processing of Dynamic Tests

```
clear all
close all
clc
```

```
import1=xlsread('test1.2.xlsx'); %importing acc-data from test 1.2
import2=xlsread('test1.3.xlsx'); %importing acc-data from test 1.3
import3=xlsread('test2.1.xlsx'); %importing acc-data from test 1.2
import4=xlsread('test2.2.xlsx'); %importing acc-data from test 1.3
import5=xlsread('test2.3.xlsx'); %importing acc-data from test 1.2
import6=xlsread('test3.1.xlsx'); %importing acc-data from test 1.3
import7=xlsread('test3.2.xlsx'); %importing acc-data from test 1.2
import8=xlsread('test3.3.xlsx'); %importing acc-data from test 1.3
```

```
%test 1
y12=import1(:,1);                %Using data from channel 1(mid long wall)
y13=import2(:,1);                %Using data from channel 1(mid long wall)
%plot raw test data
figure(1)
plot (y12)
title('Raw data Test 1, excitation 1')
xlabel('sample')
ylabel('Magnitude')
figure(2)
plot(y13)
title('Raw data Test 1, excitation 2')
xlabel('sample')
ylabel('Magnitude')

%test 2
y21=import3(:,1);                %Using data from channel 1(mid first wall)
y22=import4(:,1);                %Using data from channel 1(mid first wall)
y23=import4(:,1);                %Using data from channel 1(mid first wall)
%plot raw test data
figure(3)
plot(y21)
title('Raw data Test 2, excitation 1')
xlabel('sample')
ylabel('Magnitude')
figure(4)
plot(y22)
title('Raw data Test 2, excitation 2')
xlabel('sample')
ylabel('Magnitude')
figure(5)
plot(y23)
title('Raw data Test 2, excitation 3')
xlabel('sample')
ylabel('Magnitude')
```

```
%test 3
y31=import6(:,2);                %Using data from channel 2(mid wall)
y32=import7(:,2);                %Using data from channel 2(mid wall)
y33=import8(:,2);                %Using data from channel 2(mid wall)

%plot raw test data
figure(6)
plot(y31)
title('Raw data Test 3, excitation 1')
xlabel('sample')
ylabel('Magnitude')
figure(7)
plot(y32)
title('Raw data Test 3, excitation 2')
xlabel('sample')
ylabel('Magnitude')
figure(8)
plot(y33)
title('Raw data Test 3, excitation 3')
xlabel('sample')
ylabel('Magnitude')
```

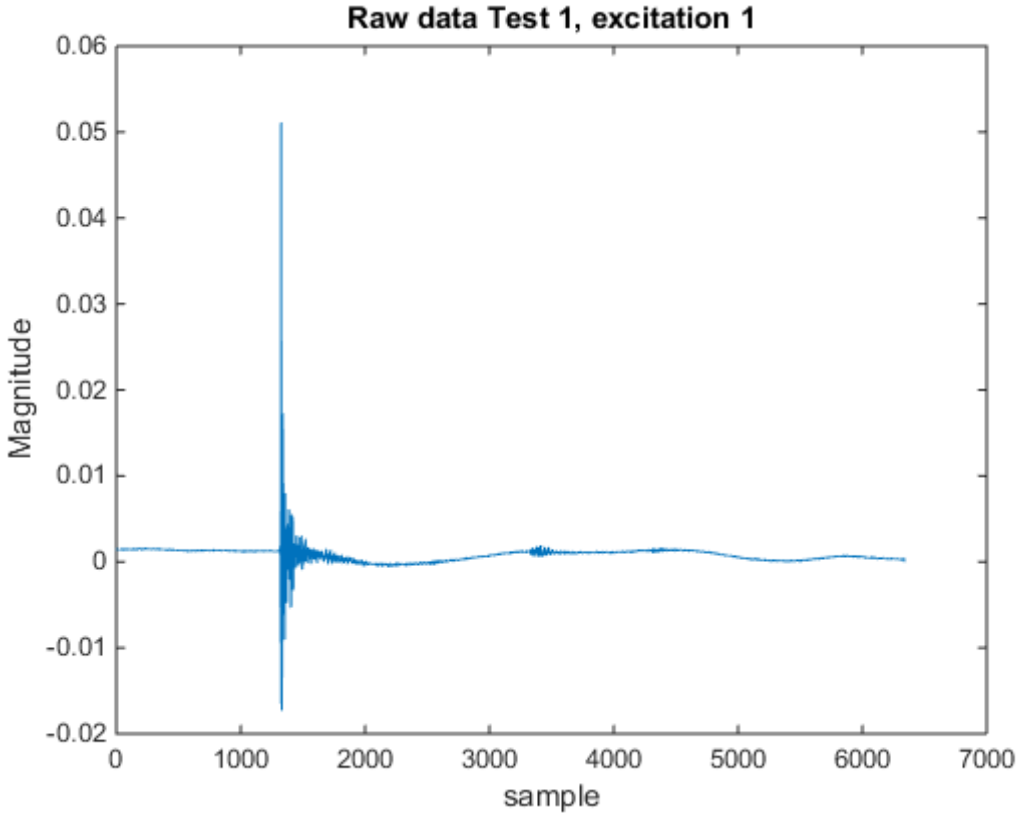
Raw data Test 1, excitation 1
Magnitude
sample
0.06
0.05
0.04
0.03
0.02
0.01
0
-0.01
-0.02
0
1000
2000
3000
4000
5000
6000
7000

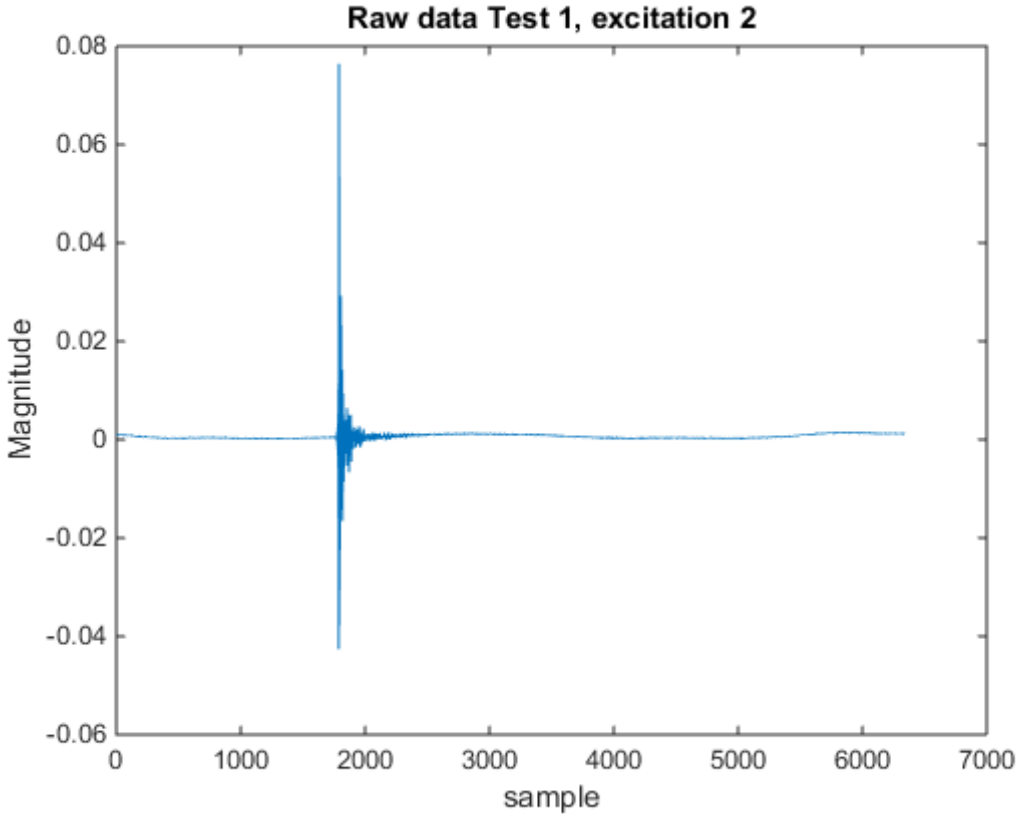
Raw data Test 1, excitation 2
Magnitude
sample
0.08
0.06
0.04
0.02
0
-0.02
-0.04
-0.06
0
1000
2000
3000
4000
5000
6000
7000

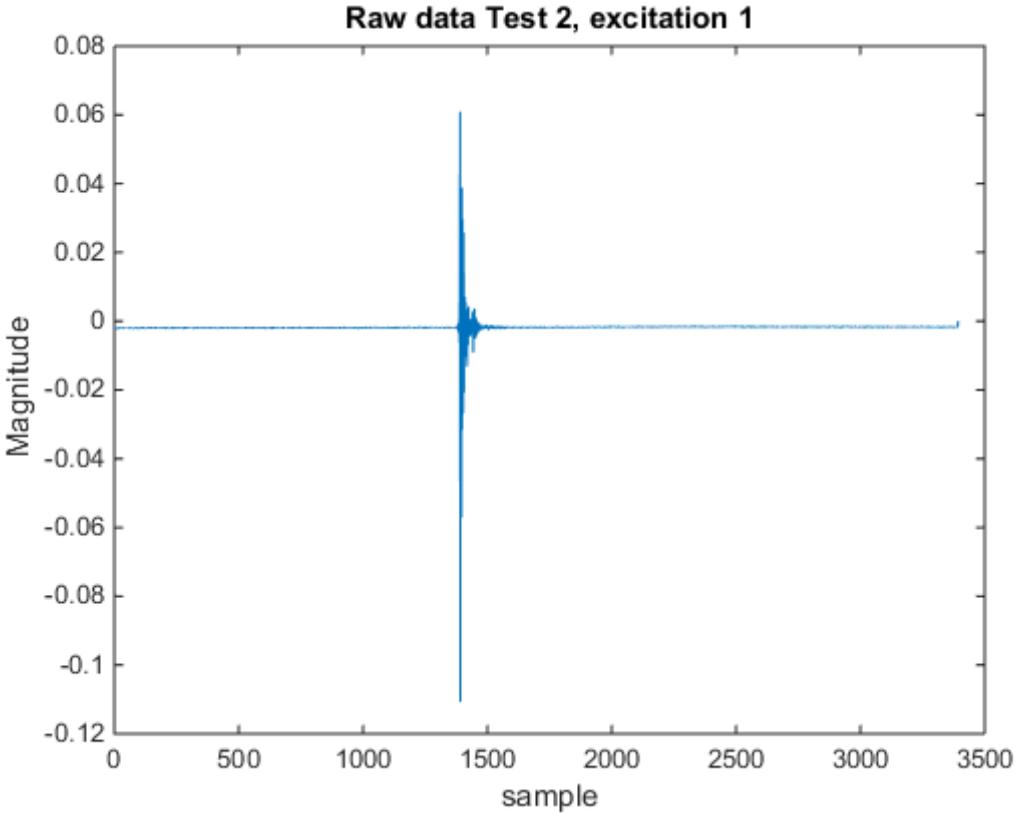
Raw data Test 2, excitation 1
Magnitude
sample
0.08
0.06
0.04
0.02
0
-0.02
-0.04
-0.06
-0.08
-0.1
-0.12
0
500
1000
1500
2000
2500
3000
3500

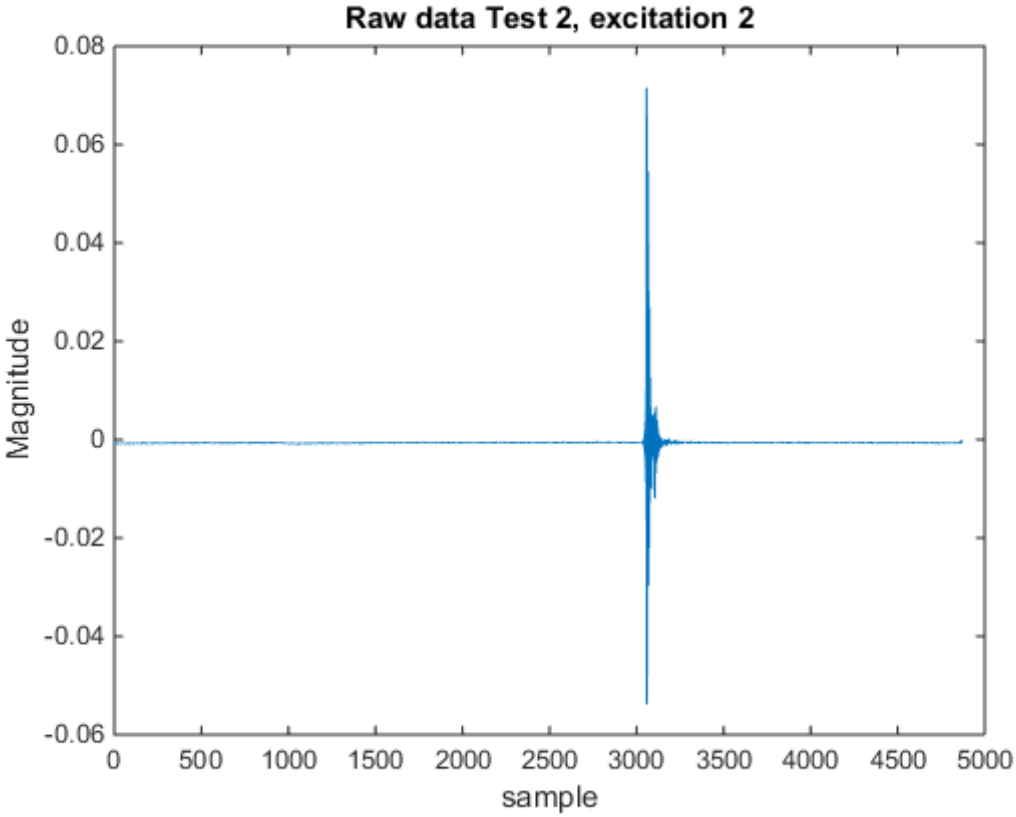
Raw data Test 2, excitation 2
Magnitude
sample
0.08
0.06
0.04
0.02
0
-0.02
-0.04
-0.06
0
500
1000
1500
2000
2500
3000
3500
4000
4500
5000

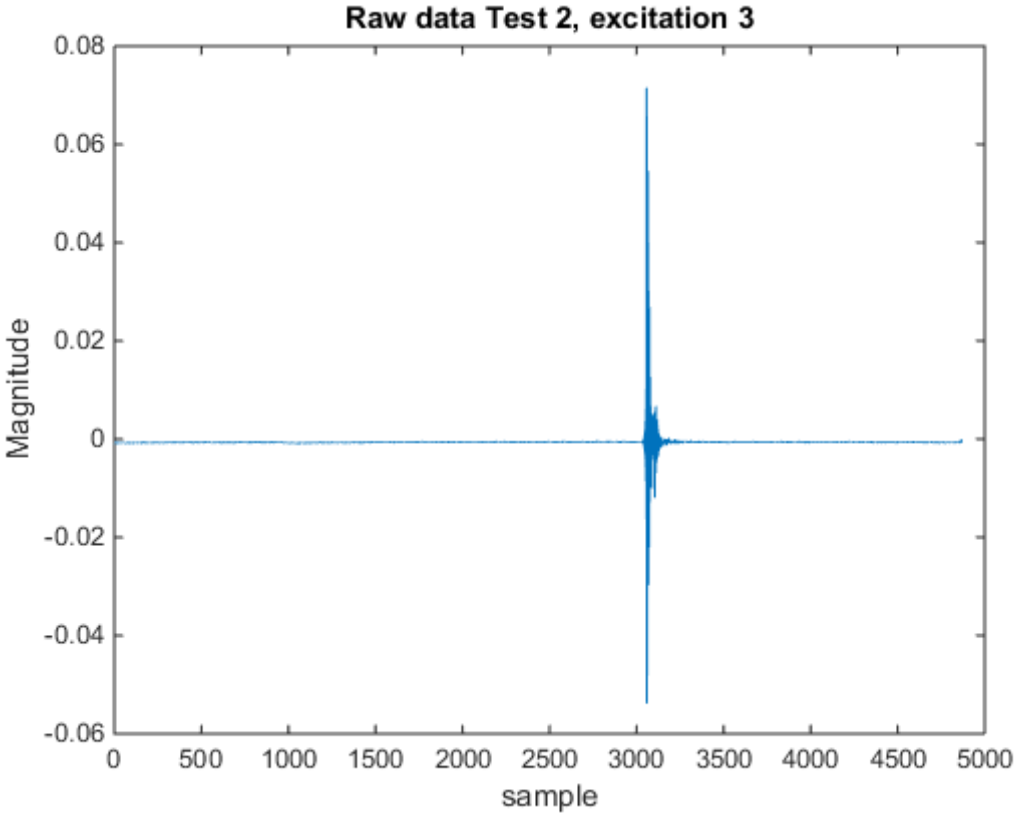
Raw data Test 2, excitation 3
Magnitude
sample
0.08
0.06
0.04
0.02
0
-0.02
-0.04
-0.06
0
500
1000
1500
2000
2500
3000
3500
4000
4500
5000

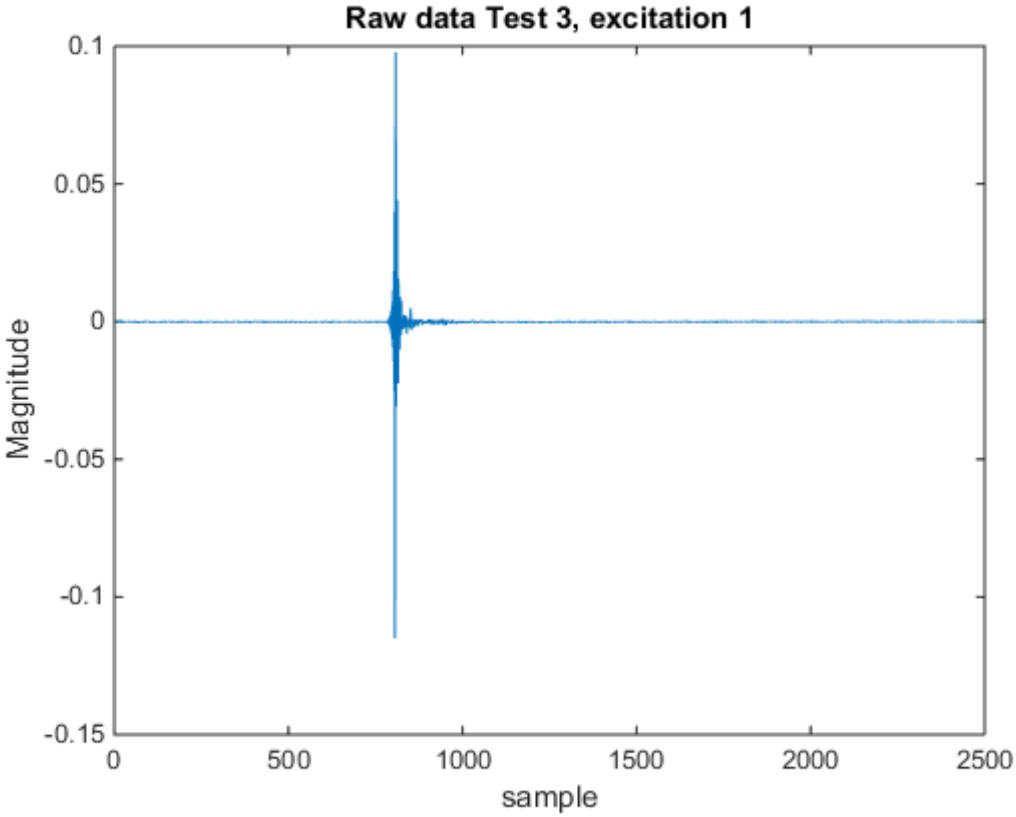
Raw data Test 3, excitation 1
Magnitude
sample
0.1
0.05
0
-0.05
-0.1
-0.15
0
500
1000
1500
2000
2500

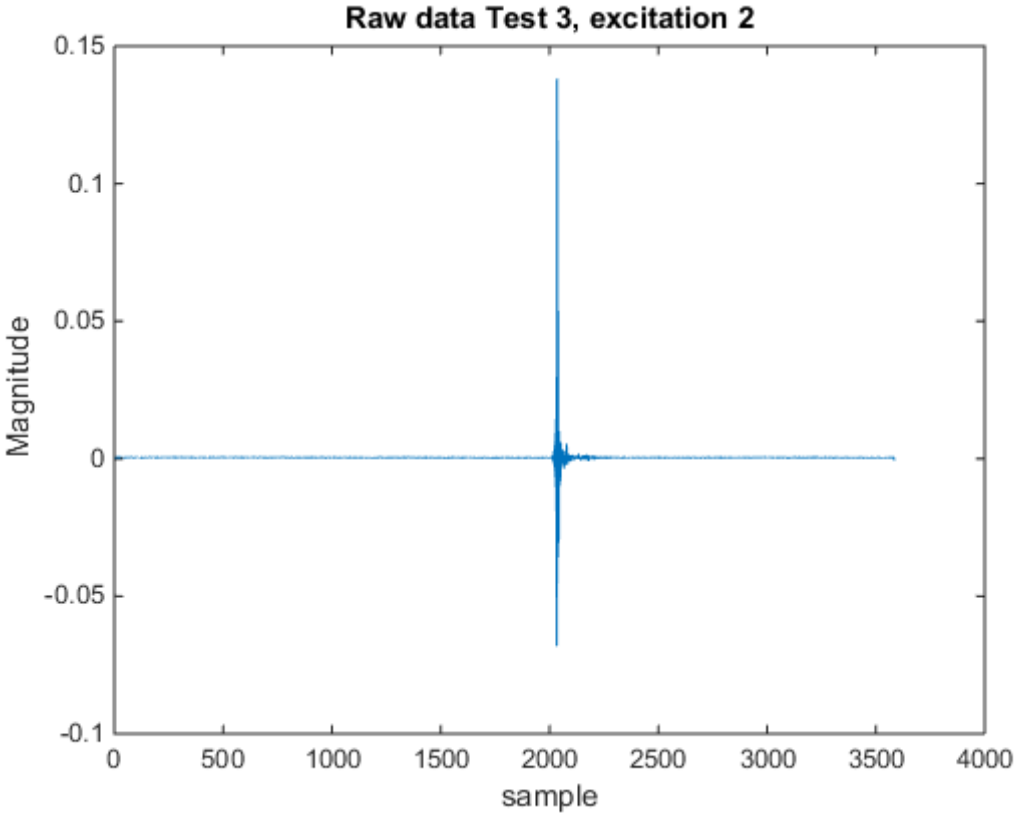

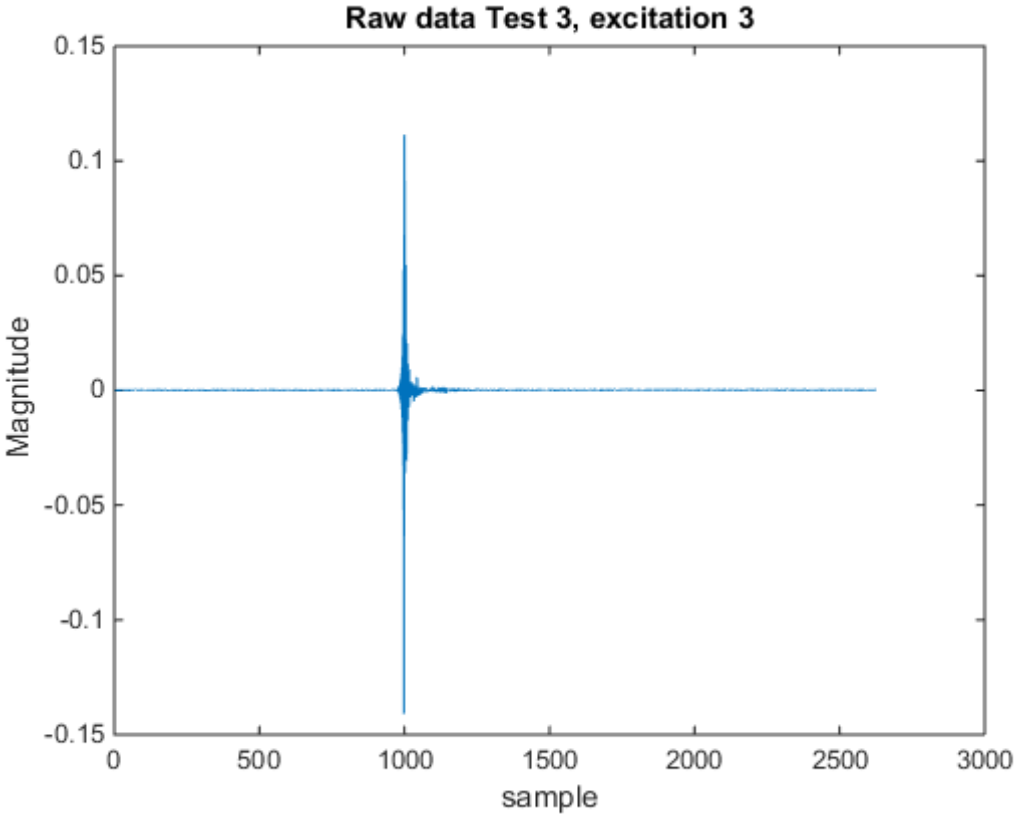


```
fs=600;                          %[Hz]-Sampling rate
```

```
%test 1
y1={y12, y13};
yal1=[];
for i=1:length(y1);
    yinitial=y1{i};
y1{i}=y1{i}-yinitial(1);              %shifting for start at 0
yshift=y1{i};
[mx,ind]=max(yshift);                 %find time of impact test
yshift=yshift(ind-25:ind+1775);       %cut series 25 samples before impact
                                      %and after 1750 samples
yal1=[yal1,yshift];
yal1(:,i)=yal1(:,i)/max(yal1(:,i));   %Norming data for absolute max value
end
yav1=(yal1(:,1)+yal1(:,2))/2;              %Averaging of the two tests
yfilt1=idfilt(yav1,[0, 0.8 ],'noncausal'); %filtering function with cut-off
                                           %at 60% of Nyqf=300 hz
%test 2
y2={y21, y22, y23};
yal2=[];
for i=1:length(y2);
    yinitial=y2{i};
y2{i}=y2{i}-yinitial(1);              %shifting for start at 0
yshift=y2{i};
[mx,ind]=max(yshift);                 %find time of impact
yshift=yshift(ind-25:ind+1775);       %cut series 25 samples before impact
                                      %and after 1750 samples
yal2=[yal2,yshift];
yal2(:,i)=yal2(:,i)/max(yal2(:,i));   %Norming data for absolute max value
end
yav2=(yal2(:,1)+yal2(:,2)+yal2(:,3))/3;    %Averaging of the three tests
yfilt2=idfilt(yav2,[0, 0.8 ],'noncausal'); %filtering function with cut-off
                                           %at 80% of Nyqf=300 hz
%test 3
y3={y31, y32, y33};
yal3=[];
for i=1:length(y3);
    yinitial=y3{i};
y3{i}=y3{i}-yinitial(1);              %shifting for start at 0
yshift=y3{i};
[mx,ind]=max(yshift);                 %find time of impact
yshift=yshift(ind-25:ind+1500);       %cut series 25 samples before impact
                                      %and after 1750 samples
yal3=[yal3,yshift];
yal3(:,i)=yal3(:,i)/max(yal3(:,i));   %Norming data for absolute max value
end
yav3=(yal3(:,1)+yal3(:,2)+yal3(:,3))/3;    %Averaging of the three tests
yfilt3=idfilt(yav3,[0, 0.8 ],'noncausal'); %filtering function with cut-off
                                           %at 80% of Nyqf=300 hz
```

```
%Plotting data
%test 1
```

```
x1=(1:length(yav1))/fs;                         %defining x-vector
figure(9)
plot(x1',yal1(:,1),'--',x1',yal1(:,2)...
    ,'--',x1',yav1,'LineWidth',1.0) %Plotting raw data
                                    %and averaged data
xlim([0;0.25])                      %Interesting part is up to 1 sec
title('Raw Data and Averaged Data Test 1')
xlabel('t [s]')
ylabel('Rel. Acceleration')
legend('Raw-Hit1','Raw-Hit2','Average')

figure (10)
plot(x1',yav1,'--',x1',yfilt1)          %Plotting averaged raw data
                                        %and filtered data
xlim([0;0.25])                          %Interesting part is up to 1 sec
title('Filtered Data and Averaged Data Test 1')
xlabel('t [s]')
ylabel('Rel. Acceleration')
legend('Average','Filtered')


%test 2
x2=(1:length(yav2))/fs;                         %defining x-vector
figure(11)
plot(x2',yal2(:,1),'--',x2',yal2(:,2),'--',x2',...
    yal2(:,3),'--',x2',yav2)    %Plotting raw data and averaged data
xlim([0;0.25])                              %Interesting part is up to 1 sec
title('Raw Data and Averaged Data Test 2')
xlabel('t [s]')
ylabel('Rel. Acceleration')
legend('Raw-Hit1','Raw-Hit2','Raw-Hit3','Average')

figure (12)
plot(x2',yav2,'--',x2',yfilt2)  %Plotting averaged raw data
                                    %and filtered data
xlim([0;0.25])                          %Interesting part is up to 1 sec
title('Filtered Data and Averaged Data Test 2')
xlabel('t [s]')
ylabel('Rel. Acceleration')
legend('Average','Filtered')


%test 3
x3=(1:length(yav3))/fs;                         %defining x-vector
figure(13)
plot(x3',yal3(:,1),'--',x3',yal3(:,2),'--',x3',...
    yal3(:,3),'--',x3',yav3)    %Plotting raw data and averaged raw data
xlim([0;0.25])                          %Interesting part is up to 1 sec
title('Raw Data and Averaged Data Test 3')
xlabel('t [s]')
ylabel('Rel. Acceleration')
legend('Raw-Hit1','Raw-Hit2','Raw-Hit3','Average')
```

```
figure (14)
plot(x3',yav3,'--',x3',yfilt3)  %Plotting averaged raw data
                                      %and filtered data
xlim([0;0.25])                          %Interesting part is up to 1 sec
title('Filtered Data and Averaged Data Test 3')
xlabel('t [s]')
ylabel('Rel. Acceleration')
legend('Average','Filtered')
```

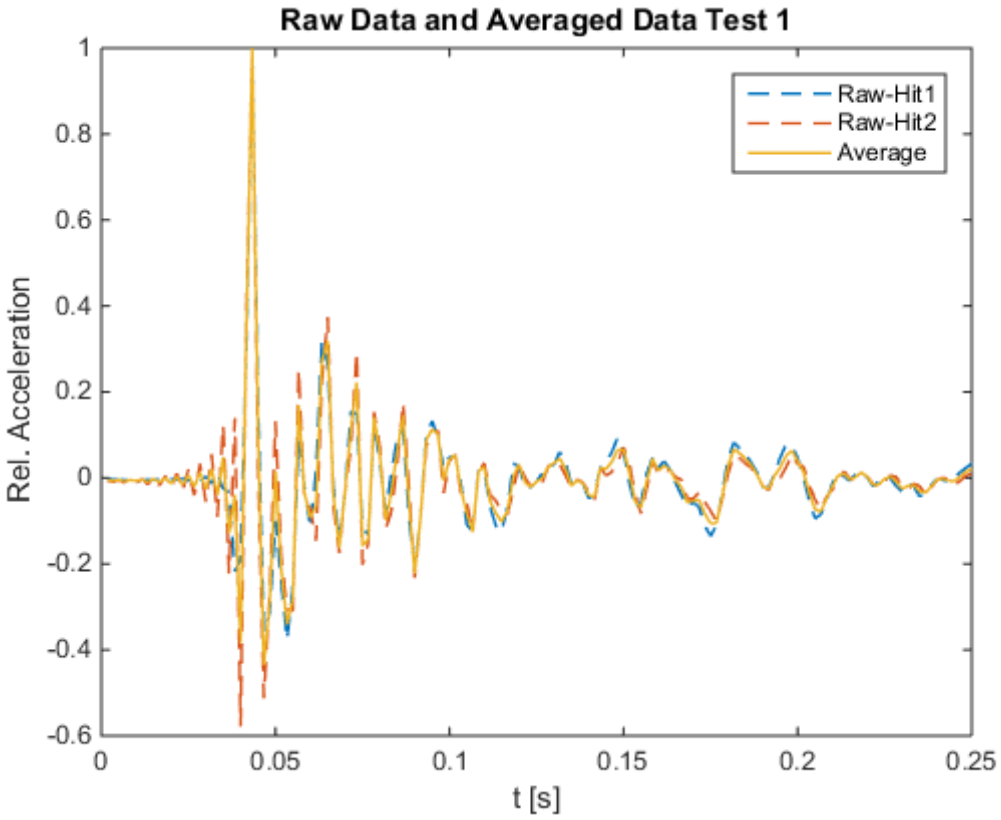
Raw Data and Averaged Data Test 1
Raw-Hit1
Raw-Hit2
Average
Rel. Acceleration
t [s]
1
0.8
0.6
0.4
0.2
0
-0.2
-0.4
-0.6
0
0.05
0.1
0.15
0.2
0.25

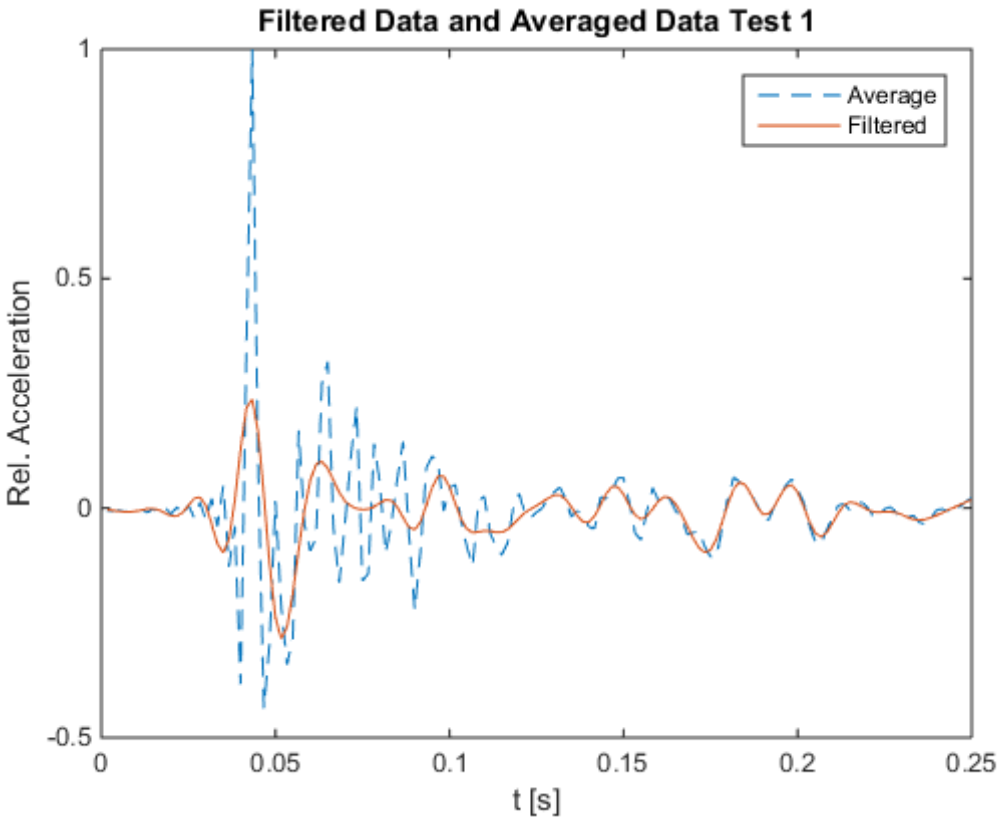
Filtered Data and Averaged Data Test 1
Average
Filtered
Rel. Acceleration
t [s]
1
0.5
0
-0.5
0
0.05
0.1
0.15
0.2
0.25

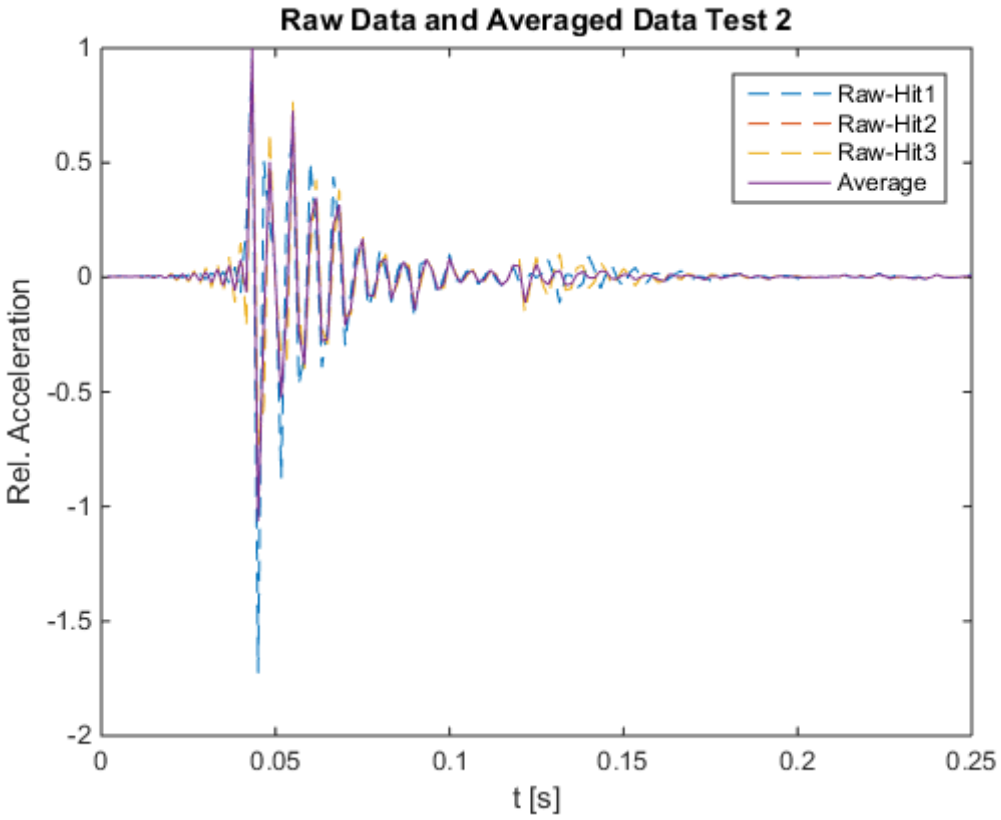
Raw Data and Averaged Data Test 2
Raw-Hit1
Raw-Hit2
Raw-Hit3
Average
Rel. Acceleration
t [s]
1
0.5
0
-0.5
-1
-1.5
-2
0
0.05
0.1
0.15
0.2
0.25

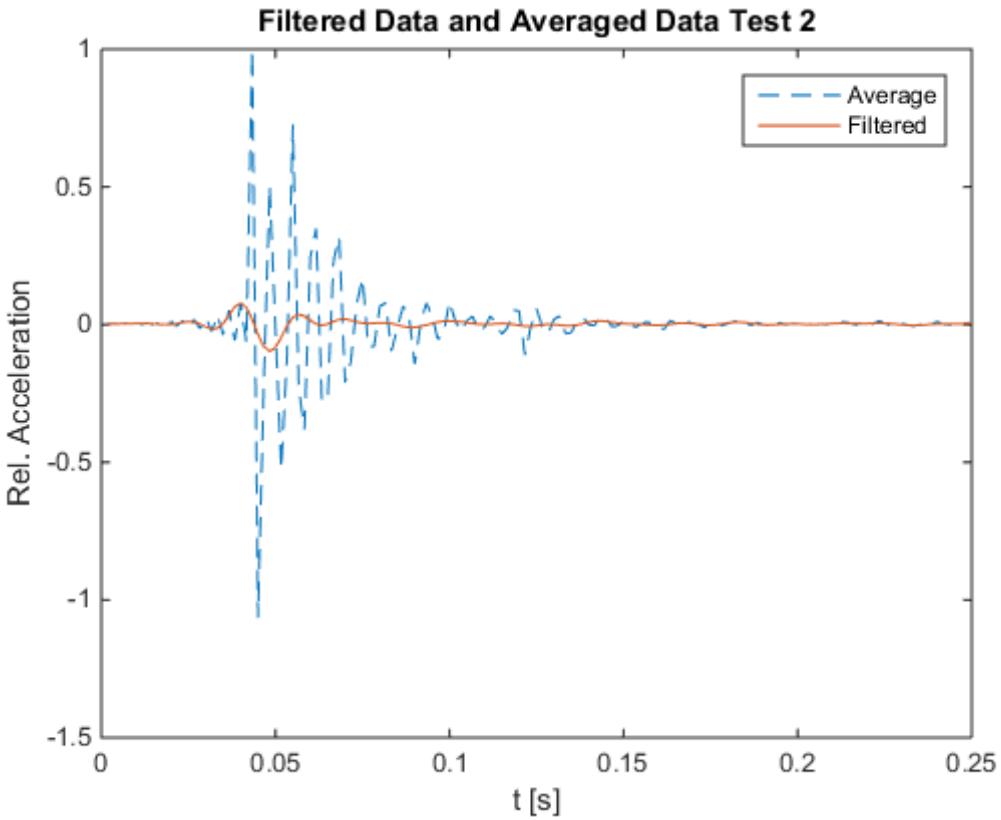
Filtered Data and Averaged Data Test 2
Average
Filtered
Rel. Acceleration
t [s]
1
0.5
0
-0.5
-1
-1.5
0
0.05
0.1
0.15
0.2
0.25

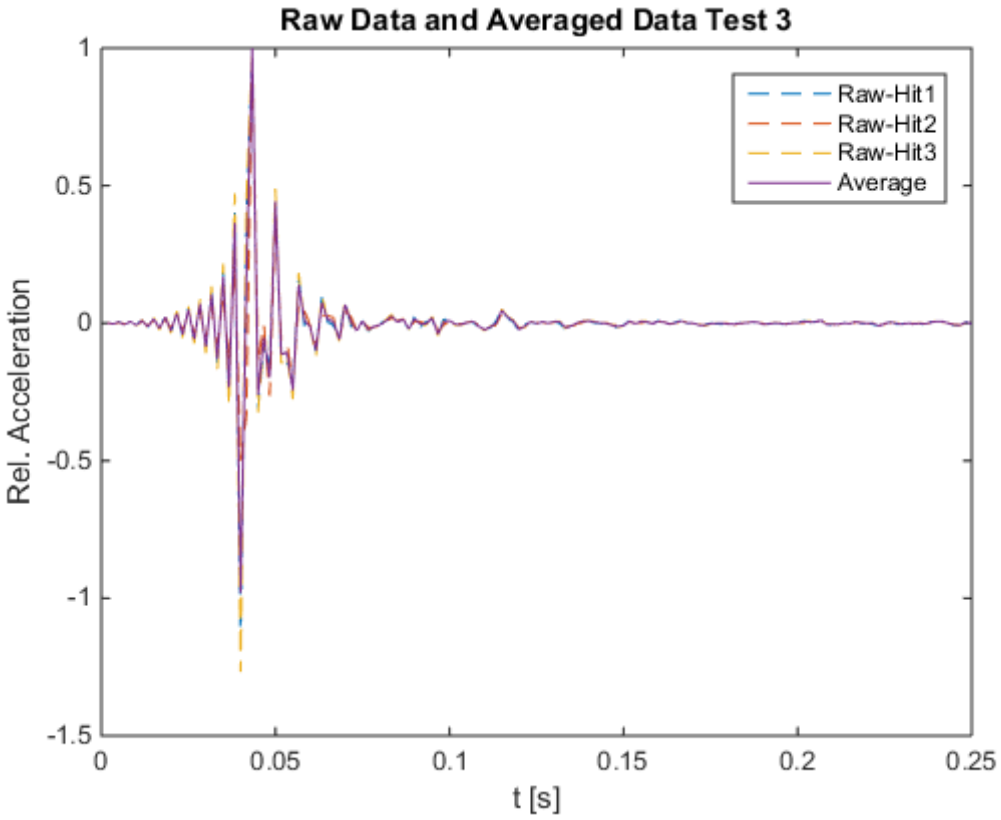
Raw Data and Averaged Data Test 3
Raw-Hit1
Raw-Hit2
Raw-Hit3
Average
Rel. Acceleration
t [s]
1
0.5
0
-0.5
-1
-1.5
0
0.05
0.1
0.15
0.2
0.25

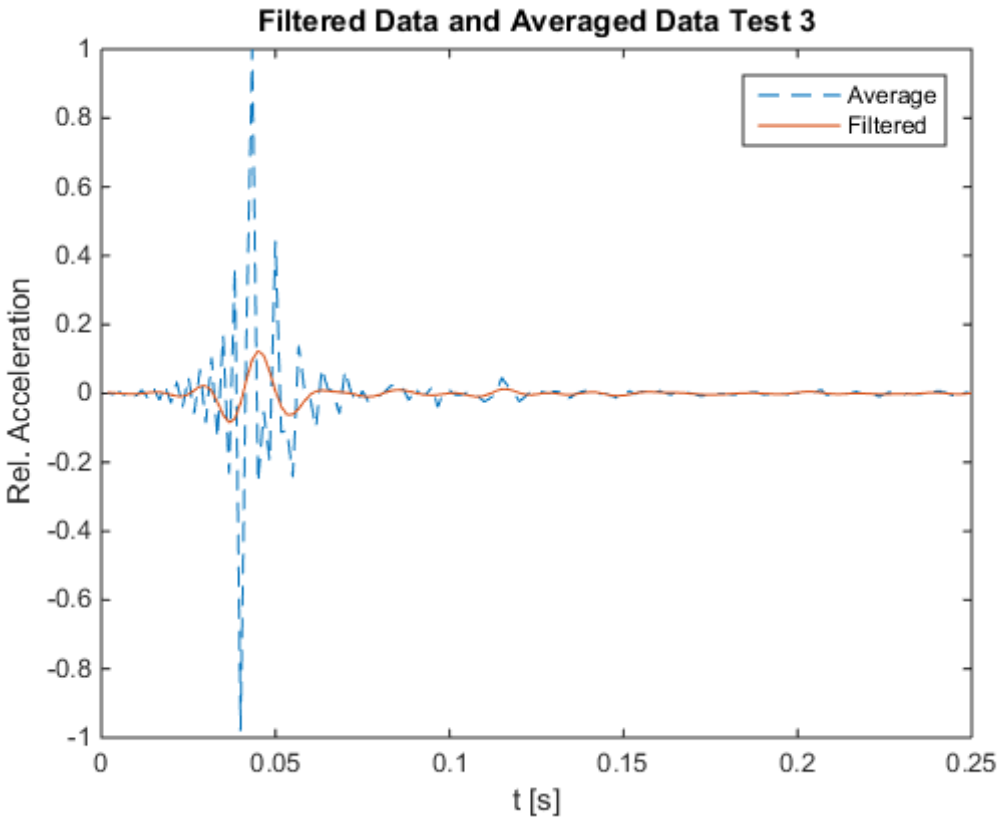
Filtered Data and Averaged Data Test 3
Average
Filtered
Rel. Acceleration
t [s]
1
0.8
0.6
0.4
0.2
0
-0.2
-0.4
-0.6
-0.8
-1
0
0.05
0.1
0.15
0.2
0.25

```
%Fast Fourier Transform of the filtered function
N=1024;                                 %Resolution of fft/number of w
k=-N/2:N/2-1;
freq1=fft(yfilt1,N);                    %fft of filtered function
freq2=fft(yfilt2,N);                    %fft of filtered function
freq3=fft(yfilt3,N);                    %fft of filtered function

%test 1
figure (15)
plot(k*fs/N,fftshift(abs(freq1)))       %plot of shifted vector with
                                        %correction of time step
xlim([1;0.6*fs/2])                      %Interesting part of the window
title('FFT of Processed Data Test 1')
xlabel('Frequency [Hz]')
ylabel('Y(freq.)')

%test 2
figure (16)
plot(k*fs/N,fftshift(abs(freq2)))       %plot of shifted vector
                                        %with correction of time step
xlim([1;0.6*fs/2])                      %Interesting part of the window
title('FFT of Processed Data Test 2')
xlabel('Frequency [Hz]')
ylabel('Y(freq.)')

%test 3
figure (17)
plot(k*fs/N,fftshift(abs(freq3)))       %plot of shifted vector with
                                        %correction of time step
xlim([1;0.6*fs/2])                      %Interesting part of the window
title('FFT of Processed Data Test 3')
xlabel('Frequency [Hz]')
ylabel('Y(freq.)')
```

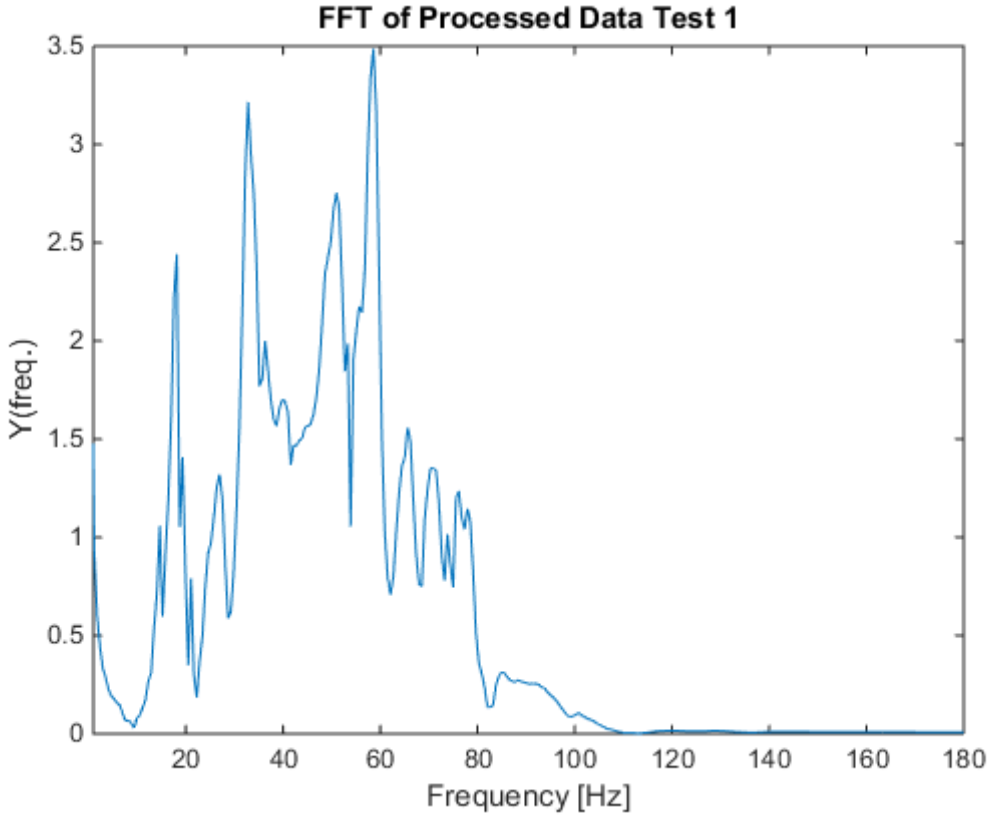
FFT of Processed Data Test 1
Y(freq.)
Frequency [Hz]
0
0.5
1
1.5
2
2.5
3
3.5
20
40
60
80
100
120
140
160
180

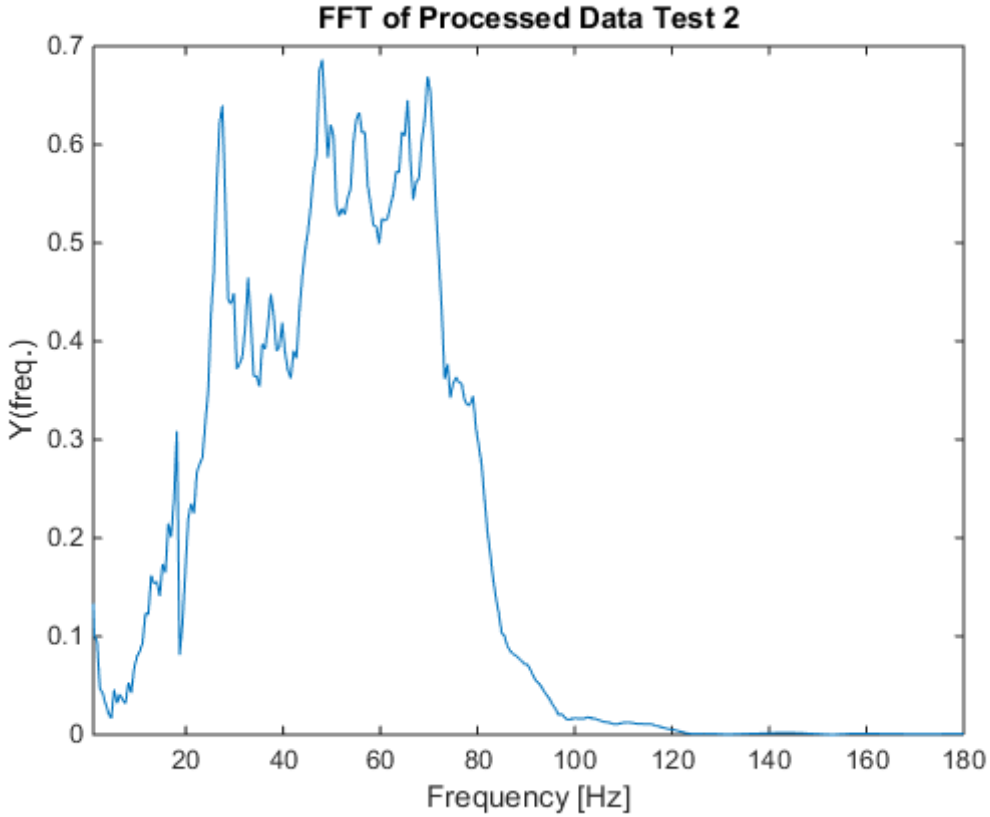
FFT of Processed Data Test 2
Y(freq.)
Frequency [Hz]
0
0.1
0.2
0.3
0.4
0.5
0.6
0.7
20
40
60
80
100
120
140
160
180

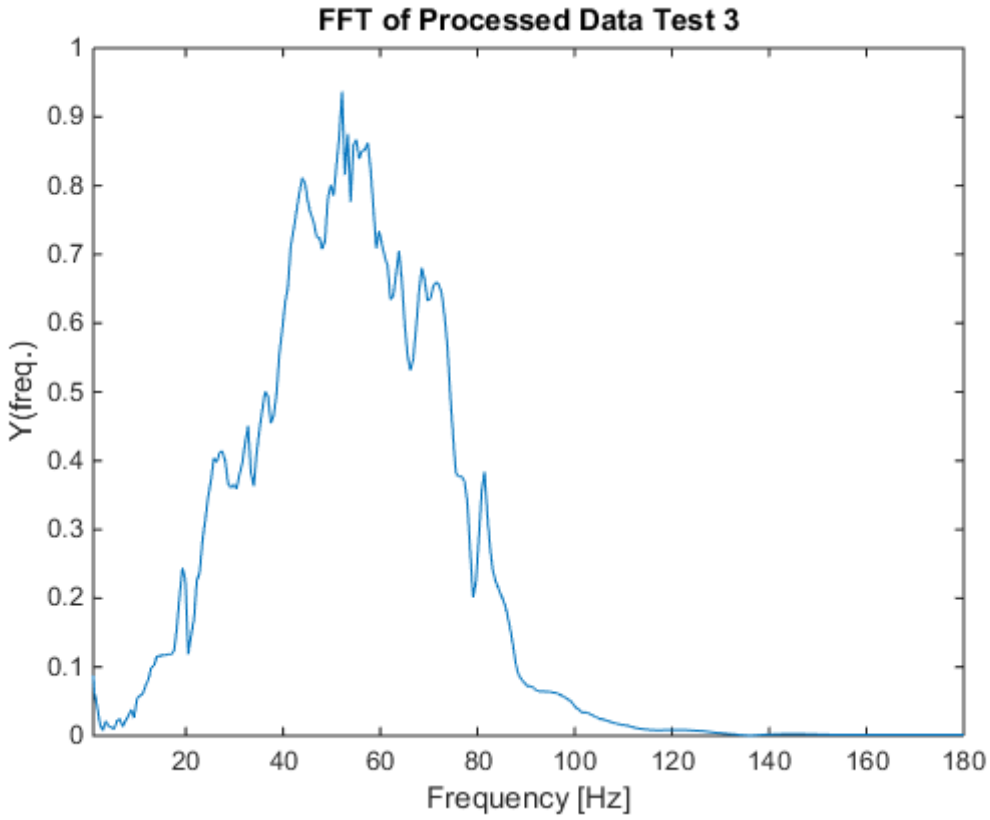

Published with MATLAB® R2014b

Appendix C

Complete Results of Modal Analyses

Appendix C

Iteration 1

In the following section all mode shapes, in the range 0-45 Hz, from the modal analysis with E=2.74 GPa and $\rho = 1548 \frac{kg}{m^3}$ are given including mode number 4 and 8 who showed to be both controllable and observable in Dynamic Test 1.

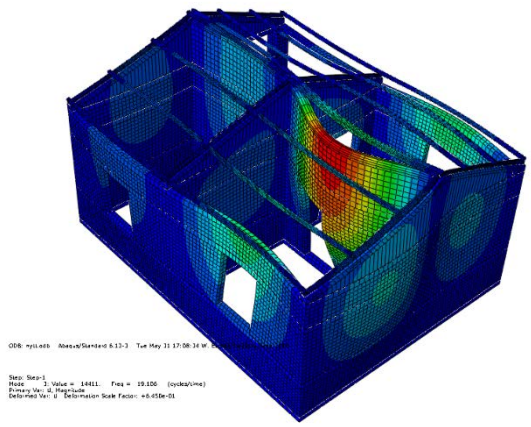

Figure 1 Mode 1

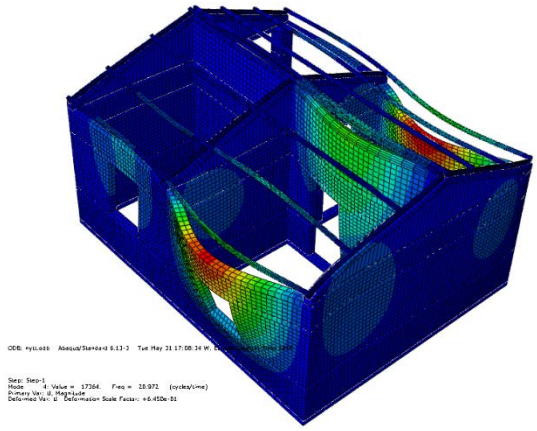

Figure 2 Mode 2

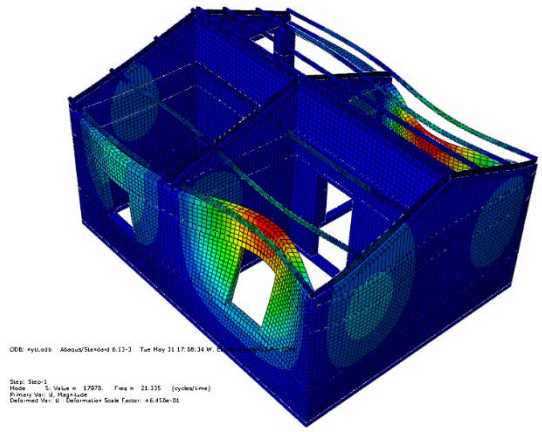

Figure 3 Mode 3

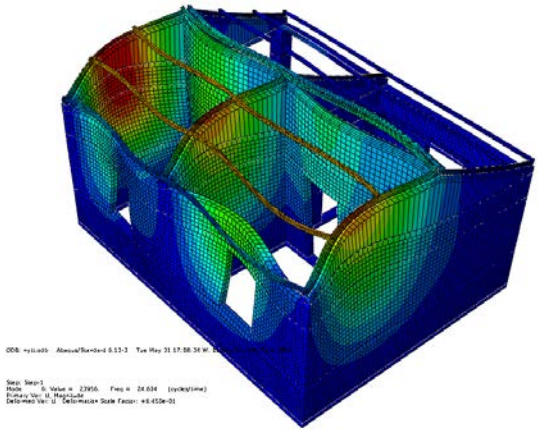

Figure 4 Mode 4

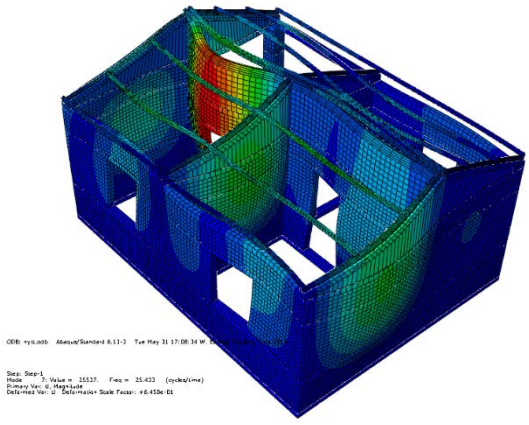

Figure 5 Mode 5

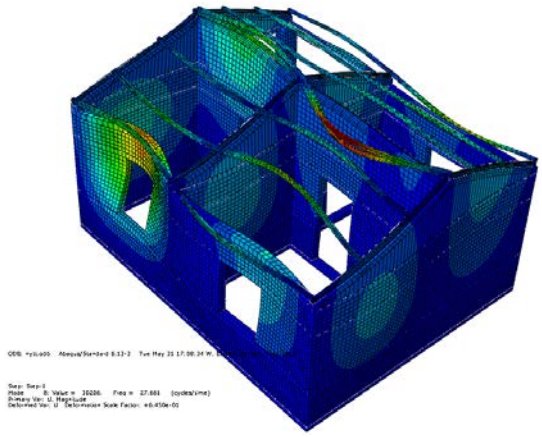

Figure 6 Mode 6

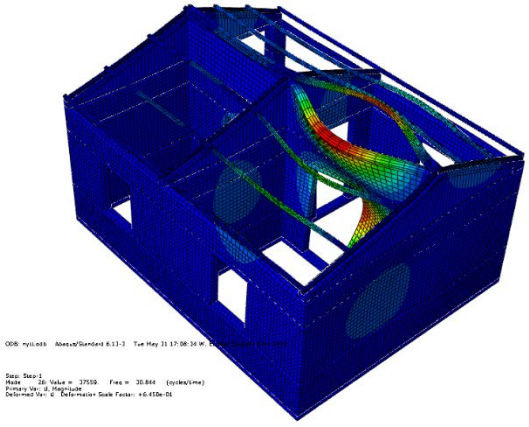

Figure 7 Mode 7

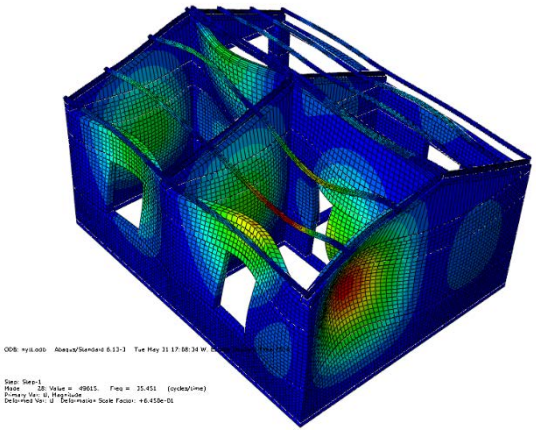

Figure 8 Mode 8

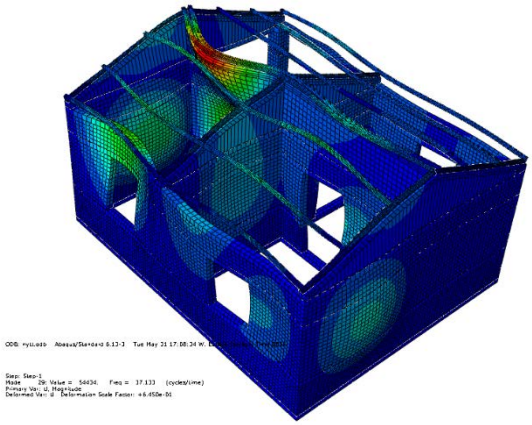

Figure 9 Mode 9

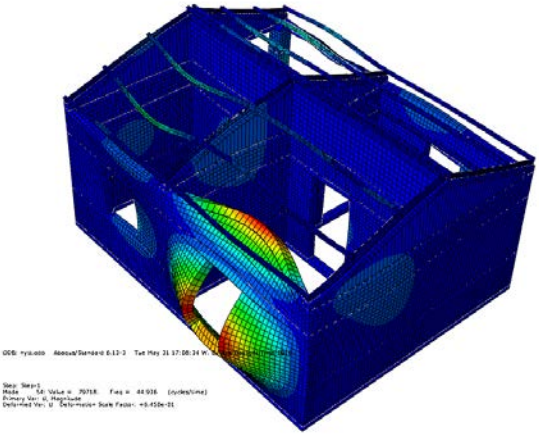

Figure 10 Mode 9

Iteration 2

In the following section all mode shapes, in the range 0-45 Hz, from the modal analysis with E=1.63 GPa and $\rho = 1470 \frac{kg}{m^3}$ are given including mode number 4, 6 and 12 who showed to be both controllable and observable in Dynamic Test 1.

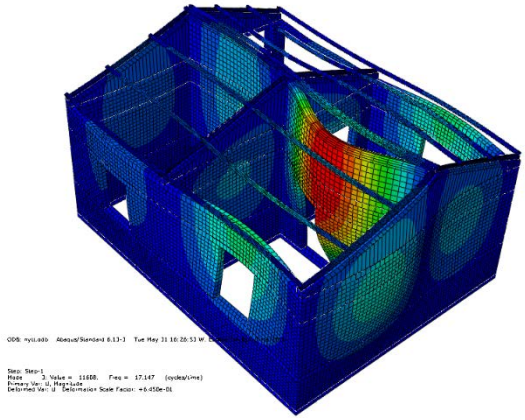

Figure 11 Mode 1

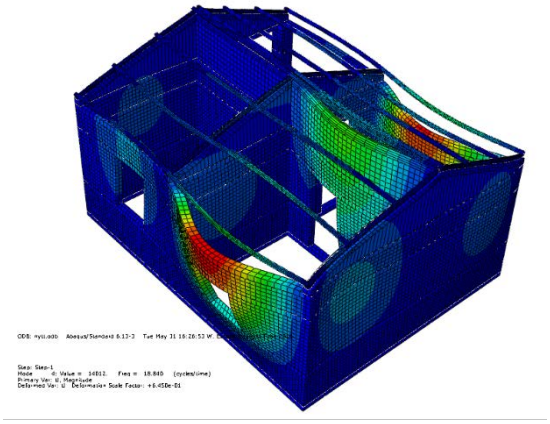

Figure 12 Mode 2

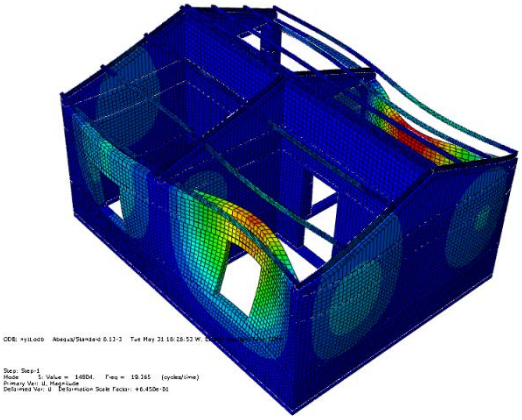

Figure 13 Mode 3

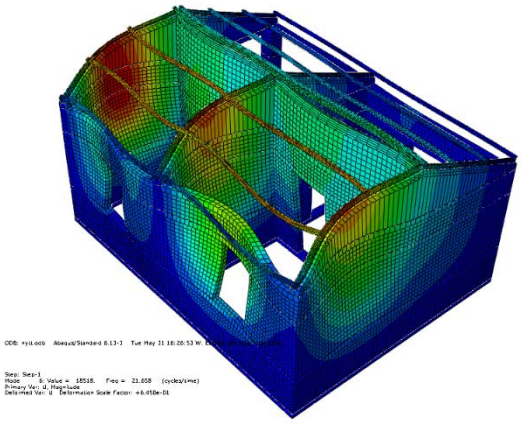

Figure 14 Mode 4

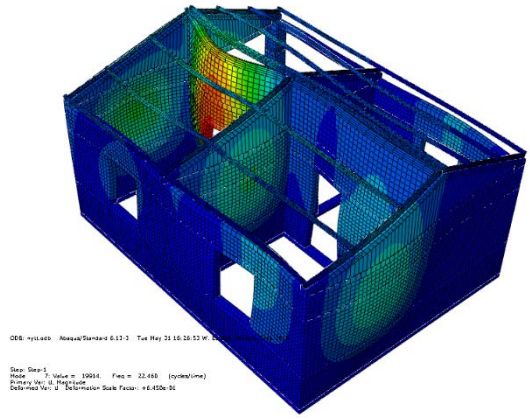

Figure 15 Mode 5

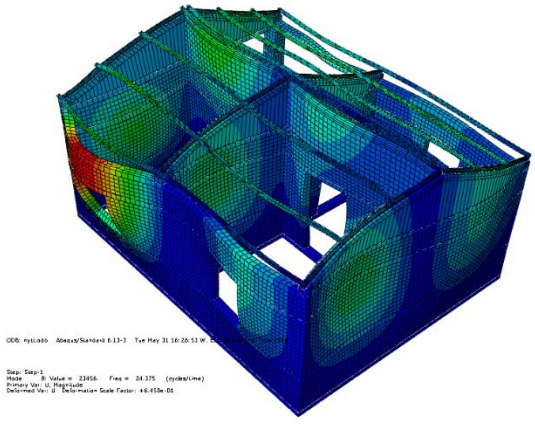

Figure 16 Mode 6

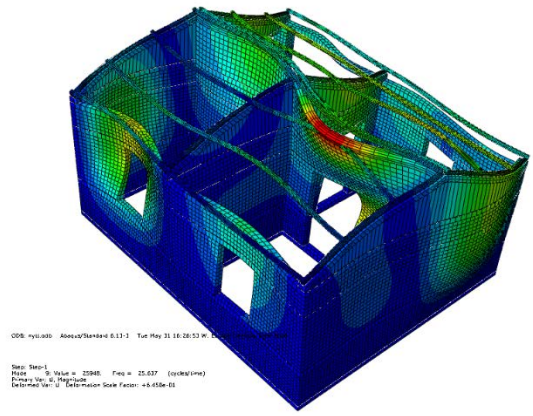

Figure 17 Mode 7

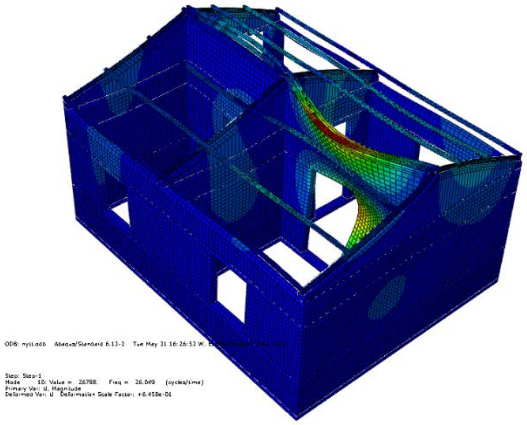

Figure 18 Mode 8

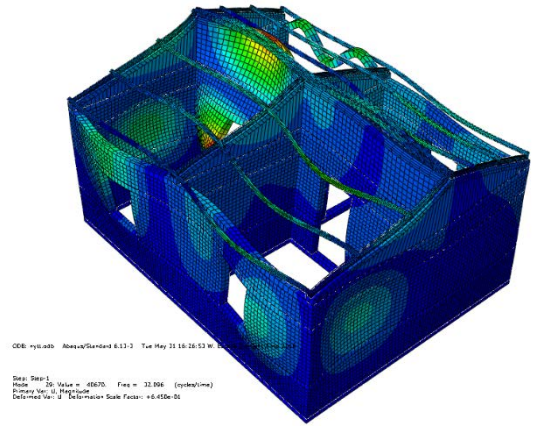

Figure 19 Mode 9

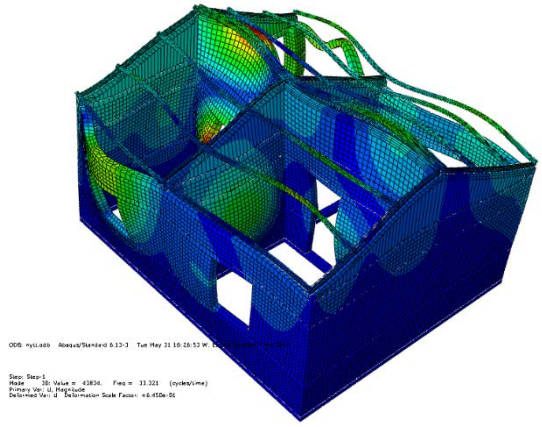

Figure 20 Mode 10

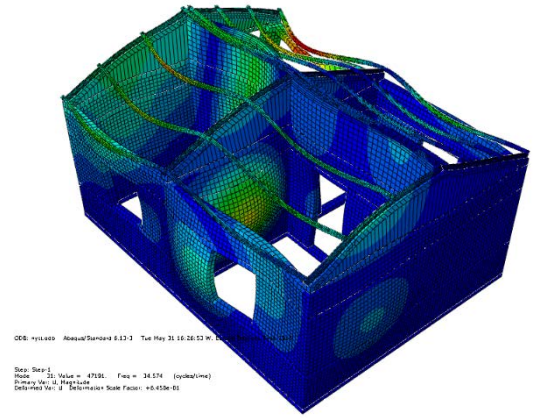

Figure 21 Mode 11

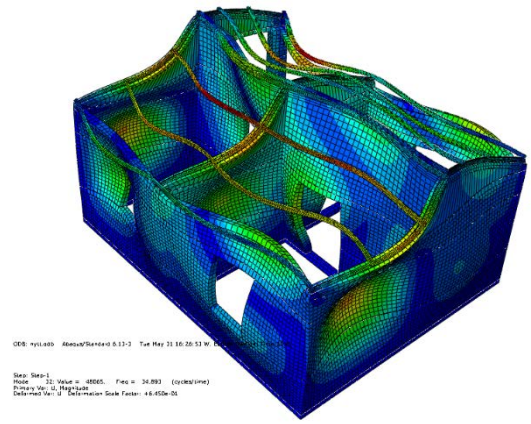

Figure 22 Mode 12

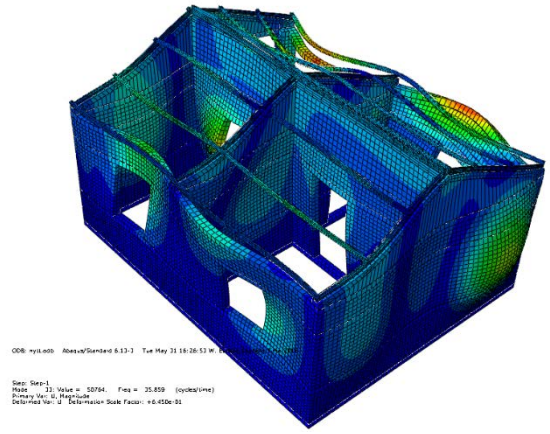

Figure 23 Mode 13

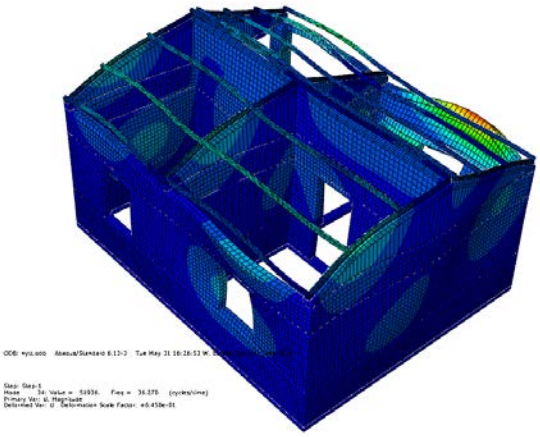

Figure 24 Mode 14

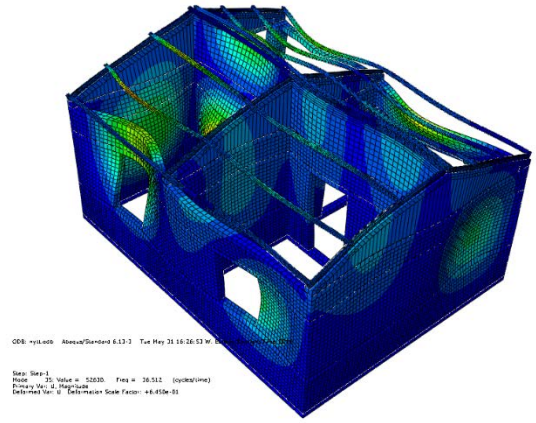

Figure 25 Mode 15

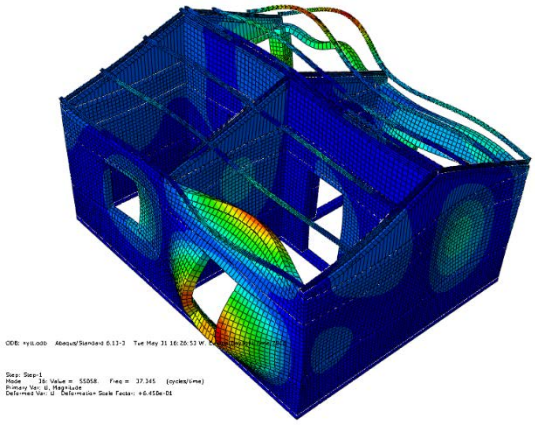

Figure 26 Mode 16

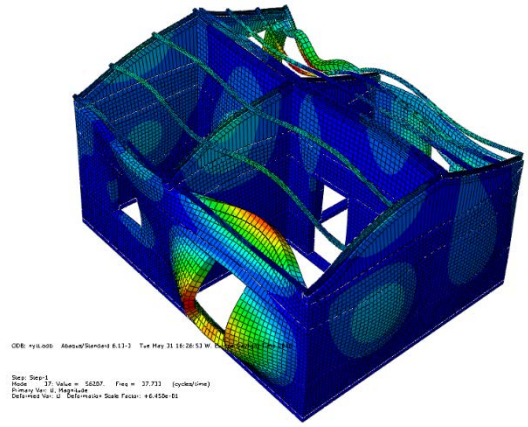

Figure 27 Mode 17

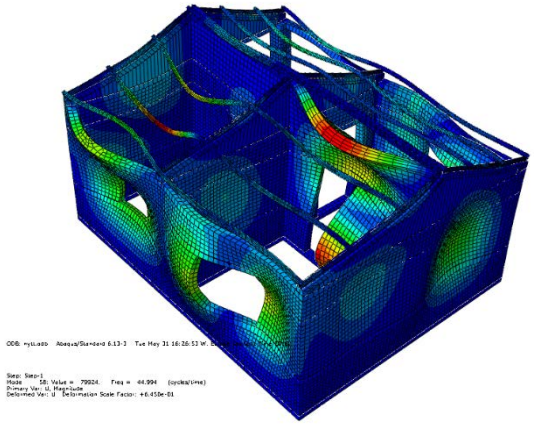

Figure 28 Mode 18

Iteration 3

In the following section all mode shapes, in the range 0-45 Hz, from the modal analysis with E=1.0 GPa and $\rho = 1700 \frac{kg}{m^3}$ are given including mode number 4 who showed to be both controllable and observable in Dynamic Test 1.

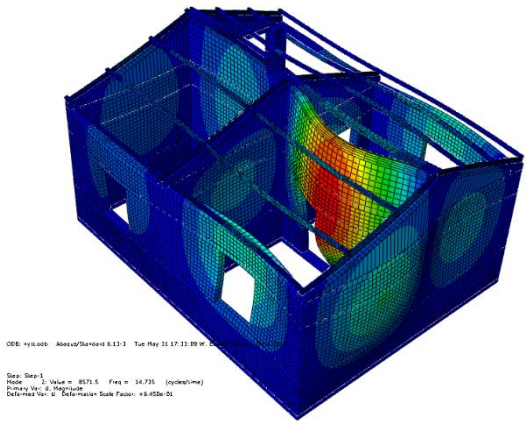

Figure 29 Mode 1

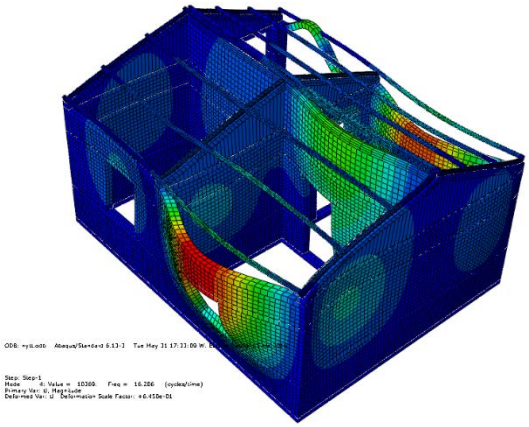

Figure 30 Mode 2

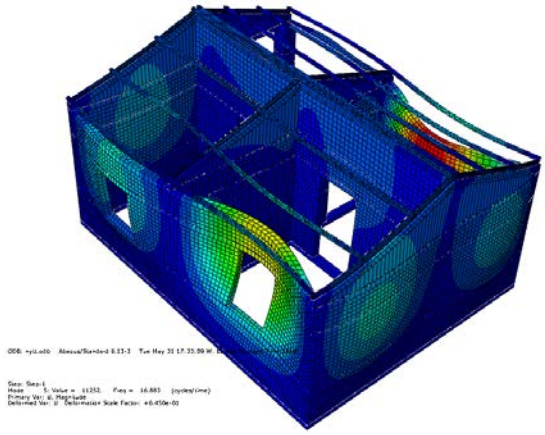

Figure 31 Mode 3

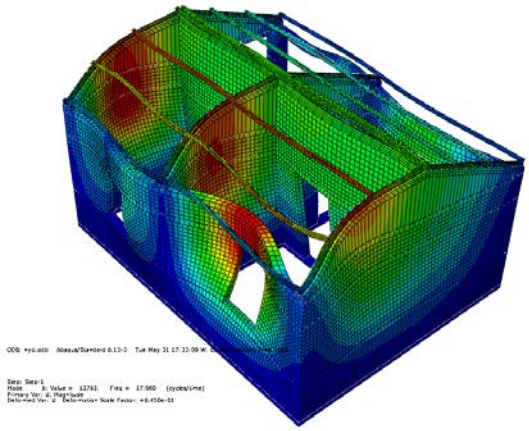

Figure 32 Mode 4

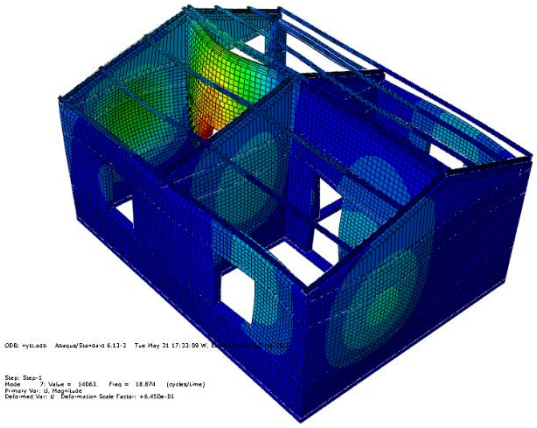

Figure 33 Mode 5

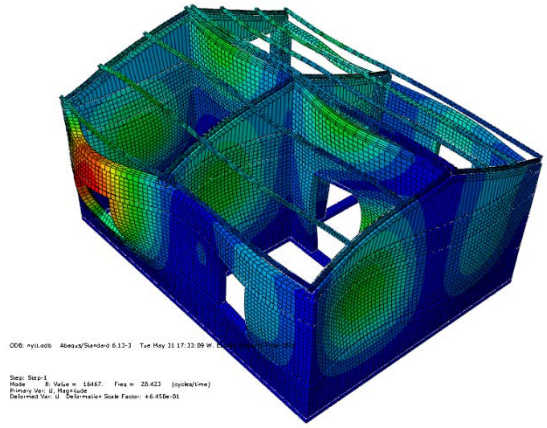

Figure 34 Mode 6

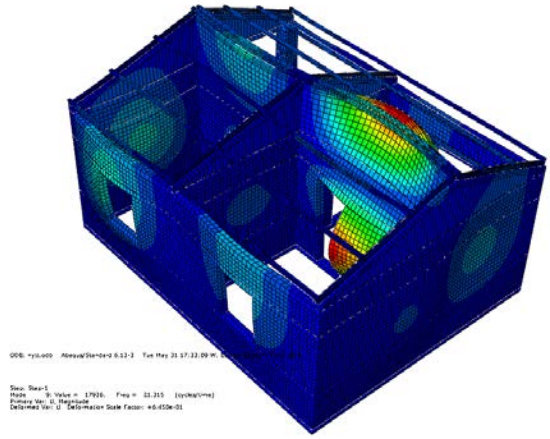

Figure 35 Mode 7

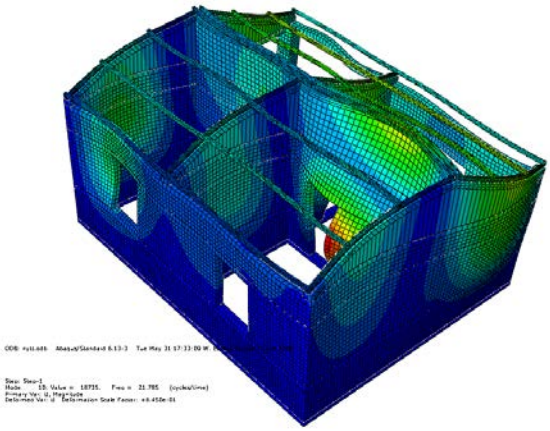

Figure 36 Mode 8

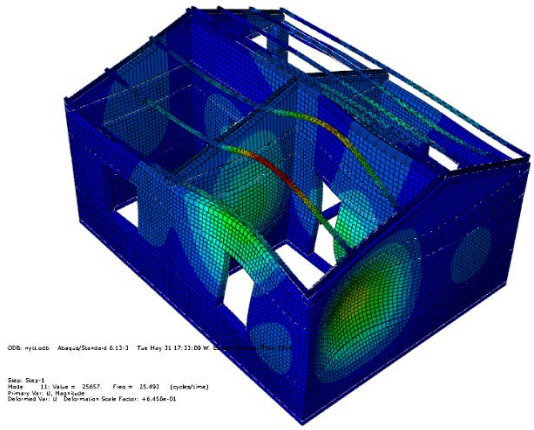

Figure 37 Mode 9

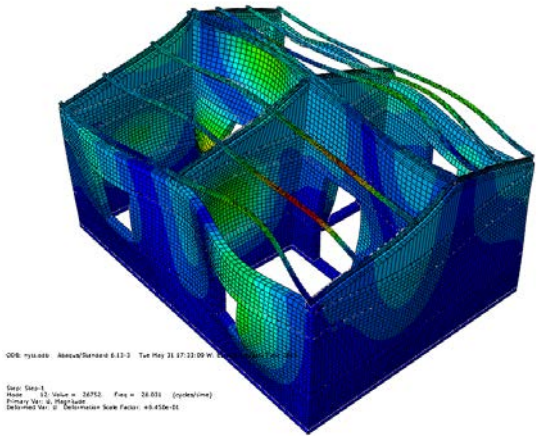

Figure 38 Mode 10

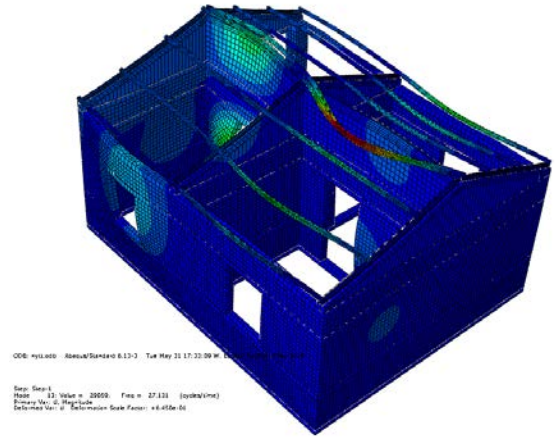

Figure 39 Mode 11

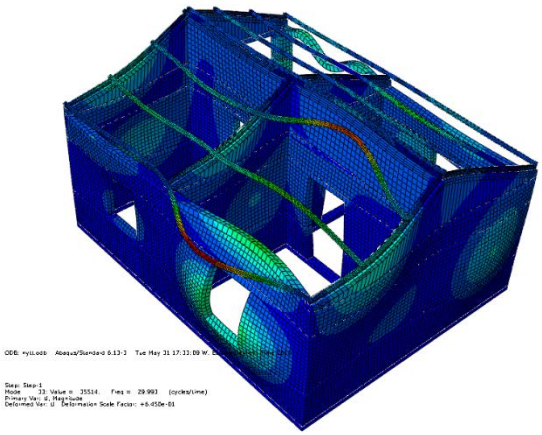

Figure 40 Mode 12

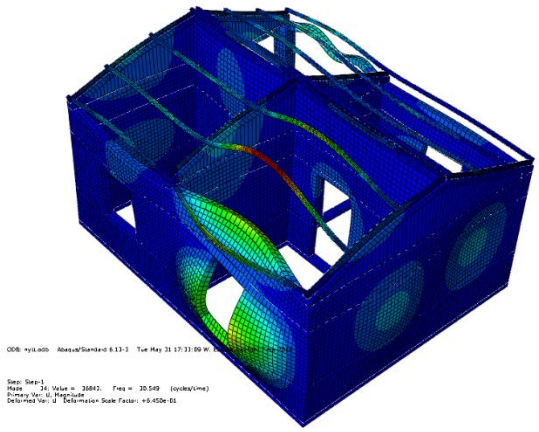

Figure 41 Mode 13

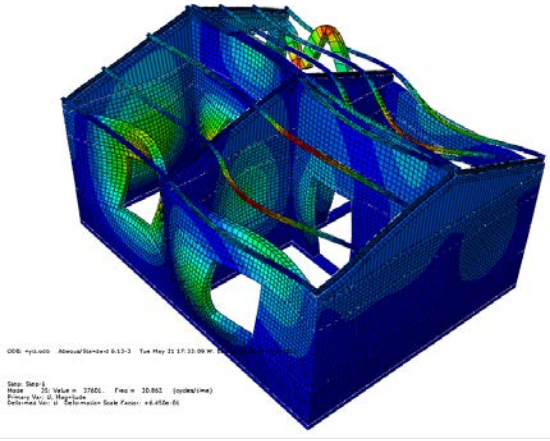

Figure 42 Mode 14

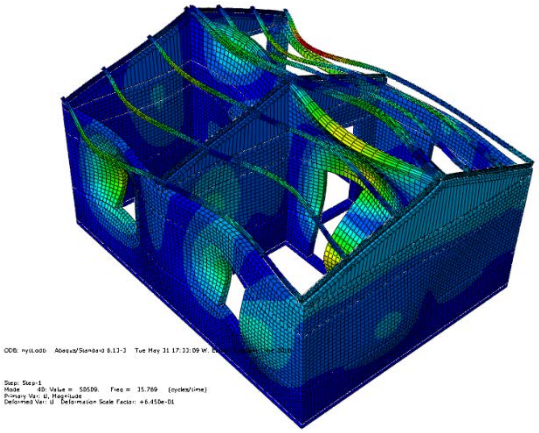

Figure 43 Mode 15

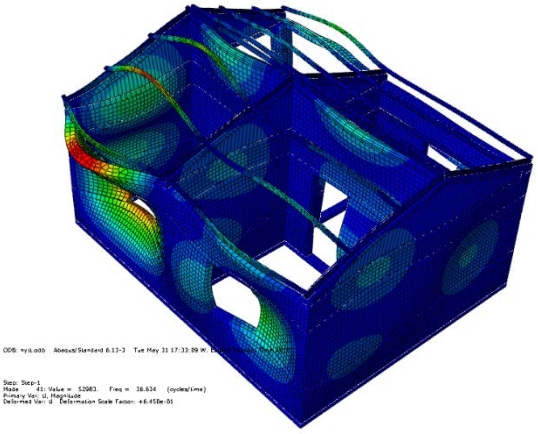

Figure 44 Mode 16

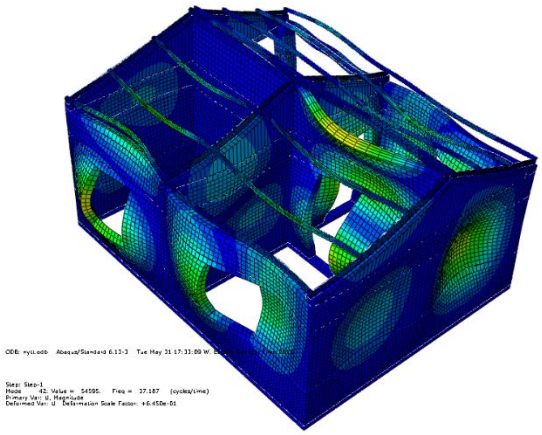

Figure 45 Mode 17

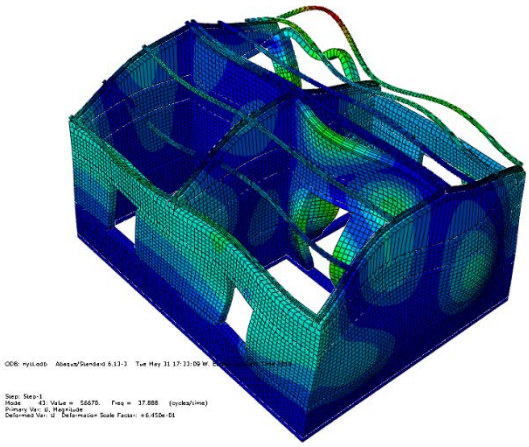

Figure 46 Mode 18

Appendix D

Force Calculations According to NBC 105:1994

Calculation of the Earthquake Effect

NBC 105:1994 5.2 provides that the analysis of earthquake effect should be in accordance with either the Seismic Coefficient Method or the Modal Response Spectrum Method.

The Modal Spectrum Method should be used for:
a) Buildings with irregular configuration
b) Buildings with abrubpt changes in lateral resistance
c) Buildings with abrupt changes in stiffneddd with height
d) Buildings with unusual shape, size or importance.

The building in Majhi Gaun was considered to be fairly regular, with no abrupt changes in neither lateral resistance or stiffness. The shape, size and the importance of the building were not considered unusual. Therefore the Seismic Coefficient Method was used.

In this method the horizontal seismic shear force acting at the base of the structure shall be taken as:

Vb=Cd*Wt

where,

Cd, is the Design Horizontal Seismic Coefficient
Wt, is the seismic mass

According to NBC 105:1994 8.2 for structures with Seismic Resisting Systems located along two perpendicular directions the specified forces may be assumed to act separately along each of these two horizontal directions.

The Design Horizontal Seismic Coefficient, Cd

Cd=C*Z*I*K

where:

C, is the basic seismic coefficient for the fundamental translational period T1.
Z, is the Sesmic Zoning factor.
I, is the Importance factor.
K, is the Structural Performance factor.

For the building considered:

Height to the top of the main portion of the building or the eaves of the building: $H_t := 3.448m$

Overall length of the building at the base in the x-direction: $D_x := 6.45m$

Overall length of the building at the base in the y-direction: $D_y := 5.1m$

1. Calculation of the Basic Seismic Coefficient

According to the NBC 105 7.3, for the purposes of initial member sizing the fundamental translation period may be calculated as:

$$T_{1x} := 0.09 \cdot \frac{H_t}{\sqrt{D_x}} = 0.122 \text{ s}$$ in x-direction

$$T_{1y} := 0.09 \cdot \frac{H_t}{\sqrt{D_y}} = 0.122 \text{ s}$$ in y-direction

$$T_{measured} := 0.06\text{s}$$

The Basic Seismic Coefficient is then aquired from NBC 105 Figure 8.1

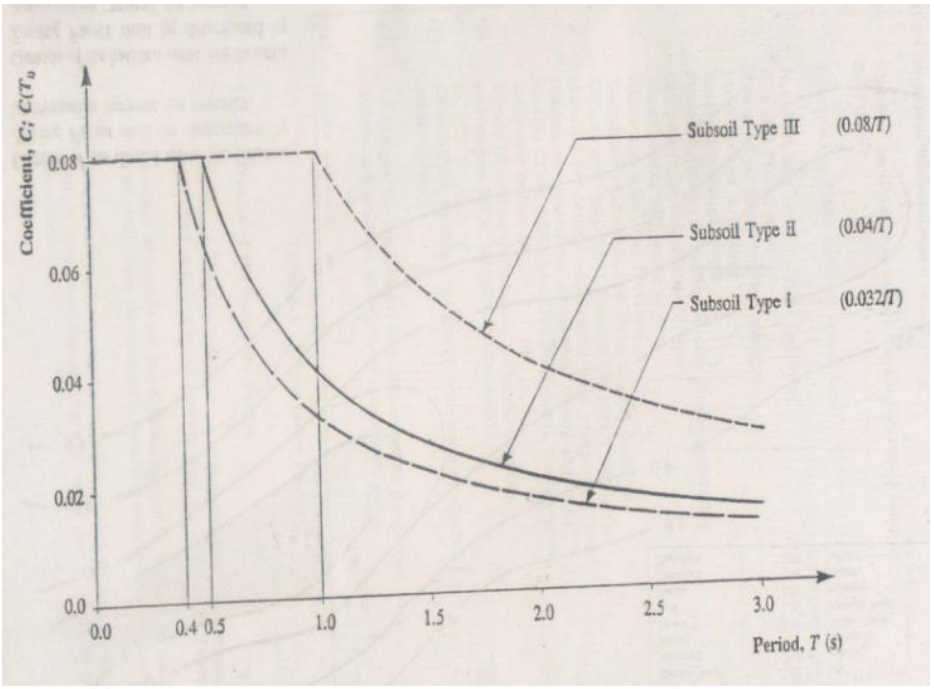

Figure 8.1 : BASIC SEISMIC COEFFICIENT, C
BASIC RESPONSE SPECTRUM, C(T1)

$$C_x := 0.08$$

$$C_y := 0.08$$

From this figure it is also clear that both the measured and the calculated values of T1 generate the same value of Cx and Cy.

2. Calculation of the Sesmic Zoning factor

The seismic zoning factor is dependent on the soil type of the location and shall be taken from NBC 105 Figure 8.2

ZONE FACTORS FOR SELECTED MUNICIPALITIES			
MANICIPALITY	FACTOR.Z	MUNICIPALITY	FACTCR.Z
Shadrapur	0.93	Dharan	1.00
Bharatpur	0.99	Dipayal	1.10
Bidur	1.00	Gaur	0.82
Birendra Nagar	1.02	Ilam	0.97
Biratnagar	0.93	Janakpur	0.89
Birganj	0.85	Kathmandu	
Butwal	0.90	Valley Towns	1.00
Byas	1.00	Mahendra Nagar	0.91
Damak	0.96	Nepalganj	0.91
Dhanagadi	0.90	Pokhara	1.00
Dhanakuta	1.00	Tulsipur	1.00

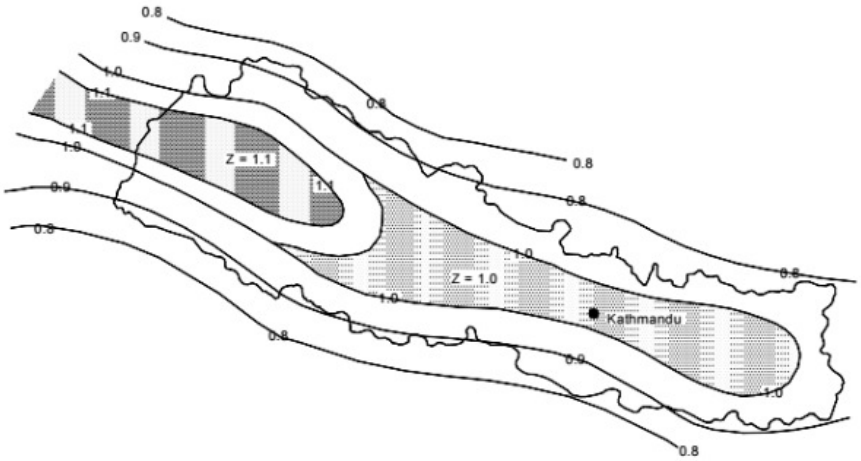

Outside of the shaded areas. the Seismic Zoning Factor shall be determined by interpolation between the contours.

Outside of the hatched areas, the Seismic Zoning Factor shall be determined by interpolation between the contours.

Figure 8.2 : SEISMIC ZONING FACTOR, *Z*

For the Kathmandu region:

$Z := 1.0$

3. Calculation of the Importance factor

The importance factor shall taken from the NBC 105:1994 Table 8.1

For a residential building: $I := 1.0$

4. Calculation of the Structural Performance factor

The Structural Performance factor was conservatively chosen as 2.5 for reinforced masonry with reference to IITK GSDMA Guidelines for Structural Use of Masonry since NBC 105:1994 Table 8.2 does not cover the use of reinforced masonry structures.

$K := 2.5$

1., 2., 3., and 4 => the Design Horizontal Seismic Coefficient:

$C_{dx} := C_x \cdot Z \cdot I \cdot K = 0.2$

$C_{dy} := C_y \cdot Z \cdot I \cdot K = 0.2$

Caluclation of the Seismic Weight, Wt

Unit weight of masonry: $W_m := 17.195 \frac{kN}{m^3}$

Width Column: $L_c := 0.3m$

Total wall area from Rhino drawing: $A_{walls} := 78.01m^2$

Thickness walls: $t_{wall} := 0.15m$

Amount of roof steel beams: $V_{steel} := 0.072m^3$

Density of steel: $\rho_{steel} := 7800 \frac{kg}{m^3}$

Seismic weights:

$W_{seismicsteel} := V_{steel} \cdot \rho_{steel} \cdot g = 5.507 \cdot kN$

$W_{seismicwalls} := A_{walls} \cdot t_{wall} \cdot W_m = 201.207 \cdot kN$

$W_{seismic} := W_{seismicsteel} + W_{seismicwalls} = 206.715 \cdot kN$

Calculation of Horizontal Base Shear

$V_{bx} := C_{dx} \cdot W_{seismic} = 41.343 \cdot kN$

$V_{by} := C_{dy} \cdot W_{seismic} = 41.343 \cdot kN$

Calculation mass distribution

The centre of mass was found by Abaqus:

$x_{cm} := 2.98m$

$y_{cm} := 2.75m$

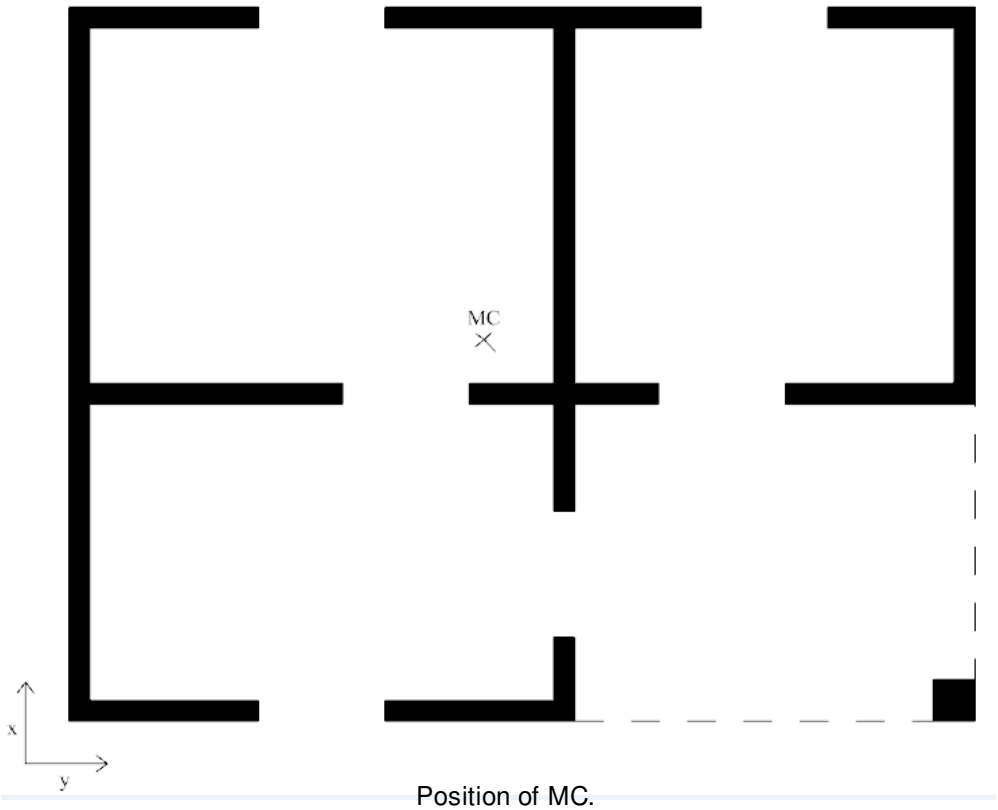

Position of MC.

Calculation of centre of rigidity

In the calculation of rotational centre the height of each shear pier is assumed to be equal. The different shear piers are shown below.

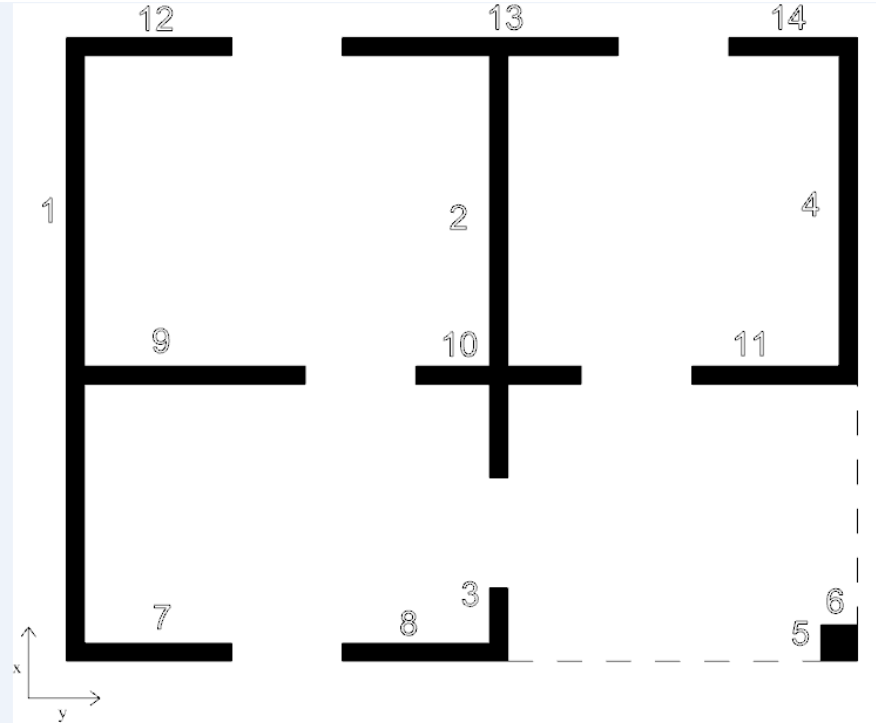

Length of shear piers in y-direction

$$L_y := \begin{pmatrix} 5.1 \\ 3.6 \\ 0.6 \\ 2.85 \\ 0.3 \end{pmatrix} m$$

Length of shear piers in x-direction

$$L_x := \begin{pmatrix} 1.35 \\ 1.35 \\ 2.0 \\ 1.35 \\ 1.35 \\ 1.35 \\ 2.25 \\ 1.05 \\ 0.3 \end{pmatrix} m$$

Position of shear piers in x-direction:

$$x := \begin{pmatrix} 0 \\ 3.45 \\ 3.45 \\ 6.3 \\ 6.225 \end{pmatrix} m$$

Position of shear piers in y-direction:

$$y := \begin{pmatrix} 0 \\ 0 \\ 2.265 \\ 2.265 \\ 2.265 \\ 4.95 \\ 4.95 \\ 4.95 \\ 0.075 \end{pmatrix} \cdot m$$

Moment of inertia of shear piers:

$$I_x := \frac{t_{wall} \cdot L_y^{\,3}}{12} = \begin{pmatrix} 1.658 \\ 0.583 \\ 2.7 \times 10^{-3} \\ 0.289 \\ 3.375 \times 10^{-4} \end{pmatrix} m^4$$

$$I_y := \frac{t_{wall} \cdot L_x^{\,3}}{12} = \begin{pmatrix} 0.031 \\ 0.031 \\ 0.1 \\ 0.031 \\ 0.031 \\ 0.031 \\ 0.142 \\ 0.014 \\ 3.375 \times 10^{-4} \end{pmatrix} m^4$$

Position of centre of rigidity:

$$x_{cr} := \left[\frac{\sum_{i=0}^{4} \left[I_{x_{(i)}} \cdot x_{(i)} \right]}{\sum_{i=0}^{4} I_{x_{(i)}}} \right] = 1.518\,m$$

$$y_{cr} := \left[\frac{\sum_{i=0}^{8} \left[I_{y_{(i)}} \cdot y_{(i)} \right]}{\sum_{i=0}^{8} I_{y_{(i)}}} \right] = 3.15\,m$$

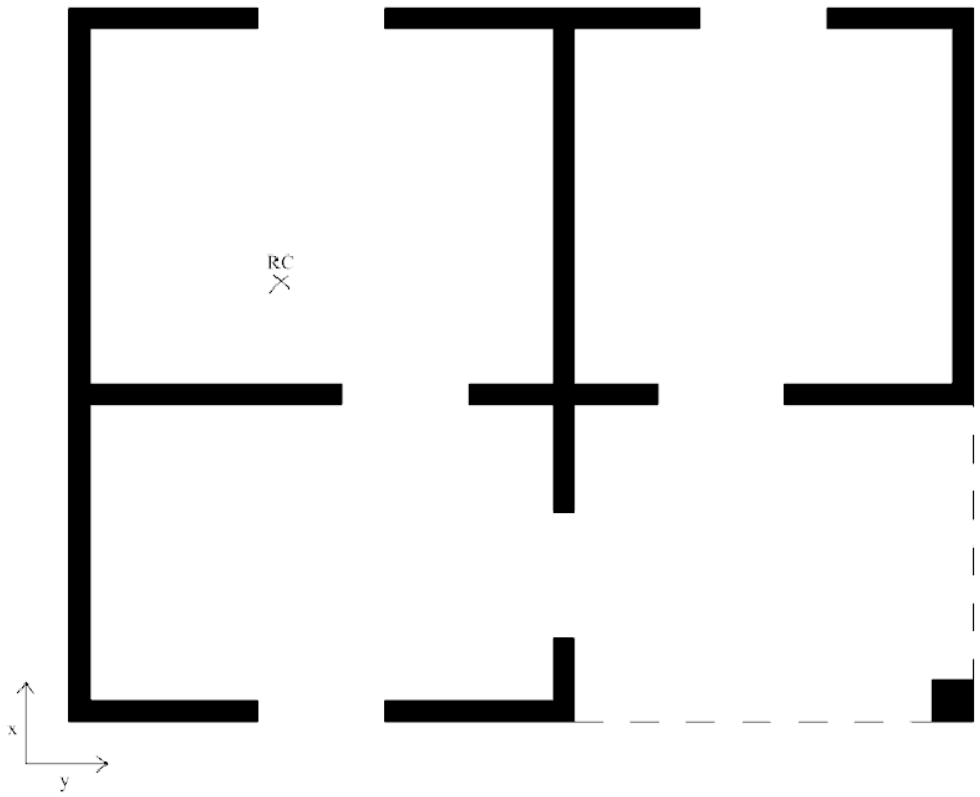

Position of RC.

Design Eccentricity

Computed eccentricity of the centre of mass from the centre of rigidity:

$$e_{cx} := \left|x_{cm} - x_{cr}\right| = 1.462\,m$$

$$e_{cy} := \left|y_{cm} - y_{cr}\right| = 0.4\,m$$

Maximum horizontal diemnsion of the building perpendicular to the the direction of loading:

$$b_x := 6.45m \qquad b_y := 5.1m$$

According to NBC:1994 8.2.2 the design eccentricity of the seismic load is:

$$e_{dx} := \begin{cases} 0 & \text{if } e_{cx} < 0.1 \cdot b_x \\ e_{cx} + 0.1 \cdot b_x & \text{if } 0.1 \cdot b_x \le e_{cx} < 0.3 \cdot b_x \\ \text{"3D modal response spectrum analysis needed"} & \text{if } e_{cx} \ge 0.3 \cdot b_x \end{cases} = 2.107\,\text{m}$$

$$e_{dy} := \begin{cases} 0 & \text{if } e_{cy} < 0.1 \cdot b_y \\ e_{cy} + 0.1 \cdot b_y & \text{if } 0.1 \cdot b_y \le e_{cy} < 0.3 \cdot b_y \\ \text{"3D modal response spectrum analysis needed"} & \text{if } e_{cy} \ge 0.3 \cdot b_y \end{cases} = 0\,\text{m}$$

=> In the y-direction no eccentricity has to be accounted for.

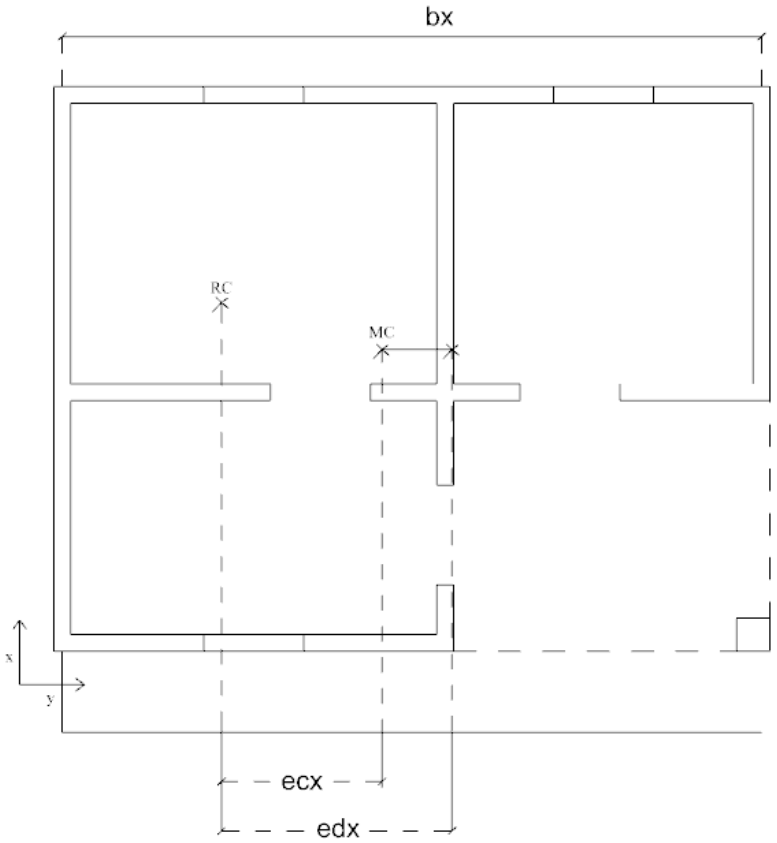

Illustration of ecx and edx.

Calculations of Force Distribution

The resultant of the force should, in x-direction, be placed at the design eccentricity, edx = 2.107 m. The loads should be applied as line loads along each section with a rebar of the three shear walls in x- and y-direction as shown below:

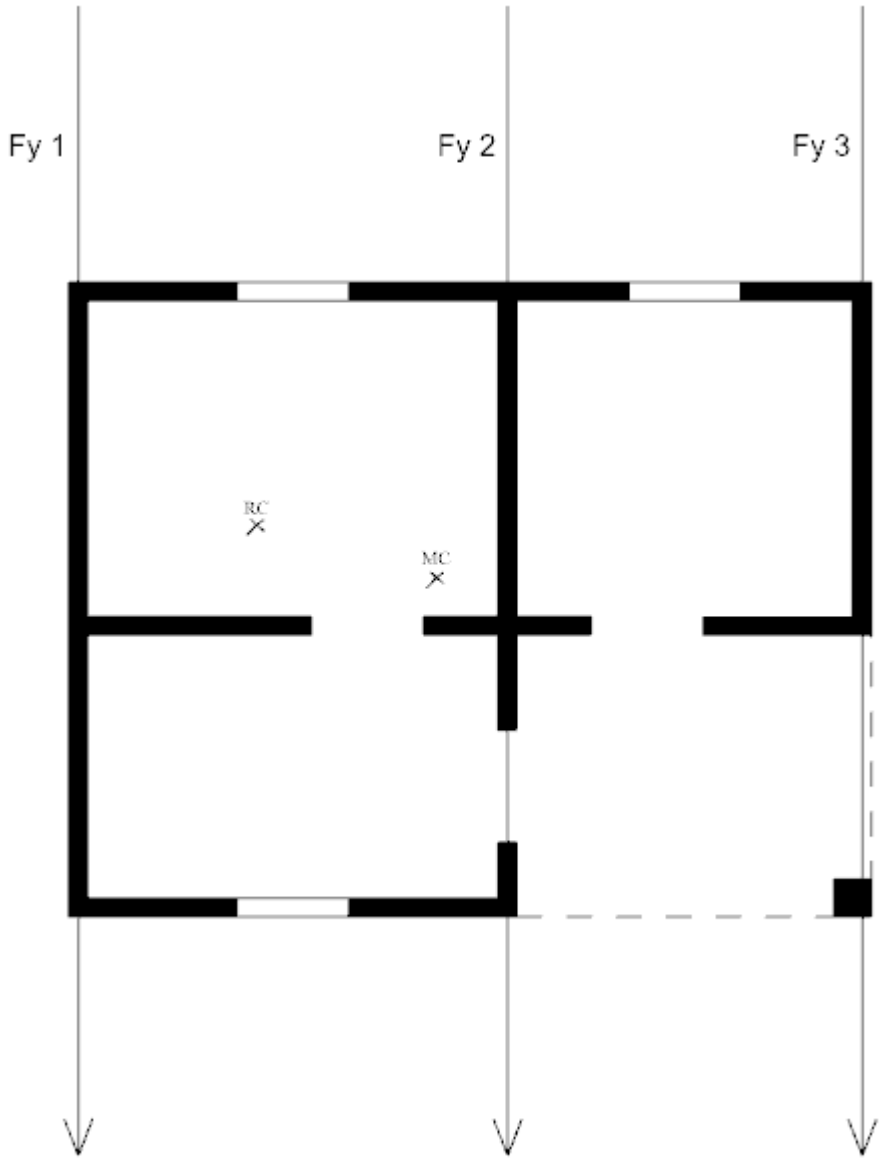

Forces in y-direction.

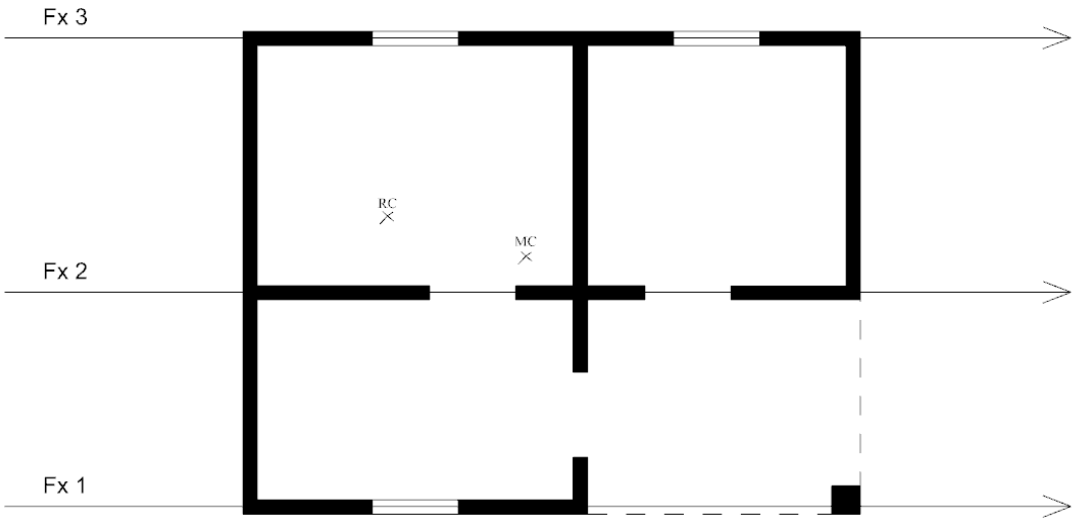

Forces in x-direction.

The magnitude of the load should, in both x- and y-direction, be distributed in relation to tributary mass of the shear wall where it is applied. A simplified calculation of this is to look at all rebars working in the direction of the force and then distribute the load with regard to geometric area of the shear wall surrounding the column.

Calculations of Forces acting in y-direction

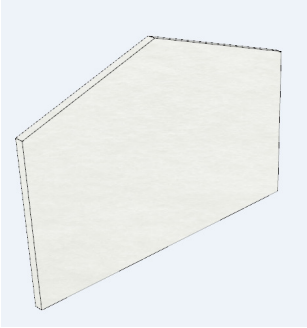

A1y

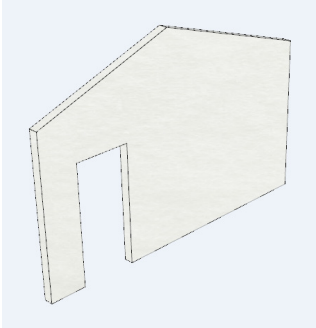

A2y

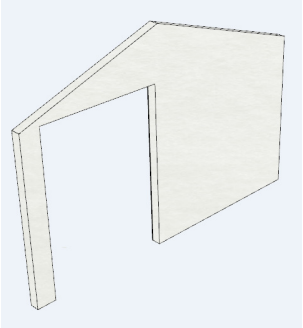

A3y

$A_{1y} := 14.64m^2$

$A_{2y} := 13.27m^2$

$A_{3y} := 10.34 \cdot m^2$

Norming for the smallest Area A3y gives the relation:

$$A_{3yn} := \frac{A_{3y}}{A_{3y}} = 1 \qquad A_{2yn} := \frac{A_{2y}}{A_{3y}} = 1.283 \qquad A_{1yn} := \frac{A_{1y}}{A_{3y}} = 1.416$$

This would give a distribution of:

$$F_{1y} := \frac{V_{by}}{\left(A_{1yn} + A_{2yn} + A_{3yn}\right)} \cdot A_{1yn} = 15.824 \cdot kN$$

$$F_{2y} := \frac{V_{by}}{\left(A_{1yn} + A_{2yn} + A_{3yn}\right)} \cdot A_{2yn} = 14.343 \cdot kN$$

$$F_{3y} := \frac{V_{by}}{\left(A_{1yn} + A_{2yn} + A_{3yn}\right)} \cdot A_{3yn} = 11.176 \cdot kN$$

But since the resulting force should be applied at edx this distribution has to be adjusted to one solution of the underspecifed equation system of R=F1+F2+F3 and R*(xcr+edx)=F1*x1+F2*x2+F3*x3. A Matlab program was developped to solve this problem (see Appendix D.2)

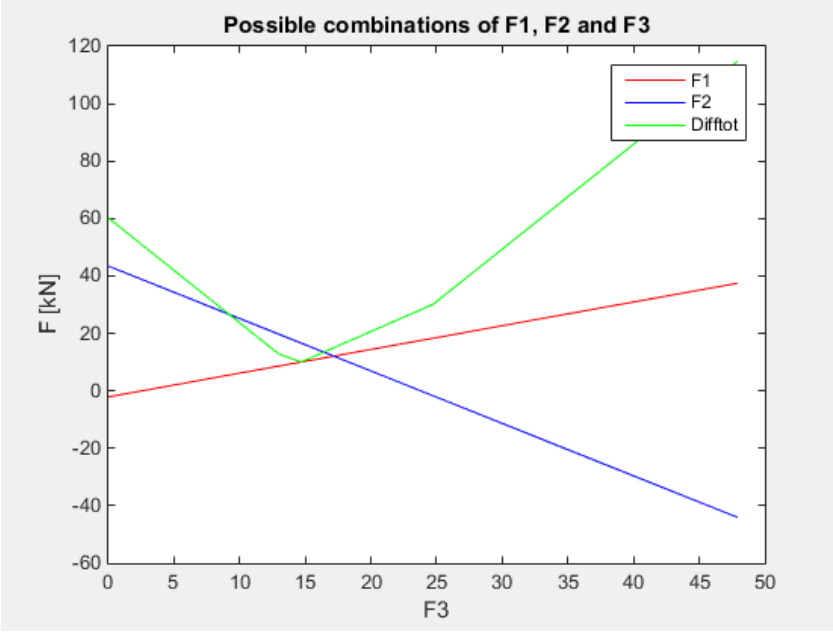

The solution that fullfils this criteria with the least deviation from the first (at min(Difftot)) is:

$F_{1y} := 10.03kN$ $F_{2y} := 16.63kN$ $F_{3y} := 14.68kN$

In each shear wall the force is applied on the sections with rebars. This distribution is done with regard to the total length of the rebars working in the force direction.

Rebar length wall y1: $L_{y1} := 31.41m$

Applied force on each column: $Q_{y1} := \frac{F_{1y}}{L_{y1}} = 0.319 \cdot \frac{kN}{m}$

Rebar length wall y2: $L_{y2} := 39.66m$

Applied force on each column: $Q_{y2} := \frac{F_{2y}}{L_{y2}} = 0.419 \cdot \frac{kN}{m}$

Rebar length wall y3: $L_{y3} := 28.1m$

Applied force on each column: $Q_{y3} := \frac{F_{3y}}{L_{y3}} = 0.522 \cdot \frac{kN}{m}$

Calculation of Forces acting in x-direction

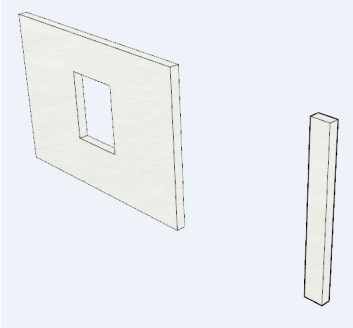

A1x

$A_{1x} := 9.3m^2$

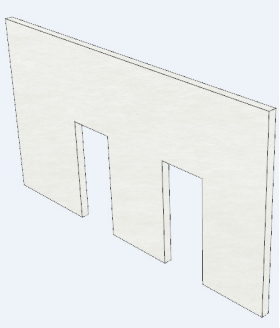

A2x

$A_{2x} := 18.1m^2$

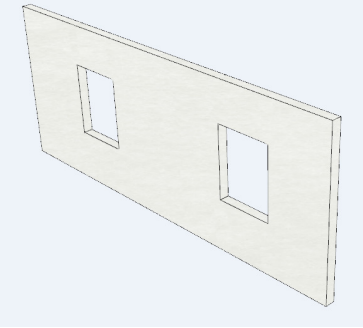

A3x

$A_{3x} := 14.7 \cdot m^2$

Norming for the smallest Area A1x gives the relation:

$$A_{1xn} := \frac{A_{1x}}{A_{1x}} = 1 \qquad A_{2xn} := \frac{A_{2x}}{A_{1x}} = 1.946 \qquad A_{3xn} := \frac{A_{3x}}{A_{1x}} = 1.581$$

This would give a distribution of:

$$F_{1x} := \frac{V_{bx}}{\left(A_{1xn} + A_{2xn} + A_{3xn}\right)} \cdot A_{1xn} = 9.133 \cdot kN$$

$$F_{2x} := \frac{V_{bx}}{\left(A_{1xn} + A_{2xn} + A_{3xn}\right)} \cdot A_{2xn} = 17.775 \cdot kN$$

$$F_{3x} := \frac{V_{bx}}{\left(A_{1xn} + A_{2xn} + A_{3xn}\right)} \cdot A_{3xn} = 14.436 \cdot kN$$

In the y-direction no adjustments for eccentric application of the forces has to be made.

In each shear wall the force is applied on the sections with rebars. This distribution is done with regard to the total length of the rebars working in the force direction.

Rebar length wall x1: $L_{x1} := 27.52m$

Applied force on each column: $Q_{1x} := \frac{F_{1x}}{L_{x1}} = 0.332 \cdot \frac{kN}{m}$

Rebar length wall x2: $L_{x2} := 50.6m$

Applied force on each column: $Q_{2x} := \frac{F_{2x}}{L_{x2}} = 0.351 \cdot \frac{kN}{m}$

Rebar length wall x3: $L_{x3} := 34.94m$

Applied force on each column: $Q_{3x} := \frac{F_{3x}}{L_{x3}} = 0.413 \cdot \frac{kN}{m}$

Appendix E

Calculations of Base Shear Distribution

```
clear all
close all
clc
x1=0;               %distance from origo to F1
x2=3.45;            %distance from origo to F2
x3=6.3;             %distance from origo to F3
xcr=1.518;          %distance from origo to RC
ed=2.107;           %distance from RC to point of resultant application
d=ed+xcr;           %distance from origo to R
R=41.34;            %Resultant=ttotal base shear

%Force distribution with regard to tributary wall area
F1id=18.34;
F2id=16.62;
F3id=12.95;

%Creating matrices
Fett=[];
Ftvo=[];
Ftre=[];
Diff1=[];
Diff2=[];
Diff3=[];

%Solving the equation given by:
syms F1 F2 F3
[F1, F2]=solve(R==F1+F2+F3, R*d==F1*x1+F2*x2+F3*x3)

 for i=0:4791;
     F3=i/100;
     F1=(19*F3)/23-4823/2300;
     F2=19981/460 - (42*F3)/23;
     Fett(i+1)=F1;
     Ftvo(i+1)=F2;
     Ftre(i+1)=F3;
     Diff1(i+1)=abs(Fett(i+1)-F1id);
     Diff2(i+1)=abs(Ftvo(i+1)-F2id);
     Diff3(i+1)=abs(Ftre(i+1)-F3id);
 end
 %Calculating the difference from these solutions to the one based on wall
 %tributary wall area
 Difftot=Diff1'+Diff2'+Diff3';
 X=1:471;
 plot(Ftre',Fett', 'r',Ftre',Ftvo,'b');
 hold on
 plot(Ftre',Difftot, 'g');
 title('Possible combinations of F1, F2 and F3')
 xlabel('F3')
 ylabel('F [kN]')
 legend('F1','F2','Difftot')
```

```
%Finding the solution with the least deviation from the one based on wall
%tributary wall area
[minwrong,index]=min(Difftot);
F1=Fett(index)
F2=Ftvo(index)
F3=Ftre(index)
```

```
F1 =

(19*F3)/23 - 4823/2300


F2 =

19981/460 - (42*F3)/23


F1 =

   10.0300


F2 =

   16.6300


F3 =

   14.6800
```

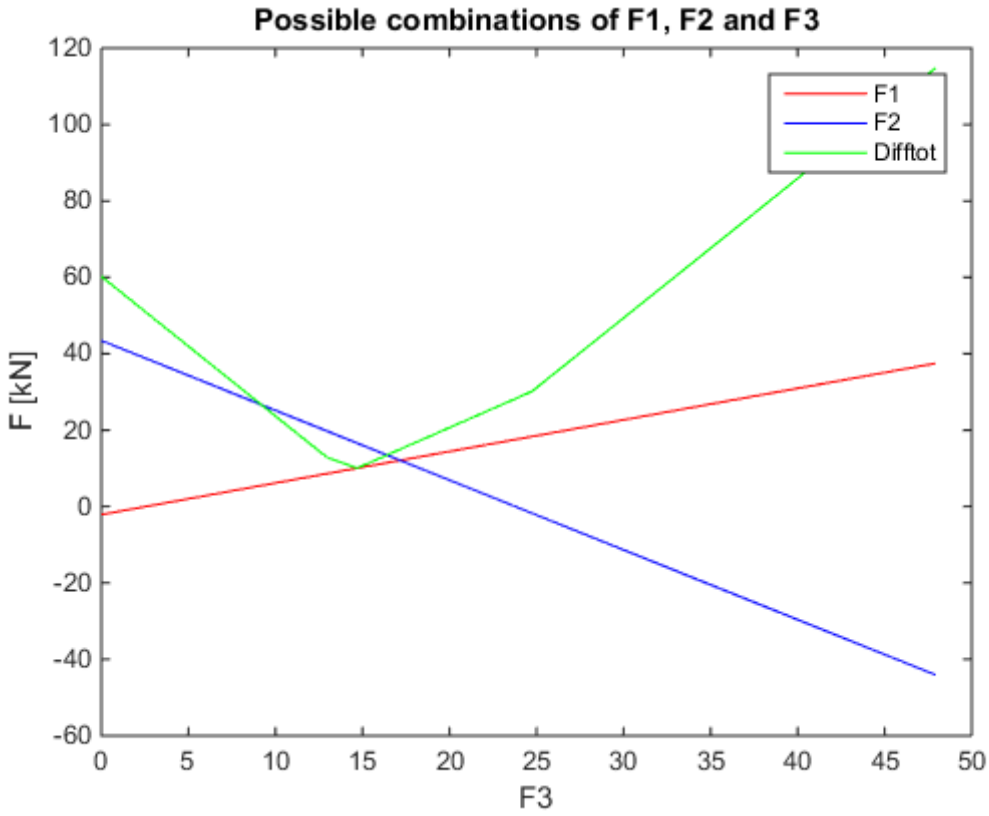

Published with MATLAB® R2014b

Appendix F

Design Calculations for Q2 and Q3

Appendix F.1

Q2. Does a bent rebar in one of the corners make the building unsafe?

Input

Maximum force at each rebar in a corner: $Q_{y3} := 0.522\frac{kN}{m}$

Number of rebars in the L-shaped corner $n := 3$

Height of the corner column: $H_c := 2.6m$

Cross-section

$h_{cs} := 300mm$

$t := 150mm$

$b := 300mm$

$b_w := h_{cs} - t = 0.15m$

$$A_c := \frac{h_{cs}}{2}\cdot t + h_{cs}\cdot t$$

For positive moment:

$$x_{tppos} := \frac{\left(b - b_w\right)\cdot\frac{t^2}{2} + \frac{b_w\cdot h_{cs}^{\ 2}}{2}}{A_c} = 0.125m$$

For negative moment:

$$x_{tpneg} := h_{cs} - \frac{\left(b - b_w\right)\cdot\frac{t^2}{2} + \frac{b_w\cdot h_{cs}^{\ 2}}{2}}{A_c} = 0.175m$$

Moment of inertia of the column:

$$I_c := \frac{\left(b - b_w\right)\cdot t^3}{12} + \left(b - b_w\right)\cdot t\cdot\left(x_{tppos} - \frac{t}{2}\right)^2 + \frac{b_w\cdot h_{cs}^{\ 3}}{12} + b_w\cdot h_{cs}\left(\frac{h_{cs}}{2} - x_{tppos}\right)^2$$

$I_c = 4.641 \times 10^{-4}\,m^4$

Material properties CSEB

$f_{ck} := 10.9MPa$

$f_{ctm} := 1.74MPa$

Calculation of bending action

$$M_{Ed} := \frac{n \cdot Q_{y3} \cdot H_c^{\,2}}{2} = 5.293 \cdot kN \cdot m$$

Condition:

The column is uncracked if $\sigma_{ct} < k * f_{ctm} \Rightarrow \sigma_{cr} = k * f_{cmt}$

$$k := 1.6 - \frac{h_{cs}}{1000mm} = 1.3$$

$$\sigma_{cr} := k \cdot f_{ctm} = 2.262 \cdot MPa$$

Naviers formula=>

For positive moment:

$$M_{crpos} := \frac{\sigma_{cr} \cdot I_c}{\left(h_{cs} - x_{tppos}\right)} = 5.998 \cdot kN \cdot m$$

For negative moment:

$$M_{crneg} := \frac{\sigma_{cr} \cdot I_c}{\left(h_{cs} - x_{tpneg}\right)} = 8.398 \cdot kN \cdot m$$

Check

For positive moment:

$M_{Ed} < M_{crpos} = 1$ **=> OK!**

For negative moment:

$M_{Ed} < M_{crneg} = 1$ **=> OK!**

Appendix F.2

Q3. Does a poorly anchored rebar next to one of the openings make the building unsafe?

Input

Maximum force at each rebar in a corner: $Q_{y2} := 0.419\frac{kN}{m}$

Height of the corner column: $H_c := 3.1m$

Cross-section

$h_{cs} := 300mm$

$t := 150mm$

$A_c := h_{cs} \cdot t = 0.045m^2$

$x_{tp} := \frac{h_{cs}}{2} = 0.15m$

Moment of inertia of the column:

$I_c := \frac{t \cdot h_{cs}^3}{12} = 3.375 \times 10^{-4} m^4$

Material properties CSEB

$f_{ck} := 10.9MPa$

$f_{ctm} := 1.74MPa$

Calculation of bending action

$$M_{Ed} := \frac{Q_{y2} \cdot H_c^{\,2}}{2} = 2.013 \cdot kN \cdot m$$

Condition:

The column is uncracked if $\sigma_{ct} < k * f_{ctm} \Rightarrow \sigma_{cr} = k * f_{cmt}$

$$k := 1.6 - \frac{h_{cs}}{1000mm} = 1.3$$

$$\sigma_{cr} := k \cdot f_{ctm} = 2.262 \cdot MPa$$

Naviers formula=>

$$M_{cr} := \frac{\sigma_{cr} \cdot I_c}{x_{tp}} = 5.09 \cdot kN \cdot m$$

Check

$M_{Ed} < M_{cr} = 1$ **=> OK!**